Impact of proteasomal immune adaptation on the early immune response to viral infection

DISSERTATION

zur Erlangung des akademischen Grades

doctor rerum naturalium

(Dr. rer. nat.)

im Fach Biologie

eingereicht an der

Mathematisch-Naturwissenschaftlichen Fakultät I

der Humboldt-Universität zu Berlin

von

Diplom-Biologin Annika Warnatsch

Präsident der Humboldt-Universität zu Berlin

Prof. Dr. Jan-Hendrik Olbertz

Dekan der Mathematisch-Naturwissenschaftlichen Fakultät I

Prof. Dr. Stefan Hecht

Gutachter:

1. Prof. Dr. Richard Lucius
2. Prof. Dr. Hartmut Hengel
3. Prof. Dr. Elke Krueger

Tag der mündlichen Prüfung: 18. Februar 2013

Those who have never entered upon scientific pursuits know not a tithe of the poetry by which they are surrounded.

Herbert Spencer

Meinen Eltern

Table of contents

Zusammenfassung

Im Kampf gegen eine Virusinfektion spielen $CD8^+$ T Zellen des adaptiven Immunsystems eine besondere Rolle. Sie patroullieren im Körper und entdecken spezifische Virusepitope, welche mittels körpereigener MHC Klasse I Moleküle auf der Oberfläche infizierter Zellen präsentiert werden. Wird eine virus-infizierte Zelle erkannt, kann diese schnell und effizient eliminiert. Für die Generierung viraler Peptide, welche auf MHC Klasse I Komplexe geladen werden können, ist das Ubiquitin-Proteasom-System von essentieller Bedeutung. Lange wurde die Funktion des Immunoproteasoms vornehmlich darin gesehen, die Generierung antigener Peptide zu verbessern. In letzter Zeit wurden weitere Funktionen des Immunoproteasoms aufgedeckt wie zum Beispiel die Regulation von Zellproliferation und -differenzierung, Zytokinproduktion oder der Schutz gegen oxidativen Stress. Diese bisher unbekannten Funktionen des Immunoproteasoms beruhen auf einer gesteigerten Abbaurate von ubiquitylierten Proteinen im Vergleich zum Standardproteasom. Innerhalb der vorliegenden Arbeit konnte die Fähigkeit des Immunoproteasoms gegen eine Akkumulation oxidativ geschädigter Proteine zu schützen mit seiner Rolle in der adaptiven Immunantwort, die Generierung von MHC Klasse I Liganden zu verbessern, kombiniert und neu interpretiert werden.

Es konnte gezeigt werden, dass während einer Virusinfektion in Nicht-Immunzellen die Produktion reaktiver Sauerstoffspezies durch die alternative NADPH Oxidase Nox4 eine bedeutende Rolle spielt. Die Aktivierung von Nox4 resultiert in der Akkumulation oxidativ geschädigter Proteine, welche potentiell toxische Eigenschaften besitzen. Dabei scheint es sich um ein generelles Prinzip zu handeln, da ähnliche Resultate anhand zwei verschiedener Virusinfektionsmodelle beobachtet wurden: die langsam foranschreitende Infektion mit dem DNA-Virus HCMV und die Infektion mit dem schnell replizierenden RNA-Virus Influenza A. Innerhalb von wenigen Minuten nach dem Eintreten von Viruspartikeln in die Zellen wurden strukturelle Virusproteine, wie das HCMV Tegumentprotein pp65 und das Influenza A Matrixprotein M1, oxidiert und anschließend ubiquityliert. Dabei zeigte sich, dass die Modifikation der Virusproteine abhängig von dem Ubiquitin-konjugierenden Enzym UBE2L6 ist. Die gleichzeitige, virusinduzierte Expression von Immunoproteasomen führte zu einem schnellen und effizienten Abbau oxidierter und ubiquitylierter Virusantigene. Infolgedessen konnten immun-dominante Virusepitope, $pp65_{495\text{-}503}$ beziehungsweise $M1_{58\text{-}66}$, vermehrt freigesetzt werden, welches sich positiv auf die adaptive Immunantwort auswirkt.

Folglich wurde ein soweit unbekannter translations-unabhängiger Mechanismus gefunden, welcher Substrate für das Proteasom zur Generierung von MHC Klasse I Liganden bereitstellt. Dabei handelt es sich um einen komplementären Signalweg zur DRiP Hypothese, welche besagt, dass defekte ribosomale Produkte die Hauptquelle für MHC Klasse I Liganden darstellen. Offenbar spielen Mechanismen der angeborenen Immunantwort, wie die Induktion von Sauerstoffradikalen, eine wichtige Rolle, um den Proteinnachschub für das Proteasom zur Generierung antigener Peptide zu garantieren. So werden neben neu translatierten, defekten Proteinen durch Oxidation stabile, exogene Virusproteine dem Proteasom zugänglich gemacht. In Anlehnung an die DRiP Hypothese wird dieser Proteinpool als DrOPs, direkt oxidierte Proteine, bezeichnet.

Zusammenfassend konnte innerhalb dieser Arbeit gezeigt werden, dass das Immunoproteasom den Schutz vor oxidativen Stress mit der Generierung antigener Peptide verbindet, wodurch eine effektive adaptive Immunantwort etabliert werden kann.

Abstract

An efficient immune control of virus infection is predominantly mediated by $CD8^+$ T cells which patrol through the body and eliminate infected cells. Infected cells are recognized when they present viral antigenic peptides on their surface via MHC class I molecules. To make antigenic peptides available for loading on MHC class I complexes, the ubiquitin proteasome system plays a crucial role. Moreover, the induction of a special subunit composition of the proteasome, the i-proteasome, is known to support the generation of MHC class I ligands. Recently, new functions of the i-proteasome, independent of MHC class I antigen processing, have been discovered. Evidence is increasing that the i-proteasome is involved in diverse processes such as lymphocyte survival, the regulation of cell proliferation and differentiation, the production of cytokines and the protection of cells against oxidative stress. These previously unknown functions of the i-proteasome likewise depend on its increased ability to degrade ubiquitylated proteins as compared to standard proteasomes. Within this thesis the characteristic of the i-proteasome to protect cells against the accumulation of oxidant-damaged proteins could be linked to its role in the adaptive immune response to improve the generation of MHC class I ligands.

It could be demonstrated that during a virus infection in non-immune cells the production of reactive oxygen species by the alternative NADPH oxidase Nox4 is of critical importance resulting in the accumulation of potentially toxic oxidant-damaged proteins. This appears to be a general principle, as shown by comparing two different virus models: the slow progressing DNA virus HCMV and the fast replicating RNA virus influenza A. Indeed, within two hours of infection structural virus proteins, such as either the HCMV tegument protein pp65 or the influenza A Matrix protein M1, were oxidized and subsequently poly-ubiquitylated. This required the activity of components of the UPS, for instance the ubiquitin-conjugating enzyme UBE2L6. The concomitant virus-induced formation of i-proteasomes led to a rapid and efficient degradation of the oxidized and ubiquitylated virus antigens thereby improving the liberation of the immunodominant viral epitopes $pp65_{495\text{-}503}$ and $M1_{58\text{-}66}$, respectively, which ameliorated the adaptive immune response.

In conclusion, a so far unknown translation-independent mechanism to fuel proteasomal substrates into the MHC class I antigen presentation pathway has been revealed. This imposes a complementary pathway to the DRiP hypothesis, which declares that defective ribosomal products represent the major source for MHC class I ligands, by making stable virus proteins available. Evidently, DRiPs represent not the sole source for virus epitopes and indeed an innate immune mechanism, i.e. the induction of oxygen radicals, can provide the protein supply for the proteasome in order to generate antigenic peptides, too. Here, a new protein pool providing proteasomal substrates in the very early phase of a virus infection has been uncovered. According to the DRiP hypothesis these proteins will be referred to as DrOPs, directly oxidized proteins, representing fully folded, exogenously delivered viral proteins which become accessible for the proteasome through their oxidation.

Within the scope of this thesis the i-proteasome has been shown to link the protection against oxidative stress, initiated directly by pathogen recognition as part of the innate immunity, with the generation of antigenic peptides. Together, an effective adaptive immune response is triggered.

1. Introduction

Our immune system protects us against numerous kinds of pathogens, such as viruses, bacteria, fungi and parasites. A successful immune response depends on: i) the detection of a wide variety of pathogens, ii) the generation of appropriate pathogen-specific effector responses, and iii) the establishment of long-term immunity, named memory. Therefore, in multi-cellular organisms specialised immune cells have evolved. These cells recognise, phagocytise and kill foreign cells as well as their own cells that became infected (Murphy, 2011). The following chapters will discuss basic immune defence mechanisms with regard to an immunological challenge caused by virus infection.

1.1 Interplay between innate and adaptive immunity

When a pathogen attacks the host, a first line of defence is provided by the innate immune system. This system is complemented with a second layer of protection, called the adaptive immune system. Specialised cells of the innate immune system, such as dendritic cells (DCs), macrophages, neutrophils etc., are activated by the recognition of so-called pathogen-associated molecular patterns (PAMPs). Through secretion of cytokines, not only the innate immune cells, but also tissue cells and a wide variety of other cells, initiate inflammatory cascades and anti-microbial defence mechanisms. They release chemokines to recruit phagocytic cells to the site of infection and modulate the strength of both innate and adaptive immune responses. Moreover, the innate system presents pathogen-derived antigens to cells of the adaptive immune system, in this way orchestrating their activation. Antigen-specific cells of the adaptive immune response comprise $CD4^+$ and $CD8^+$ T cells, B cells and plasma cells. Virus infections, as well as intracellular bacteria or transformed cells, are predominantly controlled by $CD8^+$ T cells. Upon activation $CD8^+$ T cells produce cytokines, mainly IFNγ, and acquire cytotoxic functions which mediate killing of infected and transformed cells, respectively. Notably, adaptive immune responses also exert effects on innate immune cells. For example, cytokines produced by $CD8^+$ T cells can enhance anti-microbial activities of innate immune cells. In conclusion, innate and adaptive immunity interact at various levels and mutually depend on each other (Murphy, 2011).

1.2 Antigen recognition and presentation

The innate immune response relies on germ-line encoded receptors, which are called pattern recognition receptors (PRRs). The PRRs were first detected by Charles Janeway in 1989, these receptors recognise invariant pathogen-associated molecular patterns (PAMPs) (Janeway, 1989). In contrast, the adaptive immune system generates a diverse repertoire of lymphocyte receptors which recognise numerous foreign antigens presented by major histocompatibility complex (MHC) molecules. T cell receptors (TCRs) as well as B cell receptors (BCRs) are generated *de novo* in each organism by a random rearrangement of several, repetitive gene segments allowing for highly specific adaptive immune responses (von Boehmer et al., 1988). These different strategies of antigen recognition by innate and adaptive immune system complement each other in order to enhance pathogen detection and eradication.

1.2.1 Innate immune response to viral infection

Several viral PAMPS have been identified to date, such as viral nuclear proteins, capsid proteins, envelope proteins, glycoproteins as well as viral DNA and RNA. Moreover, throughout the viral replication cycle replicative intermediates like unmethylated CpG DNA or single- and doublestranded RNA, which appear structurally different from cellular RNA, can be recognised by PRRs (Akira et al., 2001).

The signaling through most PRRs induces the expression of a set of specific genes leading to the establishment of antiviral immunity, such as the induction of the type I interferons, IFNα and IFNβ, or pro-inflammatory cytokines. Further, by increasing the expression of costimulatory molecules like CD80, CD86 or CD40 maturation of dendritic cells (DCs) is triggered. MHC class I antigen presentation is enhanced, thereby facilitating cross-presentation of viral antigens too. Antigen-specific $CD8^+$ T cell responses are induced and the secretion of chemokines stimulates the recruitment of lymphocytes and monocytes to the sites of infection. Moreover, hundreds of effector molecules directly influencing protein synthesis and cell growth are upregulated (Kawai and Akira, 2006).

According to their cellular localisation, PRRs are broadly grouped into two classes: transmembrane receptors and intracellular receptors. The transmembrane Toll-like receptors (TLRs) can be further divided into those patrolling the extracellular and those guarding the endosomal compartments (Kawai and Akira, 2010). The cytosolic retinoic acid-inducible gene I (RIG I)-like RNA helicases (RLHs) are expressed in most cell types and recognize ssRNA and some dsRNA viruses (Rehwinkel and Reis e Sousa, 2010).

Toll-like receptors represent key sensors of PAMPs and are expressed on many cell types, but the highest levels are found on DCs and macrophages. They are named after their homology to Toll proteins, which were originally discovered in 1996 in *Drosophila melanogaster* (Lemaitre et al., 1996). Subsequently, a mammalian homologue, now known as TLR4, was identified (Medzhitov et al., 1997). The TLR family consists of 13 members in humans and mice, TLR1 to 9 are common in humans and mice, TLR10 can only be found in humans, TLR11 to 13 only in mice (Thompson and Locarnini, 2007). The surface TLRs, which recognise PAMPs in the extracellular space, include TLR1, 2, 5, 6 and 11 and discover mostly lipids, lipoproteins and glycoproteins present on the surface of pathogens. The intracellular TLRs TLR3, 7, 8, and 9, reside in the endoplasmic reticulum (ER), endosomes and lysosomes, and recognise viral DNA and RNA. TLR4, which responds to LPS (lipopolysaccharides), is described to signal both at the cell surface and from intracellular locations. By formation of homo- and heterodimers TLRs detect a wide variety of pathogens (Akira et al., 2006). Due to their compartmentalisation TLRs have restricted access to host nucleic acids which protects cells against inappropriate immune responses (Thompson and Locarnini, 2007).

For the innate immune response to viruses the Toll-like receptors TLR2, 3, 4, 7, 8 and 9 play important roles. On the cell surface TLR2 and TLR4 mediate the detection of viral structural proteins like envelope glycoproteins. Compton et al. reported that TLR2 mediates the induction of pro-inflammatory cytokines via NFκB activation in response to human cytomegalovirus (HCMV) infection by detection of the envelope glycoproteins gB and gH of HCMV (Compton et al., 2003). Major ligand

of TLR4 represents lipopolysaccharide which can be found in the outer membrane of gram-negative bacteria, but recently evidence was shown that TLR4 also recognizes some viral components (Kurt-Jones et al., 2000). These interactions may serve the virus more than the host, for example pro-inflammatory cytokine responses may lead to upregulation of certain receptors which the virus uses for entry and spread.

Internal TLRs are able to recognise virus infection after invasion of virus particles into the host cells. TLR3 detects viral dsRNA which occurs as replication intermediate of many viruses but also constitutes the genome of dsRNA viruses. Activation of TLR3 can also be triggered by the synthetic dsRNA analogue poly(I:C) and mimic viral infection (Alexopoulou et al., 2001). Moreover, TLR3 was shown to be involved in the innate immune response to influenza A infection (Guillot et al., 2005). TLR7 and TLR8 recognise viral ssRNA, representing the most sensitive antiviral receptors recognising almost all RNA viruses including influenza A (Heil et al., 2004). Finally, TLR9 mediates recognition of viral unmethylated CpG nucleotides, which are rare in vertebrates but present in viruses and bacteria. Thus, TLR9 is involved in the detection of infection with dsDNA viruses such as the murine cytomegalovirus MCMV (Tabeta et al., 2004).

Upon ligand recognition, TLR signaling is initiated resulting in specific gene transcription and activation of innate immune responses. All TLRs are characterised by cytoplasmic TIR (Toll/interleukine-1 receptor) domains which interact by homo- or heterodimerisation of TLRs leading to recruitment of several downstream TIR-domain-containing adaptors, such as MyD88 (myeloid differentiation factor 88), Mal (MyD88-adaptor like; also called TIRAP), TRIF (TIR-domain containing adaptor protein inducing IFNβ) and TRAM (TRIF-related adaptor molecule) (Boo and Yang, 2010).

TLR signaling, summarized in figure 1.1A, is roughly divided in MyD88-dependent and -independent pathways. The TLRs 7, 8 and 9 use the MyD88-dependent pathway. MyD88 forms complexes with IRAK (IL1-receptor-associated kinase) family members, which themselves interact with TRAF6 (TNF receptor associated factor 6), an E3-ligase. This causes the recruitment of ubiquitin-conjugating enzyme NEMO (NFκB essential modulator) and IκB kinases into a multi-protein complex. Subsequently IκB, the inhibitor of NFκB, is phosphorylated, ubiquitylated and degraded. As a result, NFκB is released and translocates into the nucleus, where the expression of pro-inflammatory cytokines (ICs) like IL1, IL6 or TNFα is induced (Karin and Ben-Neriah, 2000).

TLR3 uses an alternative MyD88-independent pathway by interaction with the adaptor protein TRIF (figure 1.1A). Next, TRIF interacts with TRAF3 (TNF receptor associated factor 3) to activate TBK1 (TANK-binding kinase 1) and IKKε (inhibitor of NFκB kinase), which subsequently directly phosphorylate IRF3 (IFN regulatory factor 3). Phosphorylated IRF3 dimerises and shuttles to the nucleus where it activates the transcription of IFNβ. Signalling via TRIF also leads to NFκB activation. Therefore, the C-terminal non-TIR region of TRIF associates with TRAF6 (Kawai and Akira, 2006). In the case of TLR4, firstly the MyD88-dependent pathway is activated at the plasma membrane. Primarily, Mal recruits MyD88 to TLR4 which leads to initial activation of NFκB. Subsequently, TLR4 is taken up by endocytosis. Inside the endosome the adaptor TRAM recruits TRIF inducing activation of IRFs and NFκB (Kagan et al., 2008).

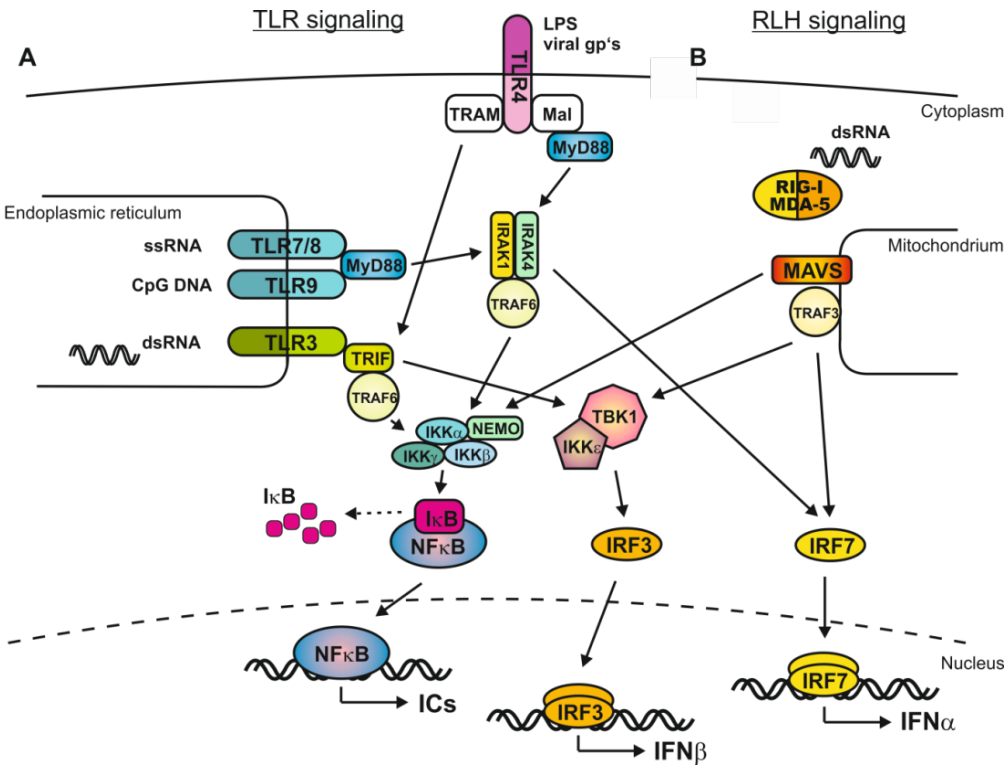

Figure 1.1 Signaling pathways of Toll-like receptors and RIG-I-like helicases. A) The endosomal TLRs, TLR7/8 and 9, use the adaptor MyD88 to activate transcription factor NFκB, which in turn induces transcription of pro-inflammatory cytokines (ICs) such as TNFα. In contrast TLR3 uses MyD88-independent signaling via TRIF to induce transcription factor IRF3, which initiates the expression of IFNβ. TLR4 is able to induce by usage of further adaptor proteins MyD88-dependent and –independent signaling. B) The RLHs RIG-I and MDA-5 both activate the mitochondrial located adaptor MAVS, which is able to activate IRFs and NFκB. For further explanations see text.

RNA helicases In 2004 Yoneyama and colleagues discovered a TLR-independent mechanism that senses viral infections and identified RIG-I (retinoic acid inducible gene 1) (Yoneyama et al., 2004). Shortly after, also the structurally related MDA-5 (melanoma differentiation-associated protein 5) was identified. Both proteins represent DExD/H box RNA helicases which interact with dsRNA, a common intermediate during the replication cycle of many RNA viruses, and thereby trigger the production of type I IFNs and pro-inflammatory cytokines. RIG-I for example was shown to play a crucial role during the innate immune response to orthomyxoviruses like influenza A (Pichlmair et al., 2006).

Downstream signal transduction of RNA helicases is mediated through N-terminal CARD (caspase activation and recruitment) domains. Upon binding to dsRNA CARD domains dimerise and interact with adaptor proteins (figure 1.1B). An important adaptor protein was identified simultaneously by 4 different groups and therefore is known under 4 different names: MAVS (mitochondrial antiviral signalling protein (Seth et al., 2005)), Cardif (CARD adaptor inducing IFNβ (Meylan et al., 2005)), VISA (virus-induced signalling adaptor (Xu et al., 2005)) or IPS-1 (IFNβ promoter stimulator (Kawai et al., 2005)). MAVS is targeted via a C-terminal hydrophobic transmembrane domain to mitochondria and signals via TRAF3 to activate Tbk1 and IKKε, which in turn phosphorylate and activate IRF3 as well as IRF7.

Further in a parallel pathway MAVS also interacts with FADD and RIP1, which represent death domain containing proteins and activate the transcription factor NFκB (Kawai and Akira, 2006) (figure 1.1B).

Type I interferon response The type I interferons IFNα and IFNβ represent the key cytokines during an immune response against viral infection. The IFNβ promoter possesses binding sequences for the transcription factors NFκB, AP1 and IRFs, particularly activated in response to viral infection are IRF3 and IRF7. These three components along with cofactors like p300/CBP (CREB binding protein) assemble to the IFNβ-enhanceosome which binds to positive regulatory domains (PRDs) of the IFNβ promoter and stimulates its transcription (figure 1.2A). Thus, IFNβ is secreted and activates via auto- or paracrine binding the IFNα receptor (IFNαR) (figure 1.2B). Upon ligand binding the IFNαR signals to the tyrosine kinases Jak1 and Tyk2 which phosphorylate STAT1 and 2 (signal transducer and activator of transcription). Phosphorylated STATs heterodimerise and translocate to the nucleus (figure 1.2C). There they associate with IRF9 forming the heterotrimeric transcription complex ISGF3 (IFN-stimulated gene factor 3), which binds to ISREs (IFN-stimulated response elements) and induces the expression of antiviral proteins including the myxovirus-resistance protein (Mx) GTPase, RNA-dependent protein kinase (PKR), oligoadenylate synthetase (OAS), ribonuclease L (RNase L) and further ISGs (IFN stimulated genes) (Stark et al., 1998) (figure 1.2D). Notably, the IFN-stimulated gene ISG15 represents an ubiquitin-like modifier which is conjugated to target proteins in a process called ISGylation conveying different cellular functions. For example, it is reported that ISGylation of IRF3 inhibits its degradation, thereby further enhancing the type I IFN response (Lu et al., 2006).

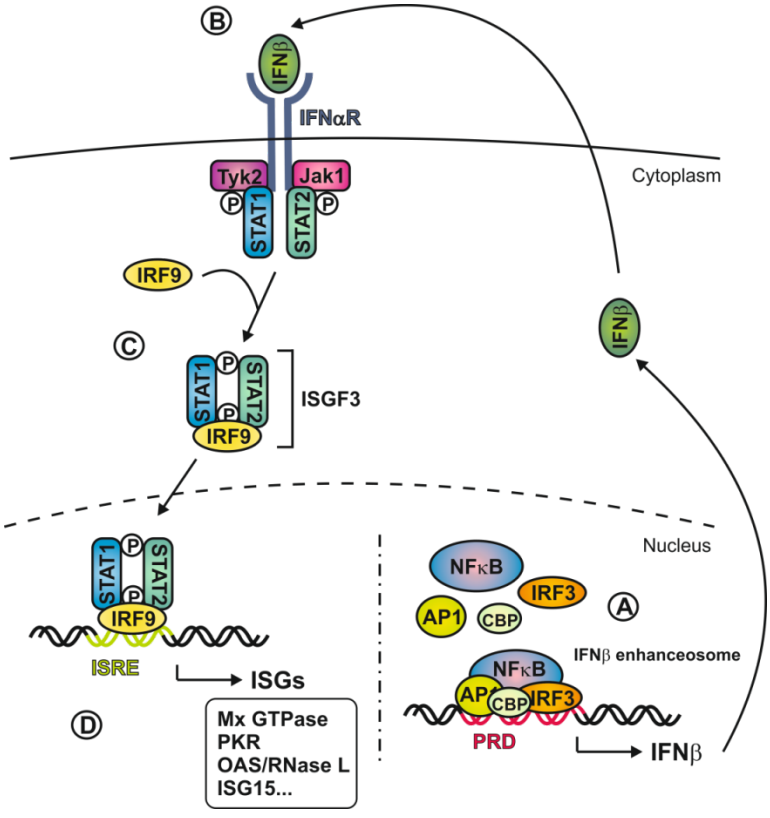

Figure 1.2 The type I interferon response. A) Assembly of the IFNβ enhanceosome which is composed of NFκB, AP1, IRFs and cofactors such as CBP. Binding to positive regulatory domains initiates the transcription of IFNβ. B) Secretion of IFNβ activates via auto- or paracrine binding the IFNα receptor. C) The IFNαR associated tyrosine kinases Jak1 and Tyk2 phosphorylate STAT1 and STAT2, which subsequently heterodimerise and constitute together with IRF9 the transcription complex ISGF3. D) ISGF3 binds to ISREs and induces the transcription of ISGs, such as Mx GTPase, protein kinase R, oligoadenylate synthetase and RNase L.

1.2.2 Adaptive immune response to viral infection

The adaptive immunity provides the most powerful defence mechanism against pathogens, using antigen-specific immune responses which can result in complete inactivation or removal of pathogens. Two major systems constitute the adaptive immunity: humoral immunity and T cell-mediated immunity. While humoral immunity is mediated by antibody producing B cells, T cell-mediated immunity can further be distinguished in $CD8^+$ and $CD4^+$ T cell responses according to the coreceptor molecules they express which are involved in antigen recognition. However, a virus infection is predominantly controlled by $CD8^+$ T cells, which will be explained in detail in the following chapter.

The antigen-specific receptor of T cells recognises peptides, which are presented by major histocompatibility complex (MHC) molecules. During their development in the thymus, T cells are determined to develop either into $CD8^+$ or $CD4^+$ T cells depending on the recognition of peptides presented by MHC class I or MHC class II molecules respectively (Singer et al., 2008). While $CD8^+$ T cells possess cytotoxic activity and are directly involved in the elimination of e.g. virus-infected cells, the function of $CD4^+$ T cells is to shape immune responses and to support other immune cells.

MHC class II molecules are only found on specialised antigen-presenting cell types (APCs), like macrophages, DCs and B cells. The peptides presented by MHC class II molecules derive from extracellular or membrane proteins, that have been internalized by APCs through endocytosis (Ramachandra et al., 1999). The resulting endosomes fuse with lysosomes, where the pathogens are digested. Thereby, antigenic peptides are generated which are loaded onto MHC class II molecules. Finally, the peptide-MHC class II complex is transported to the plasma membrane and displayed at the cell surface to $CD4^+$ T cells (Medd and Chain, 2000).

The antigen presentation of intracellular pathogens like viruses, but also in case of for instance transformed cells expressing aberrant, mutated proteins, is mediated by another system, the **MHC class I pathway**. For this, intracellular proteins are degraded in the cytosol and the resulting peptides are transported via TAP (transporter associated with antigen processing) into the lumen of the ER, where they are bound to MHC class I molecules. Thus peptide-MHC class I complexes are presented on the cell surface for detection by the immune system (Goldberg and Rock, 1992; Rock and Goldberg, 1999).

The TAP transporter is a heterodimeric ABC transporter composed of the subunits TAP1 and TAP2 (Spies et al., 1992). The TAP1 and TAP2 genes are inducible by IFNγ and encoded within the MHC class II gene locus. Peptide binding is mediated by both subunits and upon an ATP-dependent change in conformation the peptide is translocated through the ER membrane (Neumann and Tampé, 1999). The binding preferences of TAP have a selective influence on the availability of antigenic peptides in the ER for loading on MHC class I molecules (Neefjes et al., 1995; Van Endert et al., 1995). TAP prefers the transport of peptides with a length of 8 to 16 amino acids and with a hydrophobic or basic C-terminus, which indeed correlates with peptide binding to MHC class I complexes.

The MHC class I molecule is a transmembrane glycoprotein which is constituted by the non-covalent association of heavy α-chain and $\beta_2$microglobulin (β_2m). Its expression is also induced by IFNγ in all

cell types with few exceptions. As mentioned, MHC class I molecules prefer the binding to peptides with basic C-terminus comprising 8 to 10 amino acids (Falk and Rötzschke, 1993; Rammensee et al., 1993). The peptide binding groove of MHC class I is encoded within a highly polymorphic gene cluster, in humans referred to as human leukocyte antigen (HLA) complex (Geraghty et al., 2002). The classical human MHC class I genes are HLA-A, -B and –C. Thereby, MHC molecules gain highly variable binding specificities and thus provide the specificity for efficient T cell responses.

Peptide loading on MHC class I is carried out in association with TAP and takes place within a peptide loading complex (PLC) under the assistance of several chaperones like calnexin, calreticulin and tapasin. Notably, tapasin provides direct proximity to TAP thereby building a bridge between MHC class I and TAP. After binding of an antigenic peptide, the fully folded MHC class I complex dissociates from the PLC and subsequently leaves the ER. Only by peptide binding MHC class I acquires stability and can be transported to the cell surface. In case of TAP deficiency MHC class I surface expression is strongly reduced due to defective assembly, transport and consequently cytosolic degradation of MHC class I molecules (van Kaer et al., 1992). In uninfected cells, retention of empty MHC class I molecules in the ER by tapasin provides MHC class I in a surplus to antigenic peptides, so that MHC class I molecules are immediately available for peptide loading upon an immunological challenge (Schoenhals et al., 1999). In figure 1.3 the MHC class I antigen presentation pathway is summarized.

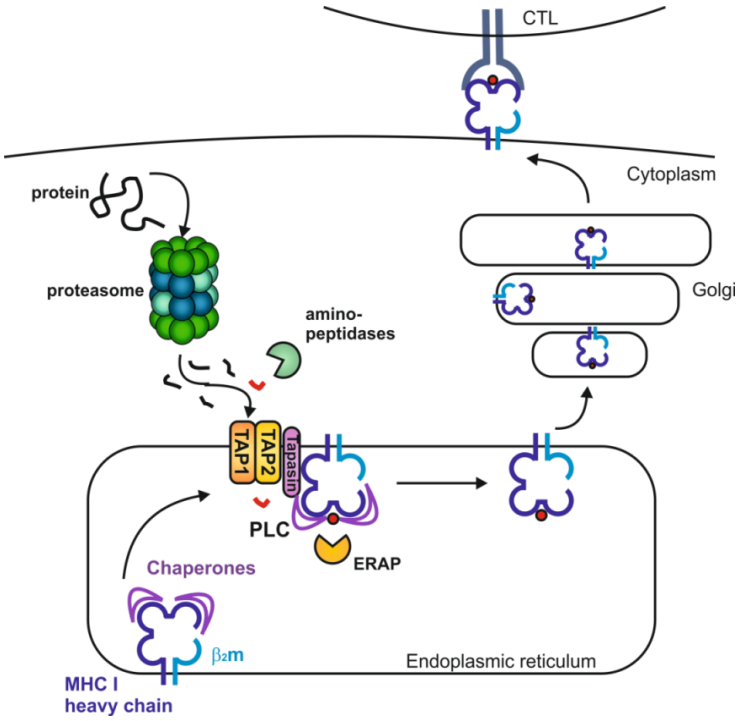

Figure 1.3 The MHC class I antigen presentation pathway. In a first step pathogens are degraded in the cytosol by a multicatalytic enzyme complex, the proteasome. Generated peptides can be further trimmed by cytosolic aminopeptidases or are transported directly via TAP into the ER lumen. Assembly of MHC class I molecules occurs inside the ER with the help of chaperones. Upon binding of β_2m the peptide loading complex (PLC) assembles including tapasin which provides proximity to TAP, so that transported peptides can be loaded directly on MHC class I molecules. At the same time further trimming by aminopeptidases like the ER-resident aminopeptidase (ERAP) can take place. Finally, the peptide-MHC class I complex is transported via the Golgi apparatus to the cell surface where it is presented to cytotoxic T cells (CTLs).

After transport through the Golgi apparatus and trans-Golgi network to the cell surface peptide-MHC class I complexes are recognized by the TCR of $CD8^+$ T cells. With support of costimulatory interactions by professional APCs, $CD8^+$ T cells differentiate into effector T cells, called cytotoxic T lymphocytes (CTLs). CTLs eliminate virus-infected cells by several mechanisms. Firstly, they release lytic granules which contain cytotoxic proteins like perforin and granzyme. Furthermore, CTLs express Fas ligand (Fas L) which binds to Fas on target cells thereby activating caspases (Henkart, 1994). Finally, they secret numerous cytokines like IFNγ, IL12, TNFα and TNFβ (Callan et al., 2000).

A central question in this thesis was how viral antigenic peptides for loading on MHC class I molecules are generated? Like displayed in figure 1.3 the degradation of intracellular pathogens in the cytosol is mediated by a multicatalytic protease complex, the proteasome. The generation of peptides with an appropriate size for transport by TAP and loading on MHC class I molecules requires degradation by the proteasome (Kloetzel, 2001; Reits et al., 2000), which was also shown by the inhibition of proteasome activity resulting in abolished MHC class I antigen presentation (Benham and Neefjes, 1997; Rock et al., 1994). Proteasomes generate peptides of 8 to 10 amino acids in length, which is a suited size for binding to MHC class I molecules and they preferentially cleave at the carboxyl terminus after hydrophobic or basic residues thereby generating the C-terminal anchor residue of MHC class I ligands. In conclusion, peptides released by the proteasome exhibit TAP and MHC class I binding preferences (Van Endert et al., 1995). To improve the generation of MHC class I ligands the immunoproteasome (i-proteasome), an isoform of the proteasome, has evolved. Likewise TAP and MHC class I chains also the subunits of the i-proteasome are encoded within the MHC gene locus and are inducible by IFNγ. The role of the i-proteasome during the presentation of certain viral epitopes was thoroughly studied within this thesis and will be described in detail in the following chapters.

Cross-presentation Before focusing on the proteasome and its role during virus infection another mechanism of antigen presentation which is of particular importance during viral infection shall be mentioned. Because most viruses infect other cells than professional APCs, like for example epithelial cells of the lung, there must exist pathways to deliver intracellular pathogens into APCs. Any infected cell can present antigens via MHC class I complexes, but due to the lack of costimulatory molecules on their surface they are not capable of priming naïve $CD8^+$ T cells. Professional APCs, like DCs and macrophages, possess the unique ability to present not only endogenous but also external antigens on MHC class I molecules, in a process called cross-presentation (Heath et al., 2004). They take up infected or dying cells by endocytosis. The endosome that forms fuses with a lysosome and degradation is initiated. Somehow, by a yet unknown process antigens pass into the cytosol where they are degraded by proteasomes. The resulting antigenic peptides are transported by TAP into the ER, where they are loaded on MHC class I molecules (Cresswell et al., 2005). A second possible pathway, called the vacuolar pathway, does not involve degradation by the proteasome and TAP transport. Instead, MHC class I molecules enter the phagosome and peptide loading occurs there (Rock et al., 2010). As described above, peptide-MHC class I complexes are subsequently displayed at the cell surface and along with surface expression of costimulatory molecules an efficient triggering of $CD8^+$ T cells to differentiate into cytotoxic T lymphocytes is possible.

1.3 Ubiquitin proteasome system

In 2004 Aaron Ciechanover, Avram Hershko and Irwin A. Rose were awarded with the Nobel Prize in Chemistry for their discovery of controlled ubiquitin-mediated protein degradation via the ubiquitin proteasome system (UPS) (Giles, 2004). The proteasome represents a complex, high molecular protease with multicatalytic activity (Tanaka, 2009) and is responsible for the major part of non-lysosomal protein degradation in eukaryotic cells of proteins in the cytosol, the nucleus and the ER (Wójcik and DeMartino, 2003). Proteasomes constitute up to 1% of the soluble protein content of a cell (Tanaka et al., 1986). This high concentration, as also determined by Kuehn and colleagues with 1 to 20 µg/mg of soluble protein in rat cell extracts (Kuehn et al., 1986), underlines the major role of the proteasome in protein degradation providing the continuous turnover of proteins and protection of cells from toxic accumulation of defect and aberrant proteins (Rock et al., 1994).

Besides the generation of the majority of MHC class I peptides (Goldberg et al., 2002; Goldberg and Rock, 1992; Kloetzel, 2004; Rock et al., 1994) the UPS fulfills several general biological functions. Ubiquitin-mediated proteasomal degradation of proteins is an essential mechanism for the regulation of numerous important cellular processes like transcription, cell cycle, cell differentiation, regulation of apoptosis or cellular stress response (Coux et al., 1996; Glickman and Ciechanover, 2002). For example, progression of the cell cycle is controlled through selective degradation of cyclins (Hershko et al., 1991). Via control of levels of transcription factors gene transcription is affected (Collins and Tansey, 2006), which is described for example for the processing and activation of NFκB (Palombella et al., 1994). Likewise, the UPS is involved in signal transduction (Taylor and Jobin, 2005), cell proliferation and apoptosis (Naujokat and Hoffmann, 2002). Further, proteasomal degradation is involved in the embryogenesis of *Caenorhabditis elegans* (Bowerman and Kurz, 2006) as well as in fertilization and gametogenesis in general (Karabinova et al., 2011; Sakai et al., 2004).

In particular, the UPS plays a central role in maintaining the protein homeostasis of cells (Goldberg, 2007). During protein synthesis a large fraction of newly synthesized proteins exhibits defects due to errors in transcription, translation or misfolding. More than 30% of the newly synthesized proteins in a cell are thought to end up as so-called defective ribosomal products (DRiPs) (Qian et al., 2006; Schubert et al., 2000). The UPS preserves cell viability by preventing accumulation of these irreversibly damaged and potentially toxic proteins (Seifert et al., 2010; Szeto et al., 2006). Recently discovered special adaptations of the UPS to situations of enhanced protein synthesis such as virus infection and oxidative stress causing an increase of oxidatively damaged DRiPs were also of major importance for the investigations in this thesis and will be discussed more detailed in chapter 1.4.3.

Further, membrane and secreted proteins which are generated inside the lumen of the ER are subjected to quality control by the ER-associated degradation (ERAD) system. Because their degradation is mediated in the cytosol as well, these proteins are transferred by retrograde translocation to the cytosol where their proteasomal degradation takes place (Smith et al., 2011).

Defects in the UPS result in severe disturbance of protein homeostasis and can cause diverse malignant diseases such as autoimmune diseases, viral infections, chronic inflammation, cancer, muscle

degradation (cachexia) or neurodegenerative diseases (Dahlmann, 2007; Golab et al., 2004; Wang and Maldonado, 2006). Further, a correlation between age and change of proteasome activity is reported (Keller et al., 2004).

The required specificity to fulfil such manifold functions is mediated by the small molecule ubiquitin (ub). Covalent labelling of protein substrates with ub delivers the protein to proteolytic degradation by the 26S proteasome (Weissman, 2001). This posttranslational modification (PTM) is carried out in an ATP-dependent enzyme cascade, in a process called ubiquitylation (Pickart and Eddins, 2004), which will be described in the following paragraphs.

1.3.1 The Ubiquitylation cascade

Ubiquitin was first isolated by Gideon Goldstein and colleagues in 1975 (Goldstein et al., 1975) and represents a highly conserved small ubiquitous protein of 76Aa (8.6 kDa) which can be found in the cytoplasm and nucleus of all eukaryotic cells (Wilkinson et al., 1980). The major function of a post-translational modification with ub is the regulated degradation of protein substrates (Ciechanover et al., 1984; Hershko et al., 1980; Hough et al., 1986; Wilkinson et al., 1980). In mammalia, ubiquitin is encoded by four ub genes which express ubiquitin either as poly-ubiquitin (poly-ub) in tandem repeats or as fusionprotein with ribosomal subunits (Baker and Board, 1987; Kimura and Tanaka, 2010; Ozkaynak et al., 1987; Wiborg et al., 1985). Special proteases, so called deubiquitylating enzymes (DUBs), cleave poly-ub into single ub molecules (Reyes-Turcu and Wilkinson, 2009), which makes them thereby available for ubiquitylation to protein substrates. Further functions of DUBs will be described later.

Ubiquitylation The carboxyl group of the C-terminal glycine of the ub molecule is linked to an ε-amino group of a lysine residue of the target protein via an isopeptide bond. Connection of the single ubiquitin moieties within the poly-ub chain occurs in the same way. The process of ubiquitylation is carried out in a three step enzyme cascade (figure 1.4) by the interaction of three enzymes: E1 ub-activating enzyme, E2 ub-conjugating enzyme and E3 ub-protein ligase (Hershko and Ciechanover, 1998). The cascade is initiated with the ATP-dependent activation of ubiquitin by an E1. Thereby, a thioester bond between the cysteine in the active centre of the E1 and the carboxy terminus of ub is generated forming an E1-ub-conjugate. Subsequently, ub is transferred to a cysteine residue in the active centre of an E2 again via thioester bond. The E2 enzyme conveys already specificity regarding ub linkage control and selection of the E3. Finally, E2 and E3 associate so that an isopeptide bond between the C-terminal Gly76 of ubiquitin and an ε-amino group of a lysine residue within the substrate bound to the E3 can be established (Hershko et al., 1983). This process is repeated several times building an ub chain (Li et al., 2007). Alternatively, the whole ub chain can be pre-assembled while bound to the E2 and is later transferred en bloc to the substrate. In humans two E1 enzymes (Haas et al., 1982; Jin et al., 2007), around 35 E2s (van Wijk and Timmers, 2010) and several hundred E3s (Pickart and Eddins, 2004) are described. The E3 enzymes confer substrate recognition,

recruitment of the E2 and transfer of ub from the E2 to the substrate. In conclusion, substrate specificity is given by the selection of different E2 and E3 enzymes.

E3 ligases can be grouped into two classes based on their catalysis mechanism: HECT domain (homologous to E6-AP carboxyl terminus) and RING (really interesting new gene)/U-Box domain (UFD2 homology) E3 enzymes. While HECT domain ligases bind ub via a thioester bond to a cysteine in their active centre in order to transfer ub in the next step to the substrate, RING domain E3s only function as platform to bring substrate and E2 in contact. RING domain ligases also possess several cysteine and histidine residues which coordinate two zinc ions to establish the conformation of the enzyme, which is important for the binding of the E2. Consequently, ub is directly transferred to lysine residues of the substrate (figure 1.4) (Ardley and Robinson, 2005).

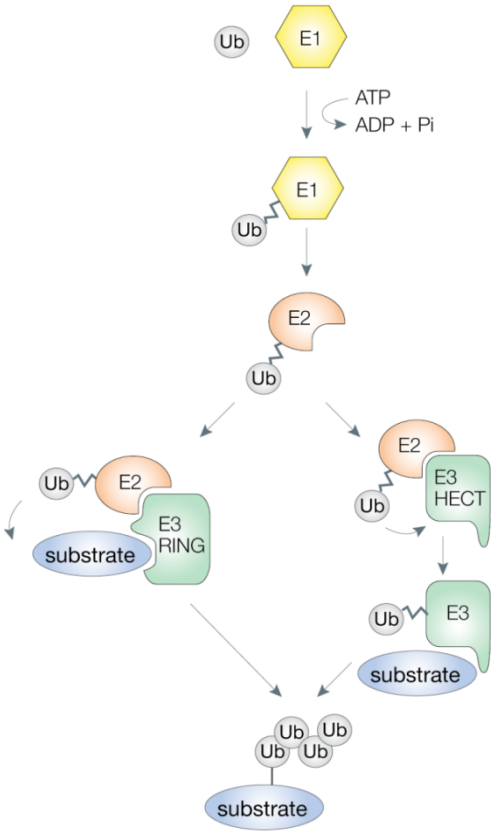

Figure 1.4 The ubiquitylation cascade. The process of ubiquitylation is initiated with the ATP-dependent activation of ubiquitin (ub) by an ub-activating enzyme (E1). Thereby, a thioester bond between E1 and ub is generated forming an E1-ub-conjugate. Subsequently, ub is transferred to an ub-conjugating enzyme (E2). Finally, E2 associates with an ub-protein ligase (E3) which conveys substrate specificity. The E3 establishes an isopeptide bond between ub and a lysine residue of the substrate bound to the E3. Based on the catalytic mechanism two classes of E3s are differentiated. HECT domain ligases bind ub via a thioester bond and transfer ub in a second step to the substrate. RING E3s only function as platform and ub is directly transferred to a lysine residue of the substrate. Adapted from (Woelk et al., 2007).

Substrate recognition Substrates for ubiquitylation are recognised through specific sequence motifs (Wilkinson, 2000). For example, the PEST sequence which is rich in proline, glutamine, serine and threonine (PEST). Marchal and colleagues proposed that phosphorylation within the PEST sequence could enhance or inhibit ubiquitylation of nearby lysine residues of mostly short lived proteins (Marchal et al., 2000). Further, the N-end rule indicates that destabilising amino acids like arginine, lysine, phenylalanine or tryptophan at the N-terminus of proteins could trigger ub-mediated degradation. Notably, other substrate-specific amino acid sequences were identified as ubiquitylation signals. Moreover, hydrophobic areas at the surface of proteins which indicate misfolding or dissociation of protein complexes can initiate ubiquitylation (Wilkinson, 2000). Further, misfolded proteins are targeted for pro-

teasomal degradation with the help of chaperones. If the chaperone-mediated refolding of a damaged protein fails and the native state of a protein is unattainable, an interaction of E3 ligases with chaperones is thought to selectively target irreversibly misfolded proteins to proteasomal degradation, so that the recognition of the substrate is in fact mediated by chaperones (Kriegenburg et al., 2012).

Forms of ubiquitylation The ubiquitin molecule exhibits seven lysine residues: Lys6, Lys11, Lys27, Lys29, Lys33, Lys48 and Lys63, all of which can be used for linkage (figure 1.5). Of major importance is the generation of ub chains linked via Lys48 which labels proteins for degradation by the 26S proteasome (Chau et al., 1989). Thereby, a minimum length of four ub moieties is required for efficient targeting to proteasomal degradation (Thrower et al., 2000). Besides linkage via Lys48 several kinds of ub chains can be assembled through connection of different lysine residues. The topology of an ub chain, i.e. length and linkage type, conveys different functions (Komander, 2009) (figure 1.5). Post-translational modification with just one ub moiety, called mono-ubiquitylation, was shown to play a role in signalling during virus budding (Patnaik et al., 2000), histone regulation and DNA repair (Bergink et al., 2006; Hoege et al., 2002). A linkage of single ubs to several different lysine residues of one protein is called multi-ubiquitylation and was shown, for example, to be involved in endocytosis of receptor tyrosine kinases (Haglund et al., 2003).

Ubiquitylation via Lys63 mostly does not lead to proteasomal degradation, but plays a role in DNA repair, signalling cascades or labels proteins for lysosomal degradation (Spence et al., 1995). The formation of Lys63-linked ub chains by E3 ligase TRAF6 is an essential step in the signalling pathway leading to activation of NFκB (Deng et al., 2000; Skaug et al., 2009). Notably, ubiquitylation via Lys11 was shown to be connected to ER-associated protein degradation (ERAD) and perhaps also to cell cycle regulation (Xu et al., 2009). Lys29- and Lys33-linked ub chains were described to play a role in the regulation of kinase activity (Al-hakim et al., 2008). However, in some cases also proteins labelled with Lys11-, Lys29- or Lys63-linked ub chains can be degraded by the proteasome (Jin et al., 2008; Kim et al., 2007; Saeki et al., 2009; Xu et al., 2009). Branched ub chains which are generated by connection of ub moieties via different lysine residues poorly bind to the 26S proteasome (Kim et al., 2009). One function of branched ub chains was described by Boname and colleagues in 2010, the viral E3 ligase K3 produces branched Lys11-Lys63-linked ub chains at the cytosolic tail of MHC class I molecules thereby triggering their endocytosis (Boname et al., 2010). Forms and functions of ubiquitylation are summarised in figure 1.5.

Ubiquitin-like modifiers Numerous structurally homologous proteins to ubiquitin have been described up to date. Several so called ubiquitin-like modifiers are known, such as SUMO, NEDD8, ISG15 or FAT10. The ub-like modifiers are similarly added as posttranslational modification to specific recognition sequences on proteins in a three step enzyme cascade (Schwartz and Hochstrasser, 2003).

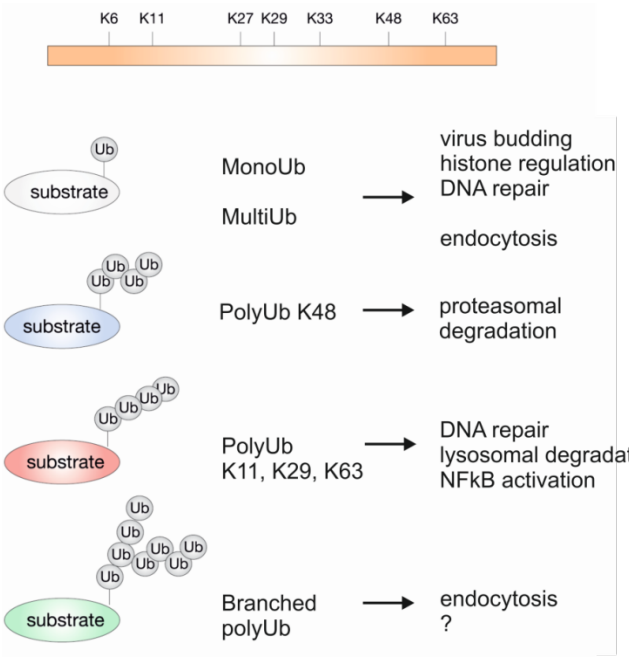

Figure 1.5 Forms of Ubiquitylation. The ub molecule exhibits seven lysine residues: K6, K11, K27, K29 K33, K48 and K63, all of which can be used for linkage. Ubiquitylation with just one ub moiety is called mono-ubiquitylation and has been shown to fulfil signalling functions during virus budding, histone regulation and DNA repair. Linkage of several single ub moieties to one substrate, called multi-ubiquitylation, is involved in endocytosis. Ub chains linked via K48 deliver substrate proteins to degradation by the 26S proteasome. Poly-ubiquitylation via the lysine residues K11, K29, K63 was shown to play a role in DNA repair, targeting of proteins for lysosomal degradation or in signalling pathways such as NFκB activation. Branched ub chains were proposed to trigger endocytosis. Modified from (Woelk et al., 2007).

Deubiquitylation enzymes (DUBs) cleave the isopeptide bond between ub and its substrate protein, but also between single ub moieties. Thereby DUBs either sequentially cleave off single ub moieties, parts of an ub chain or entire ub chains in one step. Around 80 DUBs are known, for specific linkage types and substrates specific DUBs exist. Further, specific DUBs antagonise specific E3 ligases regulating substrate degradation and activity, respectively (Komander, 2009). Thus, DUBs fulfil manifold functions, for example they cleave ub from its precursor and help to recycle ub.

1.3.2 Structure and assembly of the proteasome

Representing a high molecular, multicatayltic protease the proteasome is characterised by a complex structure displayed in figure 1.6. The 20S core of the proteasome which comprises 670 kDa represents a cylindric, barrel-like structure. The 26S proteasome spanning approximately 2.5 MDa consists of 20S core and an additional 19S regulatory particle of 700kDa (see chapter 1.3.3.) (Tanaka, 2009). The core is constituted of four stacked heptameric rings created by the assembly of 28 homolog but different subunits which range in size from 21 to 31 kDa (Baumeister et al., 1998; Coux et al., 1996). In eukaryotes, the two outer rings are composed of seven α-subunits, α1 to α7, which control the access to the catalytic chamber and interact with the regulators (Groll et al., 1997). The two inner rings are formed by seven β-subunits, β1 to β7, which build the catalytic chamber of the proteasome. Three of them, namely β1, β2 and β5, harbour the all in all six active sites of the proteasome (figure 1.6).

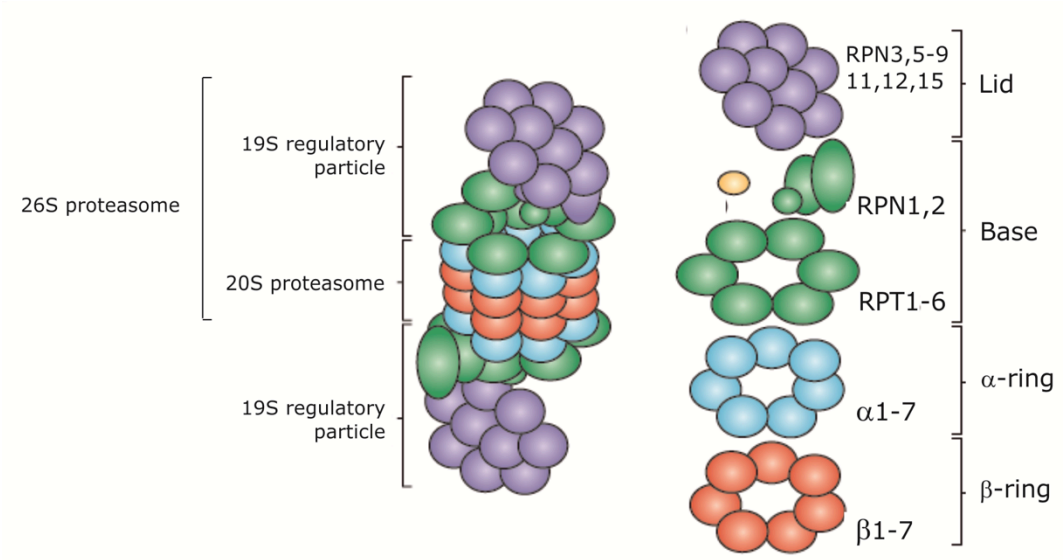

Figure 1.6 The Structure of the proteasome. The 26S proteasome is composed of two subcomplexes: the 19S regulatory complex and the 20S core proteasome. The 20S core consists of four stacked heptameric rings. The two outer rings are composed of seven homolog but different α-subunits, α1 to α7. They control the access to the catalytical chamber and interact with regulators. The two inner rings are formed of seven β-subunits, β1 to β7, which build the catalytic chamber of the proteasome. The 19S regulator is further composed of two subcomplexes: base and lid. The base caps the α-ring and is composed of six ATPase subunits, Rpt1 to 6, and two Rpn subunits, Rpn1 and 2. The lid consists of up to ten non-ATPase Rpn subunits. Modified from (Murata et al., 2009).

In order to control the access to the catalytic chamber the N-terminal tails of the seven α-subunits close the chamber under normal conditions (Groll et al., 2000; Groll et al., 1997; Unno et al., 2002). Groll and colleagues could show that a deletion of the N-termini opens the channel to the core particle (Groll et al., 2000). The group further argued that the 20S proteasome alone without binding of regulatory particles has no proteolytic activity *in vivo* because the access to the inner, catalytical β-subunits is blocked (Groll et al., 2000). Thus, opening of the gate is controlled by additional protein complexes which bind to the α-rings and induce a conformational change to the N-termini of the α-subunits (see chapter 1.3.3). The gating process also protects cells from uncontrolled proteolysis.

Belonging to the family of aminoterminal nucleophile (Ntn) hydrolases the catalytical active subunits of the proteasome β1, β2 and β5 are characterised by N-terminal threonine which protruds into the catalytic chamber and mediates the nucleophilic attack of peptide bonds (Bochtler et al., 1999). Peptide bonds are cleaved at the C-terminus of acidic, neutral or hydrophobic amino acids (Tanaka, 2009). According to their cleavage specificities the three catalytical β-subunits are distinguished: β1 caspase-like activity (cleavage after acidic amino acids), β2 trypsin-like (cleavage after basic amino acids) and β5 chymotrypsin-like (cleavage after hydrophobic amino acids) (Cardozo, 1993; Dahlmann et al., 1986; Dick et al., 1998; Orlowski and Wilk, 2000).

In mammalian, besides the mentioned standard subunits β1, β2, β5 specialised immunosubunits (i-subunits) β1i, β2i, β5i have evolved which are expressed for example after IFNγ stimulation. These i-

subunits are incorporated into nascent 20S proteasomes replacing the constitutive standard subunits in order to form i-proteasomes (Groettrup et al., 1996b; Kloetzel, 2004). In chapter 1.4 the functions and relevance of i-proteasomes will be described in detail.

The biogenesis of the proteasome in mammalian cells is a highly regulated process which comprises the biosynthesis of all subunits, their assembly and maturation. The first step during de novo synthesis of proteasomes is the expression of all 14 α- and β-subunits of the 20S core complex. These subunits are expressed as proforms with N-terminal elongation, called precursors. The heptameric α-ring assembles with the help of the heterodimeric proteasome assembly chaperones Pac1/2 and Pac3/4. Fricke and colleagues found in 2007 that main steps of the 20S proteasome biogenesis take place at the ER membrane mediated by the proteasome maturation protein (POMP) which interacts with ER membranes (Fricke et al., 2007). Further, POMP regulates the recruitment of β-subunits to the α-ring which serves as matrix for their attachment (Burri et al., 2000; Witt et al., 2000). After stepwise binding of all β-subunits a half-proteasome consisting of one α- and one β-ring is formed (Frentzel et al., 1994; Hirano et al., 2008; Nandi et al., 1997). Subsequently, two half-proteasomes come together to form an intermediate before the processing of the precursors is carried out. The catalytical active β-subunits β1, β2 and β5 cleave off their prosequence in an autocatalytic process and subsequently mature the adjacent, inactive subunits. Only after the last maturation step is completed the proteasome becomes active (Kruger et al., 2001) and degrades its first substrates represented by POMP and PAC1/2 (Hirano et al., 2005; Hirano et al., 2008; Ramos et al., 1998; Witt et al., 2000).

1.3.3 Regulators of the proteasome

Binding of regulatory complexes to the 20S core complex can influence proteasomal activity and substrate selection. While the 20S proteasome is able to degrade substrates alone (Coffino, 2001), association with different regulatory complexes occurs (Kloetzel, 2001). So far, three different regulators which bind to the outer α-rings of the 20S core complex are known: 19S, PA28α/β and PA28γ.

Proteasomal activity of 19S-bound proteasome is dependent on ATP and ub, while binding of PA28α/β and PA28γ to the 20S leaves proteasomal degradation ATP- and ub-independent. Further, also the degradation of unlabelled proteins by the 20S proteasome is independent of ATP. Moreover, the 26S proteasome can degrade substrates independent of ub, for example proteasomal degradation of ornithin-decarboxylase which is mediated by antizym (Murakami et al., 1992; Zhang et al., 2003).

The 19S regulator, which is also known as PA700, binds to 20S and activates the core particle to degrade poly-ubiquitylated proteins. Therefore, 19S mediates the binding, deubiquitylation, unfolding and translocation of substrates into the catalytic chamber in an ATP-dependent manner (Groll et al., 1997). The 19S is characterised by a complex structure composed of approximately 20 subunits which are arranged in two subcomplexes, namely base and lid (Ferrell et al., 2000; Glickman et al., 1998) (figure 1.6). The base caps the α-ring and is composed of six different ATPases of the AAA^+ family

(Rpt1 to 6) and two Rpn subunits (Rpn1 and Rpn2) which mediate substrate unfolding and gate opening in an ATP–dependent manner (Glickman et al., 1999). The lid is constituted of up to ten non-ATPase subunits which mediate the recognition and binding of poly-ubiquitylated protein substrates (Pickart 2001). The 20S proteasome can be associated with one or two 19S regulators forming the 26S or 30S proteasome, respectively.

Another regulatory particle is represented by the **proteasome activator 28** (PA28), also called 11S, which can also induce gate opening and activation of the 20S core complex (Stohwasser et al., 2000). PA28 is composed of seven alternating nonATPase PA28α and β subunits or PA28γ subunits in heptameric rings (Zhang et al., 1999). While PA28α/β is mainly found in the cytoplasm, PA28γ localises predominantly to the nucleus (Wójcik et al., 1998). PA28 does not bind to ubiquitylated subtrates and further does not mediate the degradation of large substrates (Whitby et al., 2000). The expression of the PA28α and β subunits is induced by IFNγ signalling and a role for PA28α/β in the processing of antigenic peptides for MHC class I antigen presentation is described (Kloetzel, 2001), while the mechanisms remain largely unknown.

Further complexity is given by the fact that IFNγ stimulation of Hela cells induces besides PA28α/β-20S proteasome also the formation of PA28α/β-20S-19S proteasome (Tanahashi et al., 2000). While 19S can bind to one side PA28α/β or PA28γ can bind to the other side forming a **hybrid proteasome** which is supposed to enhance the effectivity of degradation of ubiquitylated substrates (Hendil et al., 1998). Hybrid proteasome is reported to be more active than 26S and to generate a different peptide pool (Cascio et al., 2002). Thereby, the binding of PA28α/β has no direct effect on the active sites of the 20S core but the association to the outer α-rings triggers the N-terminal tails of the α-subunits to flip upwards and open the gate. Consequently, substrate entry as well as product exit are facilitated, which might support the release of longer, N-terminally-elongated peptides in order to fuel the MHC class I antigen presentation pathway (Sijts and Kloetzel, 2011). A task that the 19S regulator could probably fulfil alone and the special role of PA28 still needs to be elucidated.

1.4 Immunoproteasome

Apart from the constitutive standard proteasomes (s-proteasome) different isoforms of the proteasome are described. Accordingly, proteasomes form a heterogeneous population of enzyme complexes in the cell (Tanaka, 2009). The appearance of a certain isoform in immune cells and immune tissue led to the designation immunoproteasome (i-proteasome), which was introduced firstly in 1994 by Aki and colleagues (Aki et al., 1994).

While the s-proteasome occurs in all cell types, the i-proteasome is constitutively expressed in immune relevant cells and formed upon exposure to interferons and certain cytokines (Groettrup et al., 1996b; Shin et al., 2006). Predominantly IFNγ induces the expression of specialised i-subunits, β1i (also known as Lmp2), β2i (Mecl-1) and β5i (Lmp7), which replace the catalytical active standard sub-

units β1, β2 and β5, respectively. The i-subunits are incorporated into newly assembled proteasome complexes thereby forming the i-proteasome (figure 1.7).

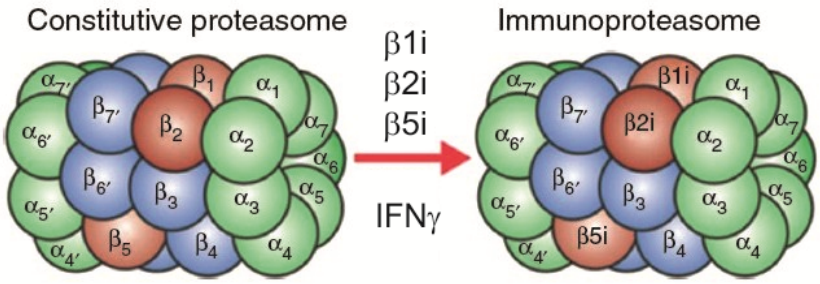

Figure 1.7 Formation of the i-proteasome. Upon certain stimuli, e.g. IFNγ signalling, the expression of the i-subunits β1i, β2i and β5i is induced leading to the formation of i-proteasomes. Adapted from (Strehl et al., 2005).

While all other proteasome genes are dispersed throughout the genome, β1i and β5i are encoded in the MHC class II region on chromosome six directly upstream of the TAP1 and TAP2 genes (Rock and Goldberg, 1999). The third i-subunit β2i was discovered later, in 1996, and is encoded on chromosome 16 (Groettrup et al., 1996a; Nandi et al., 1996).

A basal expression level of i-subunits was found in lymphoid tissue such as thymus, spleen and lymph nodes, the highest i-proteasome activity was measured in spleen (Noda et al., 2000). Moreover, also spleen of IFNγ-deficient mice was shown to exhibit similar levels of i-proteasome expression in comparison to wild type mice (Barton et al., 2002) which shows that i-proteasome abundance in lymphoid tissue is independent of further stimuli. The cells concerned in these tissues are professional APCs. Especially immature DCs exhibit high levels of i-subunit expression (Li et al., 2001; Macagno et al., 1999), further macrophages (Basler et al., 2004), B cells (Hensley et al., 2010) and T cells (Ossendorp et al., 2005).

The expression of i-subunits in non-lymphoid tissue is rather low (Murata et al., 2007). Most non-immune cells induce the formation of i-proteasomes upon an immunological challenge. In tissue culture a treatment with type I and II interferons or pro-inflammatory cytokines like TNFα up-regulates the expression of i-subunits. *In vivo* during infection with lymphocytic choriomeningitis virus (LCMV) or *Listeria monocytogenes* an exchange of the catalytical subunits has been observed in mice (Khan et al., 2001b; Strehl et al., 2006). After fungal infection with *Histoplasma capsulatum* the exchange of i-subunits was shown to be dependent on IFNγ signalling (Barton et al., 2002). While during Hepatitis C virus (HCV) infection in chimpanzees an increase of i-subunit expression in the inflamed liver was measured before IFNγ signalling occurred and coincided with the type I interferon response (Shin et al., 2006). In conclusion, in the very early stage of infection pro-inflammatory cytokines and type I interferons contribute to the formation of i-proteasome in the inflamed tissue, while later IFNγ re-

leased by NK and T cells which arrive one to several days later at the site of infection further induces the expression of i-subunits.

Though the i-proteasome represents the predominant proteasome type in lymphoid tissue, constitutive proteasomes are never replaced completely (Macagno et al., 1999). Instead, the expression of i-proteasome in non-lymphoid tissue after infection rises only slightly above 60% of the whole proteasome population (Strehl et al., 2006). Moreover, the i-proteasome is characterised by a shorter half-life of around 27 hours compared to s-proteasome with a half-life of 5 days in HeLa cells (Heink et al., 2005).

Notably, another isoform of the proteasome which is exclusively expressed in cortical thymic epithelial cells is known as the thymoproteasome. Thymoproteasomes are characterized by the incorporation of a β5t subunit, which displays a high homology to β5i, and are required during the development and positive selection of $CD8^+$ T cells in the thymus (Tomaru et al., 2009).

Moreover, mixed-type proteasomes occur when only one or two of the three catalytical β-subunits are exchanged so that proteasome complexes containing constitutive as well as i-subunits are formed (Dahlmann et al., 2000; Griffin et al., 1998).

1.4.1 Generation of MHC class I ligands

The high expression level of i-proteasomes in DCs as well as the induction of i-proteasome formation during an infection suggested a functional role for the i-proteasome during the epitope generation for MHC class I antigen presentation to cytotoxic T lymphocytes. Both, s-proteasome as well as i-proteasome, are able to generate MHC class I ligands as part of the adaptive immune response (see chapter 1.2.2), but in most instances the i-proteasome was shown to generate antigenic peptides more efficiently and at a higher rate (Sijts and Kloetzel, 2011).

First evidence for a role of the i-proteasome in epitope generation derives from *in vitro* digestion studies with β1i/β5i-containing proteasomes which generated a qualitatively and quantitatively altered set of peptides from a synthetic 25-mer polypeptide containing an immunodominant epitope of the MCMV pp89 protein (Boes et al., 1994). Further groups have confirmed altered cleavage site preferences of i-proteasomes compared to s-proteasomes (Driscoll et al., 1993; Gaczynska et al., 1993; Kuckelkorn et al., 1995; Toes et al., 2001; Ustrell et al., 1995).

In vitro experiments as well as *in vivo* mice studies underline a major role for i-proteasomes during an immune response. Altered MHC class I expression and T cell responses were observed in β1i/β5i-deficient mice already in 1994 (Fehling et al., 1994; van Kaer et al., 1994). I-proteasome deficiency was shown to impair the presentation of bacteria- as well as virus-derived epitopes to $CD8^+$ T cells (Cerundolo et al., 1995; Sibille et al., 1995). For example, in cell culture it was shown in HeLa cells infected with a Vaccinia virus expressing the Hepatitis B virus (HBV) core antigen that the efficient liberation and presentation of the $HBVcAg_{141\text{-}151}$ epitope essentially required stimulation of the cells with IFNγ and formation of i-proteasomes (Sijts et al., 2000a). During *Listeria monocytogenes* infec-

tion β5i-deficient mice showed a delayed clearance of pathogens from liver (Strehl et al., 2006). Furthermore, in a mouse model of Coxsackievirus B3 (CVB3) infection resistance to chronic infection correlated with an early type I IFN response and the concomitant up-regulation of MHC class I pathway components and i-proteasomes (Jäkel et al., 2009). Numerous other publications have demonstrated a positive influence of i-proteasome activity on the generation of MHC class I epitopes (Schwarz et al., 2000; Sijts et al., 2000b; Tu et al., 2009).

A quantification of $CD8^+$ T cell responses to seven viral epitopes during influenza A infection revealed that i-proteasomes exert different effects on the liberation of different epitopes. $CD8^+$ T cell responses in β1i-deficient mice were dramatically reduced for two immunodominant epitopes, while the frequencies of CTLs directed against two subdominant epitopes were increased compared to wild type mice (Chen et al., 2001). Similarly, during LCMV infection in mice the presentation of a subdominant epitope was enhanced in the absence of β1i or β5i (Basler et al., 2004). Another group observed that LCMV infection was cleared with similar kinetics in β1i/β5i-deficient and wild type mice (Nussbaum et al., 2005). Consequently, i-proteasome-deficient mice also mount $CD8^+$ T cell responses though with different immunodominance hierarchies thereby affecting the fine specificity of $CD8^+$ T cell responses (Sijts and Kloetzel, 2011). These distinct efficiencies in the processing of different antigens (Kloetzel, 2001) can be explained by altered cleavage site preferences of i-proteasomes compared to s-proteasomes producing a different set of peptides which is better suited for TAP transport and MHC class I binding. Indeed, i-proteasomes tend to cleave behind residues representing the correct C-terminus of a MHC class I epitope (Strehl et al., 2008). Due to increased chymotrypsin- and trypsin-like activity and decreased caspase-like activity i-proteasomes generate peptides with either hydrophobic or basic and less acidic C-terminus more effectively (Aki et al., 1994; Dahlmann et al., 2000). Another explanation could be that i-proteasomes generate indeed a similar set of peptides compared to s-proteasomes but in higher amounts in order to counteract the destruction of released peptides by aminopeptidases (Sijts and Kloetzel, 2011).

In 2000 Sijts and colleagues transfected a mouse embryonal cell line with an inducible TET-expression system for i-subunits to analyse the influence of i-subunit exchange on the presentation of an Adenovirus E1B-derived epitope. They observed a more efficient epitope presentation in CTL assays when i-proteasomes were expressed (Sijts et al., 2000b). Later, in 2007 another group performed experiments with DCs lacking i-subunit expression and used mass spectrometry to analyse the generation of the same E1B-derived epitope. They observed that the epitope was also generated by s-proteasome only less efficiently (Deol et al., 2007). These observations suggest that i-proteasomes mostly influence the quantity of generated peptides and therefore exhibit a greater efficiency in epitope generation.

A limiting factor for the efficient generation of MHC class I ligands and subsequently the effective induction of adaptive immunity represents the availability of substrates for proteasomal degradation. According to the DRiP hypothesis the major source of proteins for the generation of antigenic peptides is represented by defective ribosomal products (Yewdell, 2007). In case of an enhanced protein synthesis rate, as it occurs for instance during viral infection, also errors in transcription, translation and

protein folding increase resulting in elevated levels of DRiPs. DRiPs are degraded faster than the native functional gene product (Reits et al., 2000; Schubert et al., 2000; Yewdell, 2002), thereby also stable viral antigens can be targeted fast and directly into the MHC class I antigen presentation pathway (Khan et al., 2001a), so that the cellular immune systems gains early access to viral proteins (Yewdell, 2005). Within the scope of this thesis a complementary mechanism to the DRiP hypothesis providing substrates for the proteasome in order to generate antigenic peptides has been found.

1.4.2 Other functions of the i-proteasome

During an inflammation process in infected tissues the signalling of pro-inflammatory cytokines induces the formation of i-proteasomes in all cells, thus, also in uninfected, adjacent cells which do not require an up-regulation of the antigen processing machinery (Krüger and Kloetzel, 2012). Only recently, research focussed on functions which i-proteasomes might fulfil apart from antigen processing. Several research groups suggested already an influence of i-proteasome expression on cytokine production or T cell differentiation, survival and function (Groettrup et al., 2010; Nussbaum et al., 2005; Yewdell, 2005).

Indeed, i-proteasomes have been shown to occur in a wide array of non-immune cells and organs. The β5i-subunit is constitutively expressed in several normal tissues, for example colon, liver or placenta. Ebstein and colleagues recently reviewed the appearance of i-proteasomes or i-subunits in non-immune cells (Ebstein et al., 2012).

Mouse models and studies with specific proteasome inhibitors have helped to understand and explore i-proteasome functions in innate immunity and non-immune processes. Several publications report a role for the i-proteasome in the regulation of T cell proliferation and differentiation (Basler et al., 2006; Moebius et al., 2010; Zaiss et al., 2008). The contribution of proteasomal degradation during cell cycle regulation is well established while a role of the i-proteasome in this process is so far unstudied. By degradation of positive as well as negative regulators of the cell cycle (Naujokat and Hoffmann, 2002) the i-proteasome might affect these processes (Ebstein et al., 2012).

Another unexpected role for i-subunits was observed in the regulation of pro-inflammatory cytokine production (Hensley et al., 2010; Muchamuel et al., 2009; Schmidt et al., 2010; Visekruna et al., 2006). It is known that the key regulator controlling the expression of pro-inflammatory cytokines NFκB is activated by proteasomal degradation of IκB, the inhibitor of NFκB. In turn, released NFκB translocates to the nucleus and induces the transcription of cytokines. I-proteasome activity might accelerate the activation of NFκB (Ebstein et al., 2009). Seifert and colleagues observed that the turnover of IκB is much higher in cells over-expressing the three i-subunits and that i-proteasomes degrade IκB faster than s-proteasomes (Seifert et al., 2010). Further, *in vivo* during CVB3 infection β5i knockout mice show an impaired activation of NFκB (Opitz et al., 2011).

In conclusion, the capacity of the i-proteasome to accelerate the turnover of poly-ub substrates not only affects the generation of epitopes for MHC class I antigen presentation but also the degradation

of critical regulators such as cyclins or IκB, thereby influencing many cellular processes such as gene transcription, signalling, cell proliferation and differentiation.

1.4.3 Oxidative stress and the i-proteasome

During an innate immune response immune cells such as phagocytes produce large amounts of reactive oxygen species (ROS) as well as reactive nitrogen species (RNS) through activation of the NADPH oxidase 2 (Nox2) and the inducible nitric oxide synthetase (iNOS). As a matter of fact, also non-immune cells exposed to cytokines produce ROS and RNS (Rada and Leto, 2008). Possible sources for the production of free radicals in other cell types are the NADPH oxidases Nox1 and Nox4 which have been shown to be involved in host defense. Upon IFNγ signaling fibroblasts and epithelial cells induce Nox1 and almost all cell types express Nox4 (Manea et al., 2010b; Orient et al., 2007).

Oxidative stress is caused because ROS and RNS, besides foreign pathogens, also attack own cellular molecules (Krüger and Kloetzel, 2012). Protein modifications through oxidative stress include amino acid carbonylation, cross-linking of disulfide bonds and cleavage of peptide backbones. Subsequently, oxidant-damaged aberrant proteins tend to aggregate in large and dynamic ub-rich cellular inclusions called aggresome-like induced structures (ALIS). Such protein aggregations occur in neurons during ageing and age-related diseases such as Alzheimer (Mishto et al., 2006), but also transiently during physiological processes in various cell types following cytokine stimulation. For example, during the maturation of DCs and macrophages following a microbial stimulus large ub-positive protein aggregates transiently accumulate which, in this case, are called dendritic cell aggresome-like induced structures (DALIS) (Lelouard et al., 2002). Moreover, stress and starvation induce ALIS in non-immune cells as it has been shown in fibroblasts (Szeto et al., 2006).

Irreversibly oxidant-damaged proteins are potentially toxic and require elimination which is mediated by autophagy or the UPS in order to preserve cell viability (Fujita and Srinivasula, 2011; Kriegenburg et al., 2011; Seifert et al., 2010; Szeto et al., 2006). The removal of oxidized proteins by proteasomes is clearly established (Davies, 2001; Grune et al., 1997). Recently, i-proteasomes have been shown to contribute to the elimination of oxidatively damaged proteins (Pickering et al., 2010) and therefore to protect cells against oxidative stress (Seifert et al., 2010), which will be discussed together with the results of this thesis in chapter 4.3.

1.5 Virus infection

During a virus infection virus particles invade living host cells and use them to replicate and to produce new virus particles. Complete virus replication may kill the infected cell, but some viruses persist in cells without fully replicating. In this latent state they can survive for long periods. Viruses are often highly adapted to the infection of their host and interfere with the host immune response at different levels. These intracellular pathogens represent an immunological challenge in which proteasomal deg-

radation and MHC class I antigen presentation to virus-specific $CD8^+$ T cells play a crucial role for clearance of infection. In this chapter the two employed virus models will be introduced.

1.5.1 Human cytomegalovirus

Human cytomegalovirus (HCMV) is a worldwide distributed virus with an increasing infection rate of approximately 50% in developed states and up to 100% in developing countries (Reddehase, 2002). Transmission occurs intrauterine or via exchange of body fluids (Pass, 1985). Therefore, blood transfusion and organ transplantation are common causes of HCMV infection (Pass, 1985). The pathology of infection is highly variable in symptoms and progress and, interestingly, shows age-dependent differences (de Jong et al., 1998). In 10% of cases, congenital infection results in severe malformation of the fetus like microcephaly, deafness, blindness, mental retardation, hepatosplenomegaly and multi organ failure (Alford et al., 1990; Jahn et al., 1988). In healthy humans, i.e. in immunocompetent individuals, a primary HCMV infection is normally asymptomatic or shows unspecific symptoms like fever (Zaia, 1990). However, in immunocompromised humans, such as recipients of transplants and bone marrow or HIV patients, HCMV infection can cause severe complications like pneumonia, hepatitis, retinitis, enteritis-colitis and neurological disorders with life threatening consequences. This shows that the course of infection is strongly dependent on the status of the immune system of the infected individual, cytomegaly represents a disease of the immunocompromised (Reddehase, 2002). Also newborns are referred to as immunological immature, since they do not possess a fully developed immune system.

HCMV belongs to the family of β-herpesviridae (Roizman and Baines, 1991) and is also known as human herpes virus 5 HHV5 (Roizman et al., 1981). In cell culture HCMV infection shows a specific cytopathic effect (CPE), which is the characteristic enlargement of infected cells (cytomegaly) with formation of typical intranuclear inclusion bodies, also referred to as 'owl's eyes' (Reddehase, 2002).

Structure HCMV is an enveloped virus with a large DNA genome and a characteristic virion structure, comprising 200 to 300nm in diameter. The virus particle consists of three main structural components: the nucleocapsid, the tegument and the envelope (figure 1.8). The nucleocapsid contains the linear doublestranded DNA and is built of capsomers forming an icosahedral protein core. Between nucleocapsid and envelope several structural proteins are embedded forming a further layer, the tegument. During infection this protein matrix, which constitutes 40% of the protein amount of the virion (Gibson, 1996), is delivered to the cytosol. Tegument proteins like the lower-matrix phosphoprotein pp65 (UL83) or the upper-matrix protein pp71 (UL82) play roles during assembly and disassembly of virus particles, but also function as immunomodulators of the host cell immune response. The viral envelope derives from the cytoplasmic membrane of the host and presents a lipid bilayer with inserted glycoproteins, e.g. gB, gH, gM and gL (Britt and Mach, 1996). These glycoproteins play a role in the attachment to host cell receptors, penetration and uptake into the cells, as well as in the transmission of viruses from cell to cell. The genome comprises 235kb and encodes for approximately 200 proteins. Thereby, the CMV genome represents the biggest genome of humanpathogenic herpes viruses

(Crough and Khanna, 2009). The laboratory strain Ad196, which was used for the infection studies described in this thesis, has been fully sequenced and encodes the information for 180 potential open reading frames (ORFs) of which the functions are not fully known yet (Jahn and Mach, 1990). In contrast to laboratory strains like the Ad169, clinical isolates have an additional 15kb fragment, comprising 22 ORFs, which code mostly for glycoproteins. This difference in the genome results in different virulence and cell tropism, since infection with Ad169 causes seroconversion but no CMV disease (Cha et al., 1996).

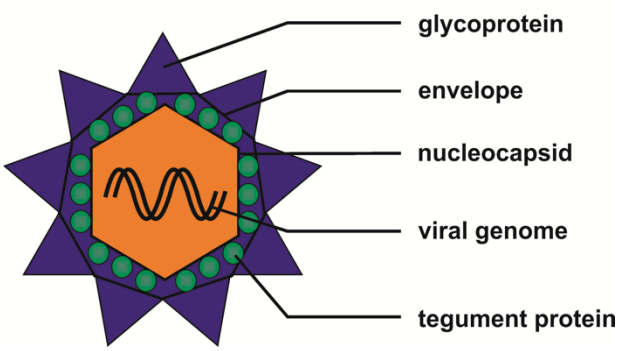

Figure 1.8 Structure of HCMV. A CMV particle consists of three structural components: envelope, tegument and nucleocapsid. The envelope is a lipid bilayer with several inserted glycoproteins. The tegument represents a protein matrix composed of several different structural proteins. The icosahedral nucleocapsid contains the dsDNA genome.

Laboratory strains versus wild type virus The wild type virus possesses the ability to infect lots of different cell types in vivo. Targets are epithelial cells, endothelial cells, smooth muscle cells and fibroblasts, but also macrophages, neutrophils and mononuclear leukocytes in peripheral blood, hepatocytes, neurons and retina cells (Gerna et al., 1992; Grefte et al., 1994). HCMV can therefore infect many different organs like brain, heart, lung, placenta and the gastrointestinal tract and occurs ubiquitiously in the organism (Sinzger et al., 1995). A possible mechanism is that infected endothelial cells may get detached from the basal lamina and circulate in the blood. In such a mechanism, infected cells eventually get trapped in the fine capillary of organs. As such, the virus may be distributed and could cause multiple organ infection (Grefte et al., 1995). Because HCMV is highly host specific, investigations in animal models are not possible. Nevertheless, several useful cell culture systems have been established to study HCMV infection *in vitro* for which mostly permissive fibroblast cell lines are employed. Consequently, laboratory strains that have been passaged over long time in fibroblasts have developed a decreased cell tropism, i.e. they have lost the ability to infect endothelial cells and are no longer human pathogenic, in contrast to less passaged clinical isolates (Quinnan et al., 1984). Genetically the loss of endothelial cell tropism might be associated to the loss of a genome region (Cha et al., 1996), which encodes a factor that is crucial for the transport of viral DNA to the host cell nucleus, since the cell tropism is not dependent on virus entry but relies on cellular transport mechanisms by which the viral DNA reaches the nucleus (Sinzger et al., 2008). Also the laboratory HCMV strain Ad169 ATCC which was employed for investigations in this thesis exhibits this characteristic.

Replication cycle HCMV infection is characterized by a slow replication cycle (Emery et al., 1999). A full infection cycle in cell culture, from adsorption of the virus to release of newly assembled virus particles, lasts 72 hours. Replication resulting in release of new virus particles occurs in epithelial cells, endothelial cells and fibroblasts (Plachter et al., 1996), while HCMV persists life long in liver, kidney

and lymphoreticulocytes, where it sporadically can be reactivated from latency (Sinclair and Sissons, 2006).

The lytic replication cycle, which is displayed in figure 1.9, begins with the adsorption of virus particles to the host cell surface which is mediated by glycoproteins (Compton, 2004). HCMV either enters the cell via the endocytotic pathway or via direct fusion of the viral envelope with the cell membrane. This process, called penetration, releases the nucleocapsid and tegument proteins into the cytoplasm of the host cell. Subsequently, the components are transported to the nucleus (Compton, 2004). The uncoating, i.e. the release of viral DNA, occurs directly into the nucleus. The expression of viral genes is coordinated in a timely cascade of three overlapping phases: immediate early (IE phase, 0 to 2h), early (E phase, up to 24h), late (L phase, after 24h) (Crough and Khanna, 2009). Despite the relatively slow replication cycle of 72h to the production of new virus particles, the expression of IE genes starts directly after virus entry and is initiated by tegument proteins. In turn these IE genes code for proteins that function as transactivators of early genes and some late genes, but also trigger expression of cellular genes. During the early phase proteins involved in viral DNA replication and repair as well as immunomodulatory gene products are synthesized. During the late phase structural proteins for the assembly of new virus particles like tegument and capsid proteins are transcribed. The assembly of the capsid and the packing of the viral DNA takes place in the nucleus. A secondary envelopment process including tegument proteins occurs at the endoplasmic reticulum Golgi intermediate compartment (ERGIC). Final envelopment and egress then releases virus particles by exocytosis at the plasma membrane.

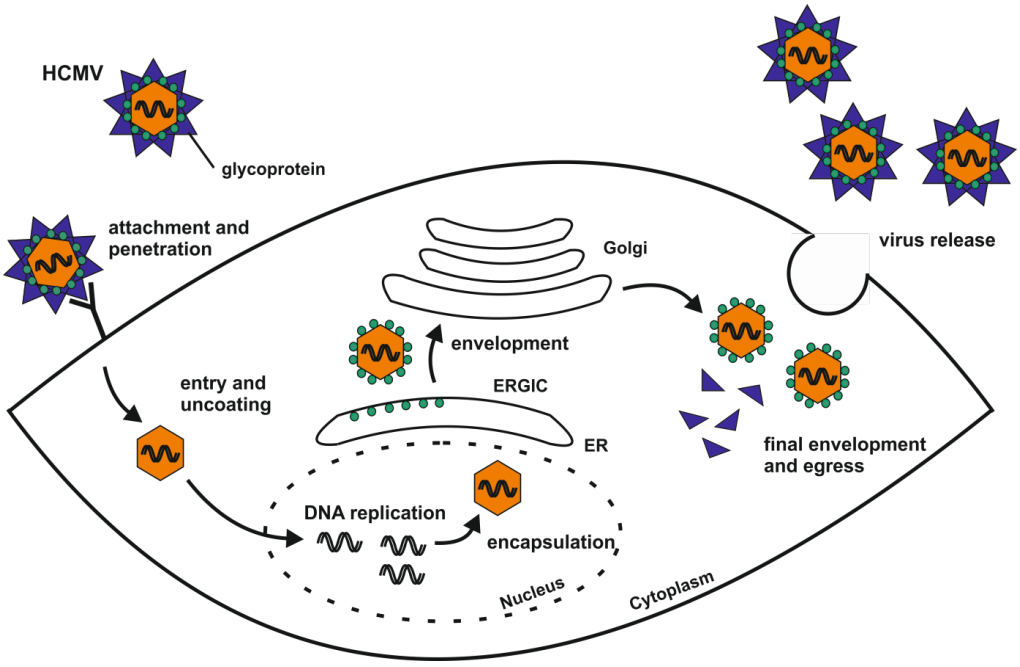

Figure 1.9 Replication cycle of HCMV. HCMV enters the cell either via direct fusion with the host cell membrane or via the endocytotic pathway. Attachment of viral glycoprotein to specific host cell surface receptors is followed by penetration, which releases the viral nucleocapsid into the cytoplasm. Subsequently, nucleocapsids are transported into the nucleus, where viral DNA is released during the uncoating. The viral gene expression cascade begins with the translation of IE genes, which in turn transactivate E genes and cellular genes and coordinate viral replication. During the early and late phase further proteins for viral DNA replication and encapsula-

tion are produced. Capsids are transported from the nucleus to the cytoplasm. The envelopment with tegument proteins occurs at the ERGIC and is followed by the final envelopment and exocytosis at the plasma membrane.

Antiviral immune response and viral countermeasures HCMV infection is efficiently controlled by the innate as well as the adaptive immune response. Most important to control the spread of the virus are cellular immune mechanisms. In particular, dendritic cells recognize viral glycoproteins (Juckem et al., 2008), internalize virus particles and present viral antigens to virus-specific CTLs (Arrode and Davrinche, 2003), which subsequently lyse infected cells and block virus replication by secretion of IFNγ (Davignon et al., 1996).

Part of the innate immune response to HCMV infection are Toll-like receptors and the type I interferon response. Activation of TLRs activates signal transduction pathways that lead to secretion of inflammatory cytokines and the upregulation of costimulatory molecules like CD80 and CD86. For example, an interaction of the viral glycoproteins gB and gH with TLR2 results in activation of NFκB (Compton et al., 2003).

The adaptive immune response to HCMV includes humoral responses as well as T cell-mediated immunity. The production of antibodies restricts viral dissemination and limits the severity of disease (Boppana and Britt, 1995). The glycoprotein gB is a major target for neutralizing antibodies (Britt et al., 1990), but the predominant mechanism controlling the spread of HCMV infection is the induction of strong $CD8^+$ T cell responses. An essential role for HCMV-specific $CD8^+$ T cells was shown by Reusser and colleagues, who found that half of the patients lacking a detectable anti-HCMV T cell response developed HCMV disease (Reusser et al., 1991). Further work showed that infusion of donor-derived HCMV-specific $CD8^+$ T cells effectively restored antigen-specific cellular immunity in BMT recipients (Riddell et al., 1992; Walter et al., 1995). Moreover, high frequencies of IE1-specific $CD8^+$ T cells correlated with protection from HCMV disease in heart and lung transplant recipients (Bunde et al., 2005).

The fine specificity of HCMV-specific $CD8^+$ T cell responses and the viral antigens against which they are directed have been comprehensively examined in healthy HCMV-seropositive donors. A variety of virus proteins was shown to be recognised, including structural proteins as well as immunomodulators, viral proteins expressed at different stages (IE, E and L antigens) and with diverse functions (capsid, tegument, glycoproteins, immunoevasins). Examples are: pp28, pp50, pp150, gH, gB, US2, US3, US6, US11, UL16, UL18. *Ex vivo* T cell assays revealed that $CD8^+$ and $CD4^+$ T cells are directed towards more than 70% of the virus ORFs (Elkington et al., 2003). To the most frequently recognised antigens belong the immediate-early protein 1 IE1, also known as UL123 or pp72 a transcription factor of 72kDa (Kern et al., 1999), and the phosphoprotein pp65 (UL83) (McLaughlin-Taylor et al., 1994).

The lower matrix protein pp65 (UL83) is a phosphoprotein of 65kDa and the major component of the tegument. Apparently pp65 has no essential function for the virus replication (Schmolke et al., 1995b), but plays an important role during the assembly of virus particles (Chevillotte et al., 2009). During virus entry, pp65 is delivered from the tegument directly into the cytosol of the host cell. Via a C-terminal nuclear localization signal (NLS) pp65 translocates directly after infection into the nucleus,

where it is observed within five minutes after infection (Schmolke et al., 1995a). Due to this processing pp65 gains access to the antigen processing machinery before the virus replication starts (Reddehase, 2002) and represents the most dominant antigen for activation of the cellular immune response (McLaughlin-Taylor et al., 1994). Therefore pp65-derived antigens play an important role for the early control and limitation of HCMV infection. Of all HCMV-specific $CD8^+$ T cells 70 to 90% recognize MHC class I presented pp65 antigenic peptids (Wills et al., 1996). Often the HCMV-specific $CD8^+$ T cell population is focused on only one peptide (Weekes et al., 1999). One of these is the immunodominant, HLA-A2 restricted pp65 epitope comprising the aminoacids 495 to 503, therefore called $pp65_{495\text{-}503}$ (sequence: NLVPMVATV). Presentation of this epitope is detected in persistent infection despite HCMV immune escape mechanism (Besold et al., 2007). The phosphoprotein 65 itself exhibits immunomodulatory effects, for example it interferes with MHC class II surface expression (Odeberg et al., 2003), limits the cytotoxicity of natural killer cells (Arnon et al., 2005), inhibits the proteasomal processing of IE1 preventing thereby the presentation of IE1-derived antigenic peptides (Gilbert et al., 1996) and impedes cell cycle progression (Castillo and Kowalik, 2002; Zhu et al., 1995).

The human cytomegalovirus is highly adapted to the infection of its host and has developed many strategies to subvert the immune control at different levels. To evade recognition and elimination by the host immune system many HCMV gene products possess specific immunomodulatory functions, such as the impairment of MHC function, inactivation of leukocytes, inhibition of cytokine production, arrest of the cell cycle and decrease of the humoral immune defense (Mocarski, 2004). The major evasion mechanism is concentrated on the inhibition of MHC class I restricted antigen presentation. Four HCMV glycoproteins interfere with this pathway and trigger rapid downregulation of MHC class I surface expression: US2, US3, US6 and US11. US2 and US11 mediate the retrograde transport of newly synthesized MHC class I molecules from ER to cytosol, where they are ubiquitylated and degraded by the proteasome (Wiertz et al., 1996). US3 inhibits the transport of loaded MHC class I complexes to the cell surface, which therefore accumulate in an ER-associated compartment (Ahn et al., 1996). US6 is a transmembrane protein that interacts with TAP and thus impairs TAP function (Ahn et al., 1997; Hengel et al., 1996). Further Halenius and colleagues found a transcriptional downregulation of TAP2 and TAP1 gene expression in HCMV-infected cells (Halenius et al., 2011).

1.5.2 Influenza A virus

According to the World Health Organisation WHO (www.who.int), each year seasonal influenza virus infections affect 3 to 5 million people resulting in up to 500.000 death cases globally. The severity of illness can range from mild, cold-like symptoms, to death (Wright et al., 2007), which occurs mainly among high-risk groups like young children, elderly or chronically ill people. Over the last century every 10 to 40 years an influenza pandemic, i.e. a global epidemic, has occurred (Wright et al., 2007). The most devastating recorded pandemic, the Spanish flu, occurred in 1918 (influenza A subtype H1N1). Worldwide 40 million humans died and an estimated number of 700 million was infected (Johnson and Mueller, 2002). Moreover, unusually large numbers of especially young people died during the 1918 influenza pandemic (Reid and Taubenberger, 2003). Less severe pandemics occurred

in 1957, the Asian flu (H2N2), in 1968, the Hong Kong Flu (H3N2), and in 1977, the Russian flu (H1N1) (Cox and Subbarao, 2000). The transmission of the influenza virus results via droplet infection, but also via contact with a contaminated surface or an infected individual.

Structure The influenza A virus belongs to the family of orthomyxoviridae, which is characterized by a linear single-stranded and segmented RNA genome of negative polarity. The virus particle is pleomorph in shape and comprises 80 to 120nm in diameter. The genome of the influenza A virus is composed of 8 RNA segments, which constitute 13kb of sequence encoding for up to 11 proteins. Nine of these proteins represent structural proteins building the virus particle: three polymerase polypeptides PB1, PB2 and PA; the nucleoprotein NP; three proteins present in the lipid envelope of the virion, the glycoproteins hemagglutinin HA and neuraminidase NA as well as the pH-dependent ion channel M2; the matrix protein M1; and the nuclear export protein NEP (also known as NS2). Furthermore two proteins, PB1-F2 and the nonstructural protein NS1 can only be found in infected cells (Figure 1.1010) (Nayak et al., 2009).

An interesting feature of the influenza genome is that it is packed in viral ribonucleoprotein complexes (vRNPs). While the nucleoprotein NP is complexed with the viral RNA (vRNA), trimeric viral polymerase complexes composed of PB1, PB2 and PA bind to the ends of the vRNPs (Klumpp et al., 1997). The transmembrane glycoproteins HA and NA fulfill important tasks during the attachment, penetration and budding of virus particles. The HA protein plays two major roles: i) binding to sialic acid receptors on the host cells; and ii) fusion of virus and host endosomal membranes (Daniels et al., 1987). The neuraminidase NA cleaves sialic acid residues of newly formed viral and cellular glycoproteins, thereby promoting the release of virus particles from the host cell (Gottschalk, 1958). The M2 protein plays an important role in the uncoating process, which ends with the release of RNP complexes into the cytoplasm of the host cell. The conduct of protons from the acid environment of the endosome into the virion through the M2 ion channel allows vRNP complexes to dissociate from M1 proteins. Furthermore, the matrix protein M1 constitutes the tegument and possesses several functions: i) it acts as a chaperone during virus assembly, ii) it aids the export of vRNPs out of the nucleus and iii) it recruits vRNPs to the virion assembly sites at the plasma membrane (Bouvier and Palese, 2008). The nonstructural protein NS1 influences the cellular transport, splicing and translation of vRNA. Further, both NS proteins, NS1 and NS2, block the induction and signaling of type I IFNs, and so they represent IFN-antagonists (Palese and Shaw, 2007; Wright et al., 2007).

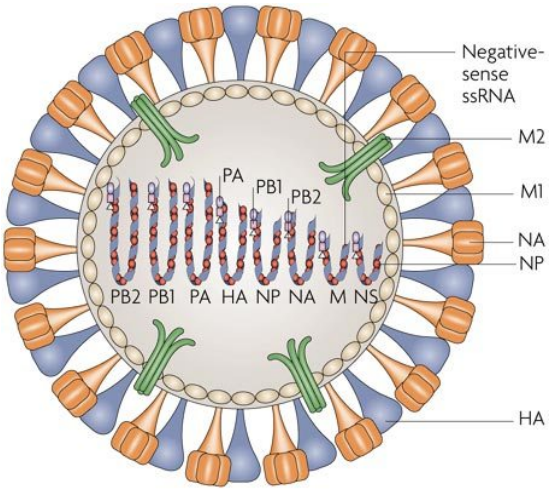

Figure 1.10 Structure of the influenza A virus. An influenza virus particle is composed of the following proteins: hemagglutinin (HA), neuraminidase (NA), matrix protein 1 (M1), matrix protein 2 (M2), nonstructural protein NS1 and NS2, nucleoprotein (NP), trimeric polymerase complex constituted of PB1 (polymerase basic 1), PB2 (polymerase basic 2) and PA (polymerase acid). Figure adapted from (Horimoto and Kawaoka, 2005).

Influenza viruses are classified into subtypes based on the antigenicity of their viral surface molecules HA and NA. There are 16 different HA and 9 different NA subtypes known, which are used for the naming of influenza subtypes according to the scheme HxNx. These different types of surface antigens have an impact on host specificity and virulence. Point mutations in the HA and NA genes result in virus variants that can no longer be recognized by pre-existing host immunity, which was directed at the 'parent' virus (Hensley et al., 2009). This process accounts for the antigenic drift that is common among orthomyxoviruses and is the reason for the yearly flu epidemics.

The segmentation of the influenza genome allows the exchange of single RNA gene segments, thereby leading to another phenomenon, the antigenic shift. When two different virus subtypes infect the same cell, they are able to reassort their genome segments and thereby can generate a new influenza strain. Antigenic shift results in high infection rates in immunologically naive populations, which can possibly lead to the occurrence of pandemics (Wright et al., 2007).

Replication cycle The primary infection site of influenza A virus represents human epithelial cells of the upper respiratory tracts. However, the virus also replicates in monocytes, macrophages and other leukocytes (Majde, 2000). The replication cycle begins with the binding of HA proteins to sialic acid-containing receptors of the host cells. This adsorption process is followed by receptor-mediated endocytosis resulting in an up-take of virus particles into endosomal vesicles. Due to the lower pH inside the endosomes a proton influx via M2 ion channels takes place and leads to conformational changes of HA glycoproteins, which results in the fusion of endosomal and viral membranes. The release of vRNPs into the cytosol is mediated with the help of matrix protein M1 which finishes the uncoating process (Bui et al., 1996). The whole process of uncoating beginning with the attachment of virus particles to the host cell takes no more than 25 minutes. Already after another 10 minutes vRNPs enter the nucleus (Martin and Helenius, 1991). This occurs because vRNPs are featured with nuclear localization sequences (NLS) which interact with host cell importing mechanisms (Boulo et al., 2007). Inside the nucleus mRNA for protein biosynthesis and complementary cRNA for synthesis of new vRNA is transcribed. The ribosomal synthesis of early viral proteins subsequently takes place in the cytoplasm. Afterwards early virus proteins are actively and passively transported back into the nucleus.

There, the replication of vRNA and the transcription of mRNA for the late structural proteins HA, NA, M1 and M2 occurs. The active export of newly synthesized nucleocapsids is dependent on the M1 protein. Subsequently the late structural proteins are translated and glycosylated. Finally, all viral components localize to the apical plasmamembrane of the polarized epithelial cells, where the packing and budding of new virus particles mediated by HA and NA takes place (Nayak et al., 2004).

Antiviral immune response to influenza A For the immune response to influenza A infection innate as well as adaptive immune mechanism play important roles. The production of cytokines like TNFα, IL1 and IL6, chemokines like MIP-1α and RANTES, but especially the type I interferon response are of crucial importance. Via interaction with Toll-like receptors TLR3 and TLR7 as well as the RNA helicases RIG-I and MDA5 the NFκB and MAPK signaling pathways are activated. Through activation of the transcription factors IRF3 and IRF7 the production of IFNα and IFNβ is induced (Wright et al., 2007).

A special relevance is attached to the innate immune response of respiratory epithelial cells. Some highly pathogenic influenza A subtypes like the avian H5N1 virus can cause massive viral pneumonia, systemic disease and death due to enhanced cytokine and chemokine production. A so-called 'cytokine storm' can damage the lung tissue and contribute to pathology instead of controlling viral replication (Oslund and Baumgarth, 2011).

Notably, the nonstructural protein NS1 represents an antagonist of the type I IFN response. Deletion of NS1 leads to 100-fold enhanced IFNα production in comparison to infection with wild type virus. One mechanism by which NS protein is believed to inhibit IFN induction is by sequestering viral replication intermediates and thus masking them from RNA sensors, e.g. preventing activation of RIG-I (Pichlmair et al., 2006). NS1 is also supposed to impair activation of the OAS/RNaseL pathway (Min and Krug, 2006) as well as of the translation inhibitory kinase PKR (Li et al., 2006).

Humoral immunity encounters a special challenge during influenza infection, since antibody responses are often strain-specific and even drive the antigenic drift, especially when directed against the hemagglutinin molecule (Kreijtz et al., 2011). Cellular immunity includes virus-specific $CD4^+$ T helper cells and $CD8^+$ cytotoxic T cells. These cells are mainly directed against conserved proteins and therefore could provide protection against different influenza A subtypes and potentially pandemic influenza viruses (Kreijtz et al., 2011). One well described immunodominant antigenic peptide represents the HLA-A2 restricted $M1_{58-66}$ epitope, which derives from Matrix protein 1 and comprises the amino acids 58 to 66 (sequence: GILGFVFTL) (Bednarek et al., 1991; Gotch et al., 1987; Morrison et al., 1992).

1.6 Aims and objectives

Recently, an important new role for the i-proteasome in the clearance of oxidatively damaged proteins has been discovered and widely discussed. It has long been accepted that the proteasome plays an important role in the elimination of toxic aggregates of accumulating oxidant-damaged proteins, but lately the i-proteasome has been demonstrated to clear ub-rich protein aggregates more efficiently

during inflammation-induced stress. Further, within a virus infection it could be demonstrated that i-proteasome deficiency contributes to tissue damage and disease progression as a consequence of lack of protection against oxidative protein damage. The concept of the i-proteasome to solely represent a component of the MHC class I antigen presentation pathway promoting the generation of antigenic peptides has profoundly changed and new functions of the i-proteasome in non-immune cells have emerged.

Within this thesis the long-established role of the i-proteasome during the generation of MHC class I ligands has been investigated and linked to its function in efficient degradation oxidant-damaged proteins. Therefore, several key questions were raised, wich have been analysed in infected target cells:

- How fast is the induction of i-proteasomes in non-immune cells in response to viral infection?
- Does the i-proteasome exhibit a special composition and does i-proteasome induction affect the generation of immunodominant epitopes?
- Which signalling pathways lead to the rapid induction of i-proteasome formation in response to virus infection?
- Where do viral proteins derive from in order to provide the supply for the proteasome to generate antigenic peptides?
- At which rate are reactive oxygen species induced and to which extent do they cause oxidative damage inside the infected cells with respect to endogenous and viral proteins?
- Does oxidative damage of viral proteins affect the antigen presentation of immunodominant epitopes?
- What is the source of reactive oxygen species in response to viral infection, focusing on the role of NADPH oxidases?

To address these questions two different virus infection models in cell culture were chosen: i) human cytomegalovirus infection in fibroblasts, as example for a large DNA virus which is highly adapted to the infection of its host, and ii) the influenza A virus which represents a small and fast replicating RNA virus. An effective immune response controlling the spread of both viruses is predominantly mediated by $CD8^+$ T cell responses directed against immunodominant virus epitopes.

In summary, this work brings together the different functions of the i-proteasome during the response to inflammation-induced oxidative stress and during antigen presentation.

2. Methods

2.1 Cell biological methods

2.1.1 Cell culture reagents

Substance	*Supplier*
Basal Iscove medium	Biochrom AG
RPMI1640	Biochrom AG
OptiMEM	Gibco
Biocoll	Biochrom AG
human AB-Serum	PromoCell
Fetal calf serum (FCS)	Biochrom AG
L-glutamine	PAA Laboratories GmbH
Trypsin/EDTA	PAA Laboratories GmbH
Dimethylsulfoxid (DMSO)	Sigma Aldrich
Penicilline/Streptomycine	PAA Laboratories GmbH
Gentamycine	LONZA
Puromycine	PAA Laboratories GmbH
Hygromycine B	Roche
Epoxomicin	Calbiochem
Sulforaphane	LKT Laboratories
Cycloheximide	Sigma Aldrich
BX-795	Axon Medchem
MMHAR-2 (CD118)	R&D Systems
Interleukin 2 (IL-2)	Chiron Therapeutics
Interleukin 6 (IL-6)	Strathmann Biotec
Interleukin 12 (IL-12)	Strathmann Biotec
Interleukin 4 (IL-4)	Strathmann Biotec
GMCSF	Fa Berlex
Phytohaemagglutinin (PHA)	Sigma Aldrich
Lipopolysaccharide (LPS)	Sigma Aldrich
human Interferon-α (hIFN-α)	Miltenyi Biotec
human Interferon-β (hIFN-β)	Miltenyi Biotec
human Interferon-γ (hIFN-γ)	Roche
Lipofectamin 2000 transfection reagent	Invitrogen
HiPerfect transfection reagent	Qiagen
DMSO	Roth
Trypane blue Solution	Sigma Aldrich
ActinomycinD	Sigma Aldrich
MTT	Sigma Aldrich
BrefeldinA	Sigma Aldrich

Table 2.1 Used cell culture reagents.

2.1.2 Cell lines and media

BASAL ISCOVE's Medium + 2mM L-glutamine + 10% FCS (heat inactivated) + antibiotics (see table 2.2)

RPMI1640 Medium + 2mM L-glutamine + 10% FCS (heat inactivated) + antibiotics (see table 2.2). For cultivation of cytotoxic T lymphocytes FCS was replaced by 10% human AB serum (heat inactivated).

All cells were cultivated in sterile cell culture dishes from Greiner in their respective media at 37°C, 5% CO_2 and 95% humidity.

Notation	*Cell type*	*Culture*	*Media*	*Antibiotics*
HeLa	human cervix epithelial carcinoma	Adherent	Basal ISCOVE	100U/ml penicillin + 100µg/ml streptomycin
HeLa $^{A2+}$	HLA-A2 positive HeLa cell, stable expressing MHC class I HLA-A*0201	Adherent	Basal ISCOVE	100U/ml penicillin + 100µg/ml streptomycin + 2µg/ml puromycin
MRC5	Human lung fibroblast (ATCC CCL-171)	Adherent	Basal ISCOVE	50µg/ml gentamycin
EBV-B	Epstein-Barr virus transformed human B-lymphocyte	Suspension	RPMI1640	100U/ml penicillin + 100µg/ml streptomycin
WEHI	Lymphoma cell line	Suspension	RPMI1640	100U/ml penicillin + 100µg/ml streptomycin
CTL	cytotoxic T lymphocyte	Suspension	RPMI1640	100U/ml penicillin + 100µg/ml streptomycin

Table 2.2 Used human cell lines, their appropriate media and respective antibiotic additive.

2.1.3 Transfection of cells

Transfection of plasmid DNA

Transfection of plasmid DNA (table 2.3) in human lung fibroblasts was conducted according to manufacturer's instructions with Lipofectamin 2000. The ratio of DNA to Lipofectamin was adjusted. After 6 to 8h of transfection the cell culture medium was exchanged with fresh medium and cells were further cultivated according to the respective protocol.

Notation	*Insert*	*Vector*	*Supplier/source*
pcDNA3.1-Zeo/lacZ	lacZ (ORF)	pcDNA3.1-Zeo(+)	Invitrogen
pCAT-PSMB9	part of the PSMB9 promoter	pCAT3basic	J. Steffen

Table 2.3 Used plasmids and DNA constructs.

Transfection of siRNA

Transient transfection of siRNA (table 2.4) was conducted with HiPerfect. Transfection reagent and siRNA were diluted in optiMEM transfection medium and added drop wise onto the cells directly after these were plated and still in suspension. Due to this fast forward procedure the transfection efficiency could be highly improved for the strongly adherent fibroblasts. All used siRNAs were employed in a final concentration of 25 to 50nM and incubated for 48h. Subsequently, the knockdown was either directly confirmed by western analysis and PCR or was followed by further experiments as described.

siRNA	*Dharmacon catalogue number*
IRF3	L-006875-00-0005
Nox1	L-010193-00-0005
Nox4	L-010194-00-0005
PSMB8	L-006022-00-0005
PSMB9	L-006023-00-0005
PSMB10	L-006019-00-0005
PSMD4	L-011365-00-0005
PSME1	L-012254-00-0005
PSME2	L-011370-01-0005
UBE2L6	L-008569-00-0005
OFF-target	D-001810-10-05

Table 2.4 All used ON-TARGET *plus* siRNAs were purchased from Thermo Scientific Dharmacon.

2.1.4 Interferon stimulation

HeLa cells and MRC5 fibroblasts were treated with 10ng/ml human IFNα, 10ng/ml human IFNβ or 100U/ml human IFNγ. Analysis of stimulated cells was carried out after indicated time points.

2.1.5 Virus infection

The human cytomegalovirus (HCMV) laboratory strain Ad169 variant ATCC was kindly provided from Prof. Hartmut Hengel (University hospital Düsseldorf). The human influenza A viruses (IAV) APR8 as well as KPV (classical bird flu) were obtained from Dr. Michael Veit (Free University Berlin).

For viral infection target cells were plated in 6-well cell culture plates with an approximated density of $1x10^6$ cells/well at the day of infection. The virus titer was diluted to a concentration of 3 to $5x10^6$ virus particles/ml in cell culture medium so that addition of 1ml virus suspension in one 6-well yielded a multiplicity of infection (moi) of 3 to 5, i.e. one cell was infected by 3 to 5 virus particles. For the timely synchronization of infection the 6-well plates were centrifuged twice for 15min at 2000rpm and

37°C, after 15min the plates were rotated by 180° in order to guarantee a fast and simultaneous attachment of the virus particles to the cells all over the well (personal communication with Anne Halenius, University hospital Düsseldorf). After several time points the infected cells were harvested and further treated according to the described protocols.

2.1.6 Generation of epitope-specific CTL

CTL clones specific for the HLA-A0201 ($A2^+$) restricted viral epitopes $M1_{58-66}$ derived from influenza A (Bednarek et al., 1991; Gotch et al., 1987; Morrison et al., 1992) and $pp65_{495-503}$ from HCMV (Diamond et al., 1997; McLaughlin-Taylor et al., 1994; Wills et al., 1996) were generated as described by Fonteneau et al. (Fonteneau et al., 2001) with the help of peptide-pulsed dendritic cells (DCs). Therefore, peripheral blood mononuclear cells (PBMCs) were isolated from fresh *buffy coats* via biocoll gradient centrifugation. PBMCs of different donors were analysed for HLA-$A2^+$ MHC class I by FACS with FITC-labeled anti-HLA-$A2^+$ antibody. In order to separate monocytes from the PBMCs of HLA-$A2^+$ donors *magnetic cell separation* (MACS® Milteny Biotec) was used. In a first step $CD14^+$ monocytes were directly labeled with MACS® microbeads, a CD14 receptor coupled to a magnetic particle. The magnetically labeled cells were detained inside the MACS® LS Column as long as the column was placed in the MACS® separator in a strong magnetic field. Removing the LS column from the magnetic field released $CD14^+$ monocytes. The flow through from the first separation step was further used for isolation of $CD8^+$ monocytes via anti-CD8 MACS® microbeads. The $CD8^+$ cells were frozen for the time being in 90% FCS and 10% DMSO. The $CD14^+$ cells were further differentiated to DCs which therefore were cultivated in big cell culture flasks under addition of 100U/ml Interleukin-4 (IL-4) and 500U/ml granulocyte macrophage colony-stimulating factor (GMCSF). After the fifth day the $CD14^+$ monocytes were transferred onto 24-well plates covered with 3% poly-MA in order to prevent adhesion of the dendritic cells and stimulated by addition of 500U/ml GMCSF, 100U/ml IL-4 and 1µg/ml lipopolysaccharides (LPS). The following day, dendritic cells were harvested and pooled, adjusted to a cell number of $1x10^6$ cells/ml and pulsed for 1h on ice with 10µg/ml $M1_{58-66}$ or $pp65_{495-503}$ peptide, respectively. Subsequently, $CD8^+$ monocytes were thawed and cocultivated with the autologous peptide-loaded DCs. Therefore, $2x10^5$ $CD8^+$ cells were combined with $2x10^4$ DCs in 96-well cell culture plates in RPMI medium supplemented with 10% human AB serum, 1000U/ml recombinant human IL-12 and 1000U/ml human IL-6. A restimulation by repeated addition of peptide-pulsed DCs and the growth factor IL-2 in a final concentration of 20U/ml was carried out after 7 days. After one further week of cocultivation T cells were tested for peptide specificity by TNFα assay (see chapter 2.1.7.1). Moreover, positive wells were verified by intracellular cytokine staining (see chapter 2.1.7.2). Finally, confirmed wells were selected for cloning of an epitope-specific T cell clone by limiting dilution in the presence of irradiated feeder cells, IL-2 and phytohaemagglutinin (PHA).

2.1.7 CTL assay

For testing polyclonal CTLs for peptide specificity TNFα assay and intracellular cytokine staining were performed. In order to investigate antigen presentation on virus-infected cells IFNγ assays were used.

2.1.7.1 TNFα assay

As target HLA-A2$^+$ HeLa cells were employed with and without loading of 10µg/ml peptide ($pp65_{495-503}$ and $M1_{58-66}$ respectively) for 15min on ice. 5x10^4 target cells were cocultivated for 3 to 6h at 37°C in 96-well plates with the CTLs to be tested. At the same time TNFα-sensitive WEHI cells were cultivated in RPMI1640 supplemented with 1M lithium chloride and actinomycin D. The supernatant of the cocultivation was added to 3x10^6 WEHI cells/well and incubated over night. Addition of 2.5mg/ml MTT (3-(4,5-Dimethylthiazol-2-yl)-2,5-diphenyltetrazoliumbromid) and incubation for 3h at 37°C induces a colour reaction based on the reduction of the yellow tetrazolium salt into purple formazan by enzymatic activity reflecting the glycolysis rate. A decreased colour change therefore indicated decreased cell viability. The insoluble purple formazan was dissolved by addition of 10% SDS and the absorbance of the coloured solution was measured at 550nm. Thus, TNFα-sensitivity of WEHI cells showed peptide-specific activation of the CTLs.

2.1.7.2 Intracellular cytokine staining

Again HLA-A2$^+$ HeLa cells with and without peptide loading were co-incubated in 96-well cell culture plates with the CTLs to be tested for peptide specificity. The addition of 10µg/ml Brefeldin A impeded the transport of IFNγ through the Golgi apparatus out of the cell. After incubation over 5 to 6h at 37°C the cells were analysed by flow cytometry with PE-coupled anti human IFNγ antibody (see table 2.6).

2.1.7.3 INFγ assay

To analyse epitope presentation after viral infection of MRC5 fibroblasts with HCMV or HLA-A2$^+$ HeLa cells with IAV, respectively, the release of IFNγ by activated epitope-specific CD8$^+$ T cells was measured. Target cells were seeded and infected in 6-well cell culture plates and depending on the experiment pre-treated according to the protocol. Cellular proteasome function was inhibited by adding 200nM epoxomicin directly after virus infection. Viral gene expression was abolished either by UV radiation (5000 J/m²) or by adding 50 µg/ml of the translation inhibitor cycloheximide 1h prior to virus infection. To prevent ROS formation the isothiocyanate sulforaphane was added in a final concentration of 10µM 24h prior to virus infection. 1µM of the kinase inhibitor BX-795 and 10µg/ml neutralizing monoclonal antibody MMAHR2 were added to the cells 1h prior to virus infection. Application of siRNA (see chapter 2.1.3) was performed 48h prior to infection and analysis of antigen presentation.

The assay was performed in round bottom 96-well cell culture plates. The target cells were harvested, washed, adjusted to a cell number of 6x10^5 cells/ml and seeded in an 8-fold dilution series starting with 50µl i.e. 3x10^4 cells. The epitope-specific CTLs generated as described in chapter 2.1.6 were freshly thawed, washed and also adjusted to a cell number of 6x10^5 cells/ml. Per well 3x10^4 CTLs were seeded resulting in different effector to target cells ratios ranging from 1:1 to 1:128. As control,

each sample was loaded with 0.5 µg/ml synthetic $pp65_{495-503}$ or $M1_{58-66}$ peptide, respectively. Target cells and effector CTLs were cocultivated at 37°C over night. The next day the culture plates were centrifuged for 7min at 2000rpm and 4°C. The supernatant containing the released IFNγ in case of CTL activation was collected and frozen at -20°C prior to the further analysis. The activation of epitope-specific CTL could then be determined by quantification of secreted IFNγ by ELISA following manufacturer's instructions (see chapter 2.3.1). The CTL response was expressed as percentage regarding the peptide-loaded control samples as 100% response.

2.1.8 CAT assay

MRC5 cells were pre-treated for 48h with 25nM off-target as well as IRF3-targeting siRNA (Dharmacon) as described above. Subsequently, $5x10^5$ cells were transfected with 2µg β1i-CAT construct provided by Dr. Janos Steffen and 2µg pcDNA3.1-Zeo/LacZ as an internal control according to the Lipofectamin 2000 manual. After 8h of transfection cells were infected with HCMV Ad169 at moi 3 to 5 and harvested 8h post infection. The CAT-concentrations in all samples were measured with CAT-ELISA kit from Roche and normalized against β-galactosidase activity, which was determined by cleavage of CPRG substrate.

2.2 Biochemical methods

2.2.1 Chemicals and antibodies

Chemical	*Method*	*Supplier*
ECL Plus™	Western Blot	GE Healthcare
BCA Protein Assay Kit	Western Blot	Thermo Fisher Scientific
OxyBlot™ protein oxidation detection kit	Western Blot	Chemicon International
Protein G Sepharose 4FF	Immunoprecipitation	GE Healthcare
Suc-LLVY-AMC	Native Gel Overlay	Bachem
N-Ethylmaleimide (NEM)	Inhibitor	Sigma-Aldrich
Epoxomicin	Inhibitor	Calbiochem
Complete® Inhibitor Mix	Inhibitor	Roche
MG132	Inhibitor	VWR International

Table 2.5 Chemicals

Antibody	*Method*	*Origin*	*Supplier*
anti-human-HLA-A2-FITC clone BB7.2	FACS	mouse	BD Biosciences
anti-human-HLA-A,B,C-PE		mouse	BD Biosciences
anti-human IFN-γ-PE		mouse	BD Biosciences
PE/FITC-labeled $IgG_{1/2a}$ isotype control		mouse	BD Biosciences

anti-pp65 (MA1-7597)	IP, IF	mouse	Thermo Scientific
anti-Ubiquitin (FK2)		mouse	Biomol
anti-pp72 (6E1)		mouse	Santa Cruz
anti-α2 (MCP21)		mouse	AG Kloetzel
anti-pp65 (CH12)	WB primary ab	mouse	Santa Cruz
anti-M1 (ab34848)		goat	Abcam
anti-Lmp7		rabbit	AG Kloetzel
anti-Lmp2		rabbit	AG Kloetzel
anti-Mecl1 (K223)		rabbit	AG Kloetzel
anti-α4		rabbit	AG Kloetzel
anti-β5		rabbit	AG Kloetzel
anti-β2 (mcp168)		mouse	AG Kloetzel
anti-POMP		rabbit	AG Kloetzel
anti-PA28α		rabbit	AG Kloetzel
anti-PA28β		rabbit	NEB
anti-Rpn10 (S5a)		mouse	AG Kloetzel
anti-GAPDH		rabbit	Santa Cruz
anti-UBE2L6		mouse	Abnova
anti-phosphoS6		rabbit	CellSignaling
anti-Stat1 (9172)		rabbit	CellSignaling
anti-phospho-IRF3 (Ser396)		rabbit	Millipore
anti-IRF3		rabbit	Santa Cruz
anti-p53 (DO7)		mouse	Novocastra
anti-Ubiquitin (FK2)		mouse	Biomol
anti-Ubiquitin (FK1)		mouse	Biomol
anti-Ubiquitin		rabbit	Dako
anti-rabbit-HRP	WB secondary ab	goat	Dianova
anti-mouse-HRP		rabbit	Seramun
anti-goat-HRP		donkey	Dianova
Alexa Fluor 633 anti-mouse IgG	IF secondary ab	goat	Invitrogen
Alexa Fluor 488 anti-mouse IgM		goat	Invitrogen
Alexa Fluor 488 anti-rabbit IgG		goat	Invitrogen

Table 2.6 Antibodies (ab: antibody; IF: immunofluorescence; IP: immunoprecipitation; WB: Western blot)

2.2.2 SDS-PAGE and Western analysis

2.2.2.1 Cell lysis

RIPA lysis buffer: 50mM Tris-HCl, 150mM NaCl, 1% (v/v) Nonidet P40, 0.5% (w/v) Sodium-deoxycholate, 0.1% (w/v) SDS and Complete, adjusted to pH 8.0 with NaOH

Triton lysis buffer: 50mM Tris-HCl, 50mM NaCl, 5mM $MgCl_2$, 0.1% (v/v) Triton X-100 and Complete, adjusted to pH 7.5 with NaOH

After harvesting the cells were washed once in 1ml ice-cold 1x PBS and centrifuged. The pellet was resuspended in lysis buffer. In case of preparation of lysate for analysis of ubiquitin conjugates the lysis buffer was additionally completed with 1µM epoxomicin and 10mM NEM. Lysis with RIPA buffer was carried out for 1h on ice with occasional vortexing. Cell pellets lysed with Triton lysis buffer were subjected 3-times to freeze and thaw in liquid nitrogen. In order to separate lysate from cell debris the lysates were centrifuged for 20min at 14.000rpm and 4°C. The supernatants were collected and stored at -80°C for further experiments such as immunoprecipitation or SDS-PAGE. The protein concentration was determined with BCA protein assay kit according to manufactures instructions in microtiter plates.

2.2.2.2 Sodiumdodecylsulfoxide-polyacrylamide gel electrophoresis

10x SDS-sample buffer: 500mM Tris-HCl pH 6.8, 60% (v/v) glycerol, 20% (w/v) SDS, 1M DTT, 1% (w/v) bromphenol blue

4x stacking gel buffer: 0.5M Tris-HCl pH 6.8, 0.4% (w/v) SDS

4x separating gel buffer: 1.5M Tris-HCl pH 6.8, 0.4% (w/v) SDS

10x electrophoresis running buffer: 250mM Tris-HCl pH 8.8, 2M glycine, 1% (w/v) SDS

For the separation of proteins under denaturating conditions SDS polyacrylamide gel electrophoresis (SDS-PAGE) adapted from Laemmli (Laemmli, 1970) was performed. Therefore, 5 to 25µg total cell lysate depending on the used antibodies for Western Blot were denaturized in SDS-sample buffer at 95°C for 5min and subsequently loaded onto SDS polyacrylamide gels with a concentration ranging between 10%, 12.5% and 15% acrylamide depending on the desired resolution range. The precise composition of the gels is given in table 2.7. The electrophoresis was performed for 1 to 2h at 120V. The protein marker PageRuler prestained protein ladder was used as standard to estimate the molecular weight of the separated protein bands.

Solution	Vol.	Separating gel					Stacking gel
		8% AA	10% AA	12,5% AA	15% AA	18% AA	5% AA
30% acrylamide	Ml	9.6	12	15	18	21.5	4.5
H_2O	Ml	17.4	15	12	9	5.5	10.5
4x separating gel buffer	Ml	9	9	9	9	9	-
4x stacking gel buffer	Ml	-	-	-	-	-	7.5
TEMED	µl	25	25	25	25	25	30

10% APS	µl	300	300	300	300	300	300

Table 2.7 Composition of SDS polyacrylamide gels. Indicated volumes of the solutions were mixed to achieve the final concentrations of acrylamide for 5 gels (Hoefer system). (AA – acrylamide)

In special cases to separate both high and low molecular weight proteins in one run gradient gels were used with a separating gel ranging from 8 to 18% AA. For one long gel (Hoefer system) 5.5ml gel solution was prepared by firstly pulling up 3ml 8% AA solution and subsequently 2.5ml 18% AA stained with bromphenol blue in one 10ml-pipette. After waiting for the gradient to establish inside the pipette the gel solution was slowly and steadily poured into the gel chamber.

2.2.2.3 Western Blot and immunodetection

Wet Blot buffer: 25mM Tris-HCl, 200mM glycine, 10% (v/v) methanol

Semidry blot buffer: 25mM Tris-HCl, 200mM glycine, 0.1% (w/v) SDS, 20% (v/v) methanol

Blocking solution: 1x TBS, 0.5% (v/v) Tween-20, 2.5% (w/v) milk powder

Washing buffer: 1x TBS, 0.5% (v/v) Tween-20

Amido black solution: 45% (v/v) MilliQ H_2O, 45% (v/v) methanol, 10% (v/v) acetic acid, 0.1% (w/v) amido black

For the transfer of high molecular weight proteins as well as the ladder-like pattern of ubiquitin conjugates from SDS polyacrylamide gels to PVDF membranes the Wet blot procedure with the appropriate buffer was used. In contrast, for the transfer of lower molecular weight proteins under 30kDa the semidry blot method was employed. The transfer was carried out over 1h at a constant electric current of 4000mA. To verify the protein transfer PVDF membranes were stained in amido black solution and washed in water.

Thereafter, free binding sites of the membrane were blocked for 1h at room temperature with blocking solution. The Incubation with the primary antibody against the antigen of interest was carried out over night at 4°C. The next day the membranes were washed twice for 20min in TBS-T followed by the incubation with the appropriate secondary antibody targeting an antigen from the first antibody diluted in blocking solution for 1h at room temperature. For the final washing the membranes were washed again twice for around 20min in washing buffer and finally soaked in water. For visualization of the horseradish peroxidase (HRP)-labeled secondary antibodies ECL Plus™ Western Blotting Detection Reagents were used. The produced chemiluminescence signal was detected on autoradiography film X-OMAT UV (Kodak) or with the CCD camera of a VersaDoc™ Imager (BioRad). The obtained signals were densitometrically evaluated with ImageJ software.

2.2.3 Native Page

Anode buffer: 50mM BisTris

Cathode buffer: 15mM BisTris, 50mM tricine

Activity buffer: 50mM Tris-HCl pH 7.5, 5mM $MgCl_2$

For the separation of proteasome complexes under native, non-denaturing conditions Native polyacrylamide gel electrophoresis was performed. Therefore, cell pellets were lysed in triton lysis buffer with the freeze and thaw method under addition of 10% (v/v) glycerol. After clearing the lysates from cell debris with a centrifugation step at 4°C and 14.000rpm for 20min, the supernatant was directly subjected to gel electrophoresis without previous storage. 50 to 75µg of total cell lysate was supplemented with 6-fold NativePAGE™ sample buffer and loaded onto NativePAGE™ Novex® Bis-Tris 3 to 12% gels from Invitrogen. The electrophoretic separation was carried out over night at 4°C and 80V. Due to the native conditions of the separation proteasome complexes in native and active conformation were obtained and could be tested for their proteolytic activity in gel. Therefore, the polyacrylamide gels were equilibrated after the run in activity buffer freshly supplemented with 1mM ATP and 100µM of the fluorogenic substrate Suc-LLVY-AMC (Suc-Leu-Leu-Val-Tyr-aminomethylcoumarin). The chymotrypsin-like activity of the proteasome was thereby visualized in gel by cleavage of the AMC group of the substrate. The free AMC was monitored by UV-excitation with a VersaDoc™ Imager from BioRad.

For immunodetection Native polyacrylamide gels were transferred onto PVDF membranes with the Wet blot method. Transfer was performed on special Hybond-LFP PVDF membranes from GE Healthcare which provide a better sensitivity due to lower background with usage of fluorescence-coupled antibodies. After the transfer membranes were blocked, incubated with primary antibodies directed against an epitope in the native conformation of the protein and washed as described for normal immunodetection above. The secondary antibodies obtained from Invitrogen were coupled to fluorescent dyes (Alexa fluorophores, see table 2.6) with different excitation wavelengths. Fluorescence signals were monitored with a VersaDoc™ Imager from BioRad.

2.2.4 Oxyblot

For the immunodetection of oxidized proteins the OxyBlot™ protein oxidation detection kit (Chemicon International) was used according to the manufacturer's instruction. The reaction relies on the immunodetection of carbonyl groups in oxidized proteins. The samples were prepared in RIPA buffer (see chapter 2.2.2.1) and 5µg of total lysate were employed per reaction.

2.3 Immunological methods

2.3.1 IFNγ ELISA

Coating buffer: 0.1M sodium carbonate pH 9.5

Washing buffer: PBS and 0.05% (v/v) Tween-20

Blocking buffer: PBS and 10% (v/v) FCS

To quantify IFNγ secreted from epitope-specific CTLs an anti human IFNγ ELISA (enzyme-linked immunosorbent assay) kit from BD Bioscience was employed according to manufacturer's instructions. ELISA plates were coated with the capture antibody diluted 1:250 in coating buffer over night at 4°C. The next morning, the plates were washed 3-times with PBST in order to remove unbound capture antibody. Thereafter, unspecific binding sites were blocked with PBS and 10% (v/v) FCS for 1h at room temperature. A standard curve was pipetted in a 1:2 dilution series of 300 pg/ml recombinant human IFNγ. The samples, i.e. the supernatants from the CTL assay, were diluted 1:20 up to 1:50 in blocking buffer and incubated for one hour at room temperature. After washing 5-times with PBST the biotinylated secondary antibody was added together with Streptavidin-HRP in one step, both in a dilution of 1:250, and incubated for 1h. Again the samples were washed 5-times before the substrate reagent TMB (Tetramethylbenzidine, BD Bioscience) and hydrogen peroxide was added and incubated for 30min in the dark. The colour reaction was stopped by addition of 50µl 1M H_3PO_4 per well and measured in a photometer at 450nm wavelength. The absolute IFNγ concentration was determined with a double logarithmic standard curve. To each sample a peptide loaded control sample was carried along (see chapter 2.1.7.3). The IFNγ release measured with peptide loading was set as 100% response and the IFNγ secretion in each sample then displayed as relative response.

2.3.2 Immunoprecipitation

By immunoprecipitation (IP) a certain protein is targeted and pulled out of total cell lysate. Depending on the IP conditions modifications of the proteins as well as interaction partners can be identified (co-immunoprecipitation, Co-IP). In this work, either for investigation of ubiquitylation and oxidation of certain viral proteins or the incorporation of i-subunits in proteasome complexes (Co-IP) different protocols were used.

2.3.2.1 Ubiquitylation and Oxidation of viral Proteins

IP buffer: 20mM Tris-HCl pH 7.5, 10mM EDTA, 100mM NaCl, 1x Complete + freshly added: 1% (v/v) Nonidet P-40, 10mM NEM, 1µM Epoxomicin, 1mg/ml BSA

Protein pellets retrieved from virus infection experiments were lysed in RIPA buffer for 1h on ice and centrifuged for 15min at 14.000rpm and 4°C to separate cell debris (see chapter 2.2.2.1). After determination of the protein concentration approximately 150µg of total cell lysate was employed and adjusted with IP buffer to a volume of 1ml. The fresh supplements were added together with 5µg of the appropriate antibodies (see table 2.6) per sample. The samples were incubated over night at 4°C and gently agitated on a wheel to form immune complexes between the specific viral antigen and the antibody. The following day immune complexes were precipitated by Protein G-Sepharose. Therefore, 30µl protein G slurry was employed per sample. The beads were washed 3-times for 15min in cold 1x PBS and equilibrated in IP buffer without supplements for 20min. After centrifugation of the beads for 5min at 3000rpm and 4°C the supernatant was discarded and replaced with the 1ml samples. As control only lysate without antibody was added to the sepharose beads. For the specific binding of Protein

G to the Fc portion of the IgG antibodies to isolate immune complexes the samples were incubated for another 4 to 6h at 4°C on a rotating wheel.

After washing the samples 3-times in 2x PBS plus 0.1% Nonidet P-40, once in 1x PBS and once with MilliQ H_2O to remove unbound proteins, 30µl 2x SDS sample buffer were added. To elute bound proteins the samples were heated for 5min at 95°C and centrifuged at 3000rpm and 4°C for 5min. For analysis of ubiquitylation of viral proteins half of the eluate (15µl) was loaded on SDS-PAGE gels, blotted and stained with αubiquitin antibody from Dako. In order to investigate oxidation of virus proteins the DNPH reaction for the Oxyblot kit (see chapter 2.2.4) was modified. The 30µl beads coupled to immune complexes which were obtained after all washing steps were complemented with 15µl RIPA buffer, 6.4µl 20% (w/v) SDS and 21µl 1x DNPH. The reaction was incubated for 15min at room temperature and then stopped by adding 12.7µl of the neutralization solution and 5.5µl 1mM DTT. Subsequently, a mild elution for 10min at 80°C was carried out. Evaluation of the oxidation was performed by loading 40µl sample onto SDS-PAGE and immunoblot with the antibodies from the Oxyblot kit according to the manufacturer's instructions.

2.3.2.2 Co-immunoprecipitation

IP buffer: 50mM Tris-HCl, 50mM NaCl, 5mM $MgCl_2$, 0.1% (v/v) Triton X-100 and Complete, adjusted to pH 7.5 with NaOH + freshly added: 0.1% (v/v) Nonidet P-40 and 1mg/ml BSA

A similar protocol was used to test the incorporation of certain proteasome subunits into proteasome complexes. 200µg of total cell lysate were adjusted with IP buffer to a total volume of 500µl. The specific αalpha2 antibody (MCP21, see table 2.6) was used to pull out proteasome complexes. Washing of the Protein G sepharose, incubation to form immune complexes and elution was performed as described above (chapter 2.3.2.1). 30µl of the eluate were loaded on SDS-PAGE and analysed with different αproteasome antibodies.

2.3.3 Flow cytometry

Surface expression of MHC class I molecules was analysed by labelling cells with αHLA-A2-FITC or αHLA-A,B,C-PE antibodies. Pretreated cells were harvested, washed in PBS and counted. Per 96-well $1x10^5$ cells were seeded in 150µl PBS + 1% (w/v) BSA. The FACS antibodies were added in a dilution of 1:50 and incubated for 20min at 4°C in the dark. Thus, unbound antibody was removed by washing twice with 200µl PBS. Finally, the cells were taken up in 200µl PBS, filled in FACS tubes and measured with a FACSCalibur™ flow cytometer from BD Bioscience.

2.3.3.1 DCFH-DA staining – Quantification of ROS

Induction of ROS after virus infection was quantified by FACS analysis using an adjusted protocol. Directly after infection cells were treated with 10µM 2'-7'-dichlorofluorescin diacetate (DCFH-DA) from Sigma Aldrich which was de-esterified intracellulary by reactive oxygen species into highly fluorescent dichlorofluorescein. $1x10^5$ cells were grown in 24-well cell culture plates, washed once with 500µl HBSS and incubated with 10µM DCFH-DA in 500µl medium without FCS for 30min in the dark at 37°C.

Afterwards, cells were washed twice with 500µl HBSS, harvested with Trypsin/EDTA and diluted in 500µl medium in order to transfer them into FACS tubes. Dichlorofluorescein was measured in the FITC channel of a FACSCalibur™ flow cytometer from BD Bioscience.

2.3.4 Immunofluorescence

Cells were grown in 24-well cell culture plates and allowed to adhere to cover slides. After viral infection for indicated time points the cells were fixed and permeabilized with ice-cold methanol for 5min at -20°C and subsequently blocked with 3% FCS in PBS for 30min at room temperature. The staining with primary and fluorescent secondary antibodies (see table 2.6) was carried out in each case for 1h at room temperature and in between washed 3-times with PBS. Nuclei were stained with DAPI in a dilution of 1:1000 for 5min. The Immunofluorescence analysis was performed with a Leica DMR microscope.

2.4 Molecular biological methods

2.4.1 Primer

Primers employed for standard RT-PCR were generated by BioTeZ GmbH in a scale of 0.01µmol. Used primers are listed in table 2.8. Stock solutions were constituted in MilliQ to 50µM and stored at -20°C. In standard PCR a final concentration of 4µM of each primer was applied. For real time PCR primers were purchased from Applied Biosystems.

Primer	*Forward sequence*	*Reverse sequence*
Nox1	CTGGAGAGAATGGAGGCAAG	TTAACAGCACGCTGATCCTG
Nox4	CTTCCGTTGGTTTGCAGATT	TGGGTCCACAACAGAAAACA
GAPDH	ATGGGGAAGGTGAAGGTC	TTACTCCTTGGAGGCCATG

Table 2.8 Self-designed Primers for RT-PCR were ordered from BioTeZ GmbH.

2.4.2 Preparation of RNA and cDNA synthesis

Total RNA was extracted from frozen cell pellets using the High Pure RNA Isolation kit (Roche Diagnostics). Absorption at 260nm was measured to determine the RNA concentration with the following formula c (µg/ml) = 40*dilution factor*A260nm. Total RNA was stored at -80°C. 1µg total RNA was reverse transcribed using the First Strand cDNA synthesis kit (Roche Diagnostics) with oligo(dT) primers and reverse transcriptase according to manufacturer's instructions.

2.4.3 Standard PCR

The FastStart High Fidelity PCR System from Roche was applied together with primers from Biotez (see table 2.8) according to the manual. The PCR program was employed as described below, the annealing temperature was adapted to the melting temperature of the used primer pair.

	5min	95°C	denaturation
35cycles	30sec	95°C	
	30sec	55-60°C	annealing
	45sec	72°C	DNA polymerization
	7min	72°	
	∞	4°C	

6x DNA sample buffer: 50% (v/v) glycerine, 50mM EDTA, 0.25% (w/v) bromophenol blue

1x TAE buffer: 40mM Tris, 1mM EDTA, 20mM acetic acid

The PCR products were supplemented with 6-fold DNA sample buffer and separated electrophoretically on 1.5% to 3% agarose gels at 60V. The gels were stained with SYBR® safe DNA gel stain (Invitrogen) and visualized under UV light. To estimate the size of separated bands the 1kb DNA ladder from Invitrogen was used as molecular weight standard.

2.4.4 Taqman® real-time PCR

Real-time PCR in order to quantify mRNA levels of different genes after viral infection was performed in duplicates using primers and probes of TaqMan® Gene Expression Assays (Applied Biosystems) with a Rotor Gene 3000 (Corbett Research). Firstly, relative amounts of each gene were acquired and calculated with comparative cycle threshold values using the Rotor Gene Monitor Software (version 4.6) and normalised to an endogenous reference (HPRT1, hypoxanthine phosphoribosyltransferase 1). Further, for the analysed target genes cDNA was amplified and sub-cloned into the pCR2.1-TOPO TA-cloning vector (Invitrogen), which was performed by Dr. Frédéric Ebstein. The resulting plasmids were then linearized and used to prepare an 8-fold dilution series of amplification standards from 5×10^5 to 328 copies per µl in order to calculate quantitative mRNA amounts.

2.4.5 Microarray and data analysis

For microarray analysis isolated total RNA (see 2.4.2) was previously tested on a RNA gel. The human U133 2.0 Plus-Array (Affymetrix) was custom hybridized and evaluated by standard procedures from Signature Diagnostics AG. The data discussed in this thesis have been deposited in NCBIs Gene Expression Omnibus (GEO, http://www.ncbi.nlm.nih.gov/geo/) and are accessible through GEO Series accession number.

3. Results

Addressing the key questions which were raised in this thesis focus was laid on the model system of HCMV infection in permissive, primary fibroblasts. Later, investigation of particular interesting aspects was expanded to influenza A infection. Prior to the actual experiments virus infection in the appropriate cell culture system had to be established. Especially for the analysis of chronological events inside the target cells which are initiated in a very early phase of infection directly by entry of virus particles into the cells the temporal reliability of infection had to be assured.

In a first step the course of i-proteasome induction in response to virus infection and the nature of *de novo* formed proteasome complexes were scrutinized. Attention was drawn to the generation of mixed-type proteasome complexes containing constitutive as well as i-subunits and their role during the processing of viral epitopes. Thereby, very early time points of infection starting two hours post infection were included. The second point was subjected especially to the induction of i-proteasomes in response to HCMV infection. Little is known so far about the viral components or the cellular receptors which interact in order to initiate an eminent early immune response. In this work crucial roles of the type I interferon response and the transcription factor IRF3 were explored. The last part of this thesis comprised a detailed analysis of the processing of viral antigenic peptides beginning with the HCMV pp65 model antigen and later pointing out potential general mechanisms. During the investigations the DRiP hypothesis was revisited and prominent aspects of ubiquitylation and oxidation as well as their impact on epitope generation were examined.

3.1 Synchronising viral infection

In order to analyse kinetic effects of viral infection on the ubiquitin proteasome system and the MHC class I antigen presentation there was the prerequisite to establish a reproducible virus infection with a certain multiplicity of infection and certain duration. For the latter demand the process of infection needed to be synchronized. Therefore, the respective cells were subjected to an improved infection procedure which is described in chapter 2.1.5 and was adapted from Anne Halenius. This procedure provided a timely focused virus entry which played a role especially in the case of the bigger HCMV particles (about 200nm in diameter).

Synchronicity and multiplicity of infection was proven by staining for structural and non-structural viral proteins in Western blot. The HCMV phosphoprotein pp65 is a late expressed protein in the viral gene expression cascade, but also a structural component of the virus particle (Crough and Khanna, 2009; Mocarski, 2002; Stinski, 1978). As shown in figure 3.1A the structural protein pp65 was constantly detected during the whole time course of infection. The remarkable increase of pp65 levels observed after 24h post infection might be attributed to de novo synthesis of pp65, this hypothesis will be examined later in chapter 3.2.2. The pp72 viral protein is an immediate early viral protein which is not incorporated in the virion. A pp72 band in western blot was visible after 4h known as the time point of expression of immediate early genes in the HCMV gene expression cascade (Stinski, 1978).

For influenza A infection protein levels of the matrix protein M1 and the non-structural protein NS1 were assessed by Western analysis. While M1 as a structural component of the virus particle was detected during the whole time course using a longer exposure of films to the immunoblots, the NS1 protein was only detected after 6hpi (figure 3.1B), the time point of de novo synthesis of NS1 (Palese and García-Sastre, 1999). Likewise, M1 is newly synthesized approximately after 6h of influenza A infection, which could be recognised in immunoblot by the significant increase of M1 protein levels after this time point.

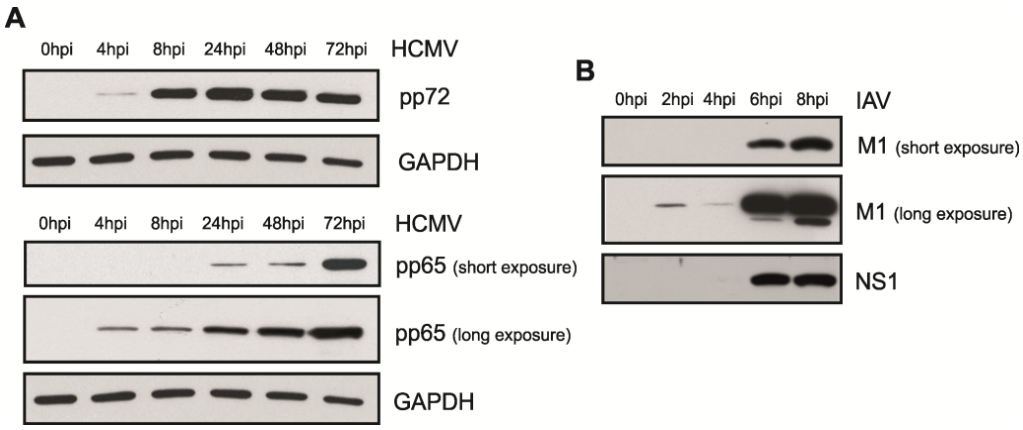

Figure 3.1 Levels of structural and non-structural viral proteins during the course of infection. A) Pp72 (upper panels) and pp65 (lower panels) protein levels analysed by immunoblot with αpp72 and αpp65 antibody, respectively, during the time course of HCMV Ad169 infection in MRC5 fibroblasts (short and long exposure time). Staining with αGAPDH antibody served as loading control. B) Immunoblot analysis of the structural matrix protein 1 (M1) and the non-structural protein 1 (NS1) during the course of influenza A virus (IAV) infection in HeLa cells (IAV data provided by Theresa Bergann).

3.2 The Mystery of the very early CTL response

The $pp65_{495\text{-}503}$-specific CTL clone, whose generation is described in chapter 2.1.6, was used to study the generation of the immunodominant $pp65_{495\text{-}503}$ epitope in HCMV-infected target cells during a time course. In this work for the first time the very early kinetics immediately after entry of virus particles into the target cell was investigated. Surprisingly, presentation of the $pp65_{495\text{-}503}$ epitope was observed on the surface of infected MRC5 fibroblasts as early as 2h post infection. Remarkably, the strongest presentation of about 60 to 70% of peptide loaded target cells was reached between 2 and 4hpi. After 24 to 72hpi a significant decrease in epitope presentation occurred (figure 3.2A black bars) which can be attributed to the expression of immunomodulatory gene products of HCMV discussed in chapter 4.

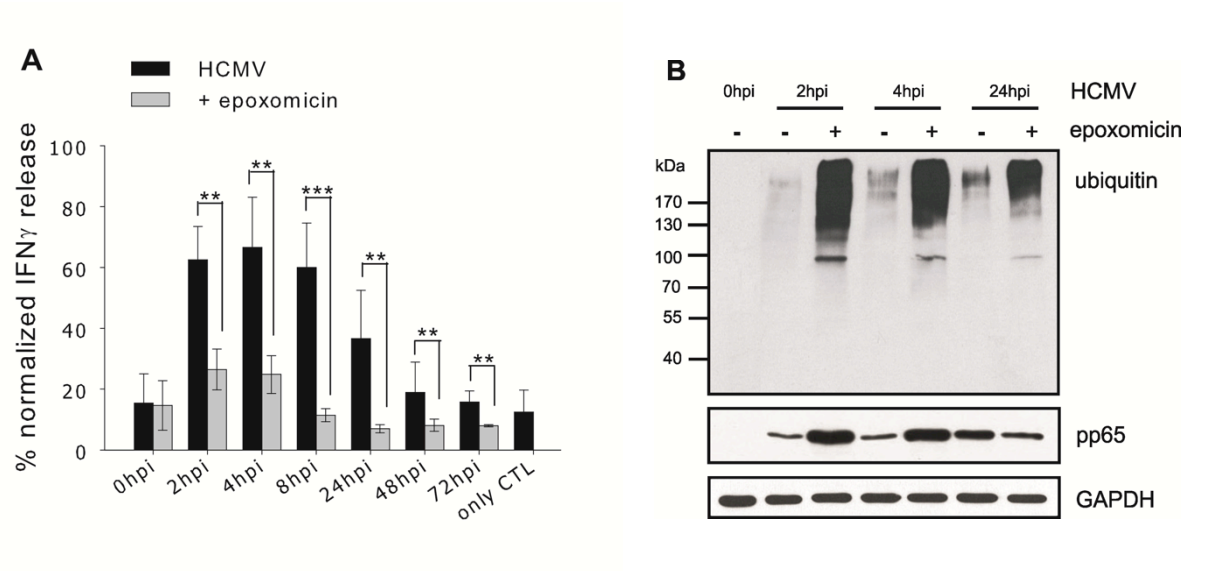

Figure 3.2 Presentation of the pp65$_{495-503}$ epitope is proteasome-dependent. MRC5 were infected with HCMV Ad169 at moi 5 for indicated time points. 200nM proteasome inhibitor epoxomicin was applied directly after infection. A) pp65$_{495-503}$ specific CTL assay analysis comparing infection of untreated MRC5 (black bars) with epoxomicin treated cells (grey bars). IFNγ release by effector T cells was measured by ELISA and displayed as percentage of the response received by loading MRC5 with 1µg/ml pp65$_{495-503}$ peptide (n = 6 of 3 independent experiments; error bars represent standard deviation ±SD; ** p<0.01 *** p<0.001). B) Effect of 200nM epoxomicin on the accumulation of poly-ub conjugates and of the viral protein pp65 2h, 4h and 24h post HCMV infection displayed by immunoblot with αubiquitin (FK2), αpp65 and αGAPDH antibody serving as loading control.

3.2.1 Support by the proteasome

In a publication of Besold and colleagues in 2007 a proteasome dependent presentation of the pp65$_{495-503}$ epitope was observed (Besold et al., 2007). To assess whether this also applies to the generation of the immunodominant pp65$_{495-503}$ epitope in the employed model system in this work cells were treated directly after viral infection with 200nM of the proteasome inhibitor epoxomicin. Epoxomicin represents a specific inhibitor of both the standard and i-proteasome by irreversible and covalent binding to the β2 and β5 catalytical subunits (Meng et al., 1999). A significant decrease of antigen presentation at each time point throughout the course of HCMV infection was observed (figure 3.2A grey bars). By Western blot analysis proper epoxomicin activity was confirmed due to the accumulation of poly-ub conjugates (figure 3.2B). Moreover, an accumulation of pp65 at the early time points 4 and 8hpi was observed which suggests that the epitope generation was affected on the level of proteasomal degradation. After 24hpi pp65 protein levels were reduced, at this time point de novo generation of pp65 in the viral gene expression cascade starts which is known to be blocked by proteasome inhibitors (Kaspari et al., 2008; Tran et al., 2010).

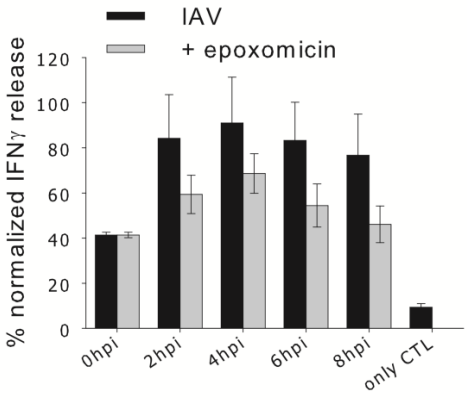

Figure 3.3 Presentation of the $M1_{58-66}$ epitope is dependent on proteasomal activity. HLA-$A2^+$ HeLa cells were infected with IAV at moi 5 during a time course of 0 to 8hpi. 200nM proteasome inhibitor epoxomicin was added directly after infection to each sample. $M1_{58-66}$ specific CTL response was measured by IFNγ release in an ELISA and displayed as percentage of the response received by loading cells with 1µg/ml $M1_{58-66}$ peptide (n = 3 of 2 independent experiments, error bars represent ±SD).

An analogous experiment was performed for the presentation of the immunodominant $M1_{58-66}$ epitope after influenza A infection. Stably transfected HLA-$A2^+$ HeLa cells were infected with influenza A virus for several time points and treated directly after infection with 200nM epoxomicin. The $M1_{58-66}$-specific CTL clone was used to assess epitope presentation. Again at each time point of infection antigen presentation decreased about 20 to 30% (figure 3.3). Presumably, also the generation of the $M1_{58-66}$ epitope was dependent on proteasomal degradation of M1.

3.2.2 Where the $pp65_{495-503}$ epitope derives from

3.2.2.1 UV-inactivation and Cycloheximide treatment reveal the source of pp65

Since pp65 represents a late transcribed gene in the viral gene expression cascade whose expression begins not earlier than 24hpi (Stinski, 1978), the question arises where the pp65 epitope derives from at earlier time points of infection. The onset of pp65 de novo synthesis in the course of the viral gene expression cascade at 24hpi was observed by western analysis of pp65 protein levels in total cell lysate of infected fibroblasts using short exposure times (figure 3.1A, lower panels). The occurrence of pp65 at early time points by using longer exposure in western analysis suggested the detection of non-translated pp65, since pp65 is a structural component of the virus, incorporated in the virus particle and delivered to the cytoplasm of the infected host cell during the virus entry process (McLaughlin-Taylor et al., 1994).

Therefore, two different approaches were used to block translation: i) treatment of the infected host cell with translation inhibitor cycloheximide and ii) in a more sophisticated approach by UV inactivation of the virus particles. Ten minutes of UV irradiation destroyed the viral genome while the virus proteins remained intact. Firstly, total cell lysate of cycloheximide pretreated cells was analysed by immunoblot. To verify translation inhibition blots were stained for the transcription factor p53, which is known to represent an unstable, short-lived protein but also to be induced during HCMV infection (Fortunato and Spector, 1998). The tumour suppressor and cell cycle regulator p53 was induced already 2h after HCMV infection and its expression was further increased at 4hpi. The induction was abolished by application of cycloheximide. As well the expression of pp72, an immediate early viral

gene product translated at 4hpi, was blocked after cycloheximide application. In contrast, protein levels of pp65 remained unaffected (figure 3.4A). Infection with UV-inactivated virus was similarly tested by assessing protein levels of the nonstructural pp72, which could not be detected, while pp65 protein levels were steady (figure 3.4B). The Western analysis revealed also slightly increasing pp65 levels at the early time points from 2 to 8hpi. This induction was not attributed to *de novo* translation, since UV inactivation and translation inhibitor completely abolished pp72 and p53 expression while not affecting pp65 levels, but to ongoing infection i.e. the entry of virus particles into cells thereby enlarging the cellular pp65 pool.

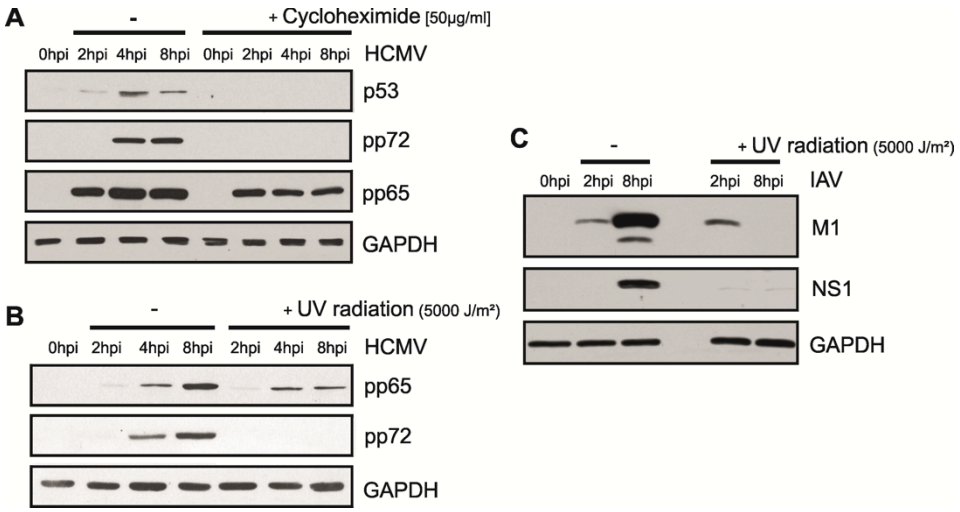

Figure 3.4 Inhibition of translation by cycloheximide application and UV-inactivation. A) MRC5 fibroblasts were left untreated or were pre-treated with 50µg/ml cycloheximide 1h prior to infection with HCMV Ad169 at moi 5. Total cell lysate was stained in immunoblot for the late expressed HCMV protein pp65 and the immediate early HCMV protein pp72. Further, tumor suppressor protein p53 was stained to prove translation inhibition. B) Infection of MRC5 with either wild-type virus or UV-irradiated HCMV at moi 5. C) Infection of HeLa cells with IAV at moi 5. Total cell lysate was employed for immunoblot with αM1 and αNS1 antibodies. αGAPDH served as loading control (IAV blots provided by Theresa Bergann).

A similar experimental approach was followed for the influenza A infection in order to analyse the origin of the $M1_{58-66}$ epitope. The matrix protein M1, likewise pp65, presents a structural component of the virus particle. Similarly, M1 could be found in the cytoplasm of infected cells before it is synthesized *de novo*, which is reported to occur around 6hpi (Palese and García-Sastre, 1999). Using long exposure times for the detection of M1, the viral protein was found already 2hpi in total cell lysate of infected HeLa cells, with a remarkable increase at the time point of M1 de novo synthesis (figure 3.4C, upper panels). When cells were infected with UV-irradiated influenza virus matrix protein 1 was still found at early time points of infection but not in later stages, when de novo synthesis should occur which was presumably blocked due to the UV inactivation. As control served the nonstructural viral protein NS1 which was expressed as seen in the lower panel after 8h and not detected earlier. NS1 expression was abolished after infection with UV-inactivated virus (figure 3.4C, lower panels). Hence, the presence of both viral proteins, pp65 and M1, at early time points of infection was independent of

translation, but dependent on the delivery of these proteins to the cytoplasm of the host cell during the virus entry process.

To complete the picture, the presentation of the $pp65_{495-503}$-epitope assessed by CTL assay of 4 and 8h HCMV-infected fibroblasts either treated with 50µg/ml translation inhibitor cycloheximide or infected with UV-irradiated virus was also unchanged and still reached 70 to 80% (figure 3.5). Together with the biochemical analysis it became clear that the $pp65_{495-503}$ epitope presented on the cell surface at the early time points was not newly synthesized in the infected host cells, but had to derive from structural components of the virus particles. The tegument protein was directly delivered into the cytoplasm of the cell during the virus entry process and thereby gained access to the antigen processing machinery before the viral gene expression started, which has been postulated already in 2000 by Matthias Reddehase (Reddehase, 2000).

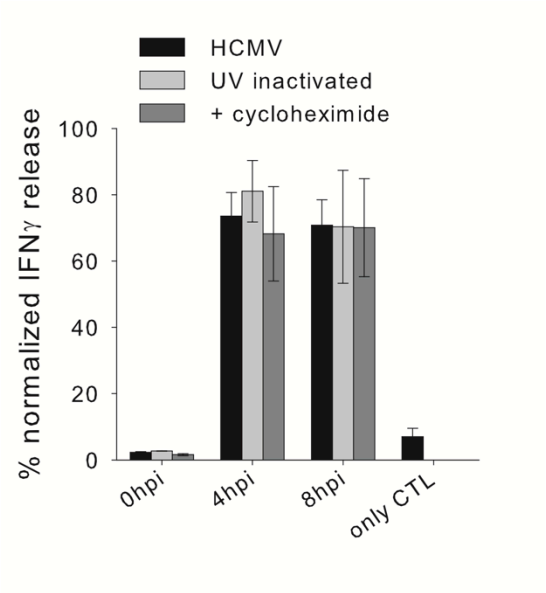

Figure 3.5 Translation-independent generation of the $pp65_{495-503}$ epitope. CTL assay analysis of MRC5 cells infected for 4h and 8h with HCMV Ad169 comparing UV-inactivated virus or pretreatment of cells with 50µg/ml cycloheximide 1h prior to virus infection. IFNγ release by $pp65_{495-503}$ specific CTL was measured by ELISA and displayed as percentage of the response received by loading MRC5 with 1µg/ml $pp65_{495-503}$ peptide (n = 5 of 2 independent experiments, error bars represent ±SD).

3.3 What happens in the infected cells?

As it is outlined in chapter 1.5 virus infection inflicts several profound changes in the infected cell, primarily on the transcription and translation of many cellular genes. In this work, focus was laid firstly on effects on the ubiquitin proteasome system. Therefore, an Affymetrix microarray analysis was performed to monitor cellular gene expression in uninfected and 4h HCMV-infected MRC5 fibroblasts, as well as in uninfected and 4h IAV-infected HeLa cells. Already in a publication from Zhu et al. expression of around 6600 human mRNAs was analysed in primary human foreskin fibroblasts after 8h and 24h infection with HCMV Ad169 (Zhu et al. 1998). They observed an induction of several UPS genes and among these a 4-fold induction of β5i mRNA 8h after HCMV infection. Similarly, in this thesis a significant upregulation of UPS components such as i-subunits and ubiquitylation enzymes was observed (see attachment).

3.4 Proteasomal adaptation

Type I interferons, IFNα and IFNβ, and type II interferon IFNγ, but also heat stress or viral infection induce the expression of the i-subunits, β1i, β2i and β5i (Callahan et al., 2006; Jamaluddin et al., 2001; Shin et al., 2006), and their subsequent incorporation into nascent proteasome complexes in order to form i-proteasomes (Frentzel et al., 1994; Groettrup et al., 1997; Nandi et al., 1997). In professional antigen presenting cells (APC) the i-proteasome represents the predominant type of proteasome, while in non-lymphoid organs the expression of i-proteasome does not exceed 60% (Strehl et al., 2006). Moreover, mixed-type proteasome complexes containing constitutive as well as i-subunits are reported (Dahlmann et al., 2000; Griffin et al., 1998). Likewise, an induction of the proteasome activator PA28 is reported in response to IFNγ stimulation (Ahn et al., 1995). In this thesis, formation of mixed-type proteasomes and induction of PA28 during viral infection were elucidated.

3.4.1 HCMV infection induces the formation of mixed-type proteasomes and the proteasome activator complex PA28

The examination of the cellular proteasome pool in infected cells during HCMV infection approved the results from microarray studies and revealed a very fast induction of mixed-type proteasome complexes as well as of the proteasome activator PA28. Real-time PCR analysis confirmed that expression of the i-subunits β5i and β2i as well as of both PA28 subunits α and β was induced on mRNA-level 4hpi and strongly reduced after 24hpi (figure 3.6A). In contrast, transcripts of the constitutive subunit β7 were only slightly but continuously elevated. An induction of the third IFNγ-inducible, catalytical subunit β2i could not be detected in RT-PCR.

In Western analysis immediately after HCMV infection a significant increase of protein levels of the i-subunits β5i and β1i, but in line with the results of real-time PCR analysis no increase for the β2i subunit was observed (figure 3.6B densitometric analysis and figure 3.6C selected blots). The densitometric analysis of several experiments showed a significant increase in the expression of both subunits within 4h followed by a reduction after 72h, known to be dependent on downregulation mediated by HCMV immune escape mechanisms (Kahn et al. 2003). The β5i antibody detected a total of three bands, the band at 30kDa represented the proprotein which was cleaved in a two-step autocatalytic process to remove the propeptide and liberate the active site threonine of the mature β-subunit (Nandi et al., 1997; Schmidtke et al., 1996; Schmidtke et al., 1997). In case of the β5i subunit the mature protein occurs in two isoforms at 22.6kDa and 21.3kDa. The β1i antibody was proven to recognise the i-subunit β1i at 21.3kDa as well as the constitutive subunit β1 at 22.6 kDa.

Similarly, an induction of PA28α and PA28β was observed between 4 and 24hpi. In contrast, the expression of the constitutive proteasome subunit α4 showed a continuous increase. Moreover, a transient induction of the proteasome maturation protein (POMP) which is essential for the incorporation of the expressed i-subunits β5i and β1i (Heink et al., 2005) was observed (data not shown). Hence, the formation of functional i-proteasomes was verified by co-immunoprecipitation (figure 3.6D). By precip-

itating the constitutive subunit α2 and staining against β5i and β1i the formation of mixed-type proteasome complexes was proven during the whole course of virus infection.

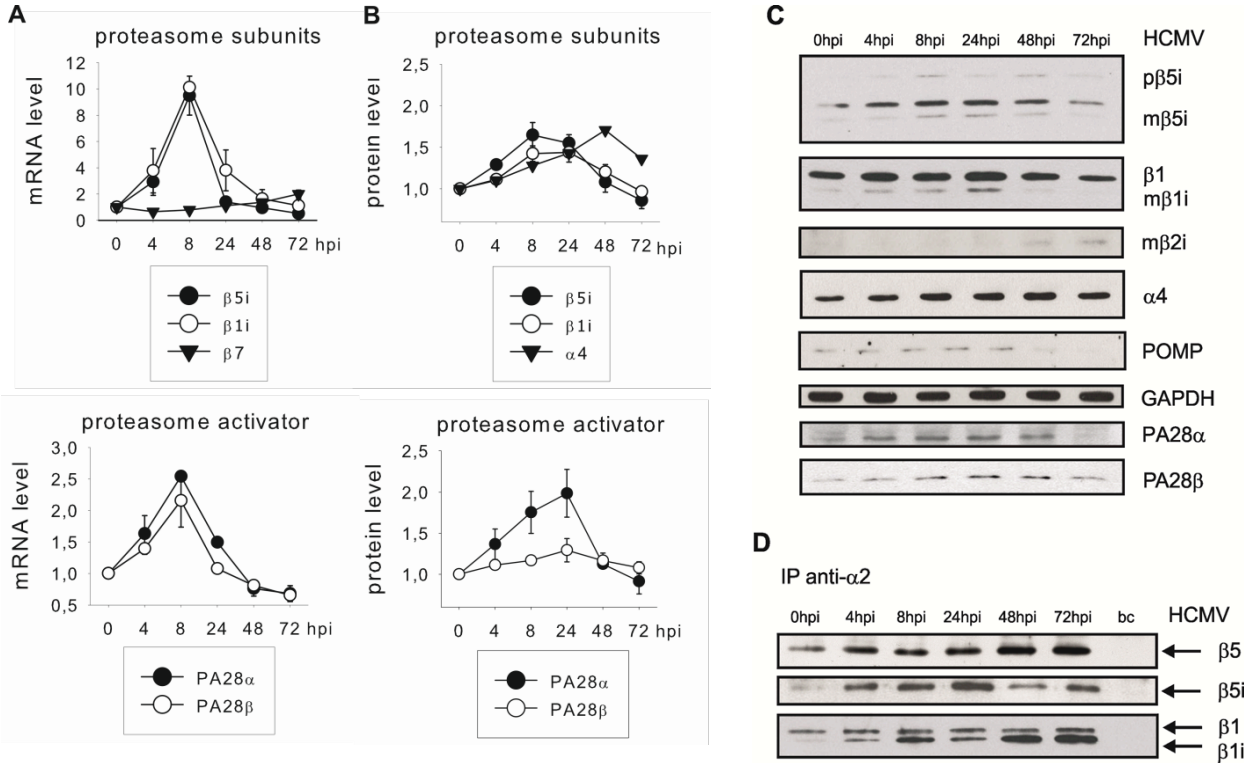

Figure 3.6 HCMV infection induces the formation of mixed-type proteasome complexes. MRC5 fibroblasts were infected with HCMV Ad169 at moi 5 for the indicated time points. A) Real-time PCR analysis of β5i, β1i and β7 mRNA (upper graph) as well as PA28α and PA28β mRNA (lower graph). Results were expressed as average fold change from uninfected MRC5 (mean values of 3 experiments, normalised to HPRT1, error bars represent ±SD. B) Densitometric analysis of β5i, β1i and α4 protein levels (upper graph) as well as PA28α and PA28β in Western blot (lower graph), (n = 6 experiments, normalised to GAPDH, error bars show ±SD). C) Selected immunoblots showing the induction of i-subunits (precursor p and mature m proteins are indicated), constitutive subunit α4 and both PA28 subunits. GAPDH served as loading control. D) Co-Immunoprecipitation of proteasome complexes with α-α2 antibody and staining in Western analysis against β5/β5i and β1/β1i.

The appearance of functional i20S complexes in response to HCMV infection was further verified by performing Native Page analysis. The electrophoretic separation resulted in discrimination of free 20S complexes, 20S associated with PA28 activator and 20S associated with 19S regulator attached to one end constituting the 26S proteasome or to both ends composing 30S complexes. Further, an attachment of PA28 to one end and 19S to the other end of the barrel-shaped 20S core was possible thus forming hybrid proteasome. The different proteasome complexes were visualized in an activity overlay with the Suc-LLVY-AMC substrate reflecting chymotryptic activity (figure 3.7). Immunoblot and incubation with fluorescent antibodies raised against β5i and β1i proved the incorporation of these i-subunits during the course of infection and showed a continuous increase. Apparently, the downregulation of i-subunit expression on the transcriptional level mediated by immunomodulatory gene products of HCMV (Khan et al., 2004) did not affect the percentage of i-proteasomes to the overall cellular

proteasome pool. Not all proteasome complexes from the gel could be detected in the according immunoblots. I-subunits seemed to be incorporated in a higher amount in free 20S or 20S complexes associated with PA28 than in 26S or 30S proteasomes, whereby methodical complications, due to the dissociation of 19S during the preparation of the lysates, could not be ruled out during this thesis.

Therefore, the formation of mixed-type proteasome complexes at the early time points from 4 to 24hpi containing β5i and β1i but no β2i and the partial formation of complexes with PA28 was concluded.

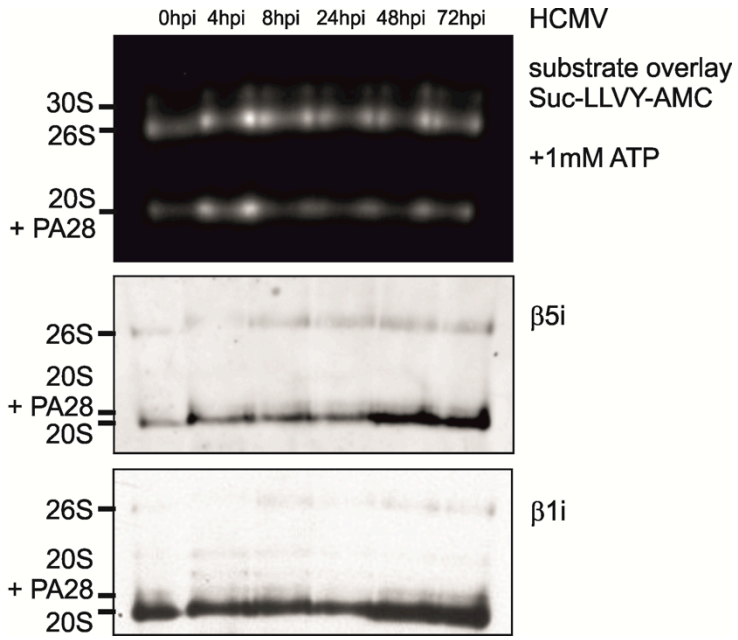

Figure 3.7 Incorporation of i-subunits in active proteasome complexes in response to HCMV infection. MRC5 cells were infected for indicated time points with HCMV Ad169 at moi 5. Total cell lysate was applied to Native PAGE analysis. Substrate overlay of Native Gel with 1μM Suc-LLVY-AMC under addition of 1mM ATP. Native Blots were incubated with α-β5i and α-β1i antibodies.

3.4.2 It's all in the mix

To verify whether the formation of mixed-type proteasome complexes also had an impact on the generation of the $pp65_{495-503}$ epitope, the expression of i-subunits β5i and β1i was knocked down and $pp65_{495-503}$-epitope presentation was monitored 4h post infection when being at maximum. For this purpose, target cells were preincubated 48h prior to virus infection with 25nM PSMB8 and PSMB9 siRNA. The downregulation of each subunit alone as well as in combination negatively affected the antigen presentation (figure 3.8A). Compared to the treatment with OFF-target control siRNA the knockdown of β1i with PSMB9 siRNA caused a reduced epitope presentation of approximately 25%, while the downregulation of β5i expression with PSMB8 siRNA resulted in almost 40% decreased presentation and treatment with both siRNAs together in an even stronger reduction of about 46%. The knockdown was verified by immunoblots with α-β5i and -β2i antibody (figure 3.8B). The expression of the constitutive subunit α4 was not affected by knockdown of both i-subunits. The protein levels of pp65 slightly accumulated due to downregulation of i-subunit expression in infected cells presumably due to decreased proteasomal degradation of pp65.

In conclusion, the effect on the presentation of the $pp65_{495-503}$ epitope demonstrated a supporting role of mixed-type proteasome complexes containing the β5i and β1i subunit for the generation of this epitope.

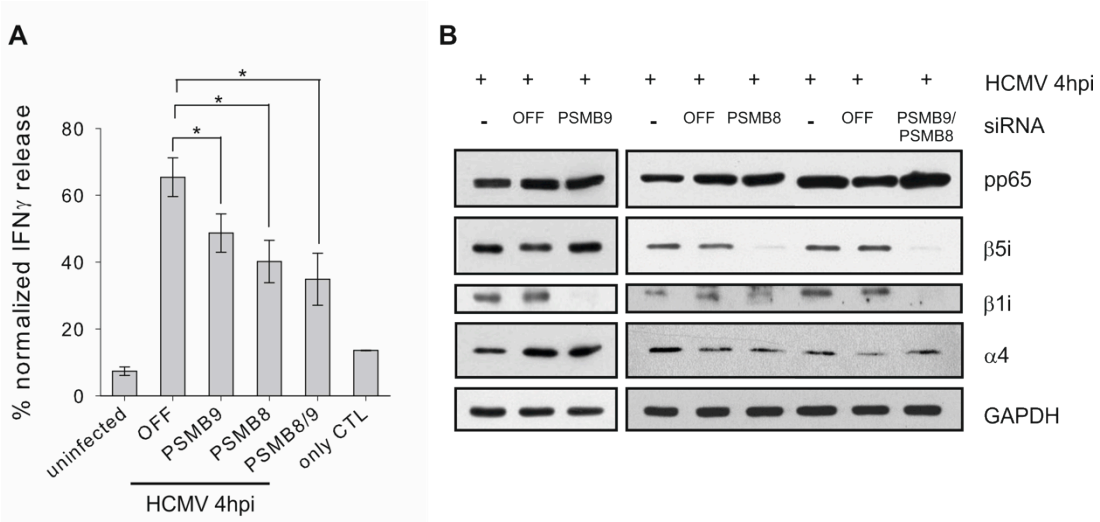

Figure 3.8 Mixed-type proteasomes support the generation of the $pp65_{495-503}$ epitope. MRC5 cells were infected with HCMV Ad169 at moi 5 for 4hpi. 25nM OFF-target, PSMB8 and PSMB9 siRNA was applied 48h prior to infection. A) IFNγ release by $pp65_{495-503}$ specific CTL was measured by ELISA and displayed as percentage of the response received by loading MRC5 with 1µg/ml $pp65_{495-503}$ peptide (n = 6 of 3 independent experiments; error bars represent ±SD; ∗ $p<0.05$). B) Western analysis of siRNA knockdown. α-α4 antibody was used to control equal amounts of proteasome, αGAPDH served as loading control.

3.4.3 With a little help from PA28

Moreover, a potential supporting role of proteasome activator PA28 for the generation of the $pp65_{495-503}$ epitope was tested. Downregulation of both PA28 subunits with PSME1 and PSME2 siRNA impaired the epitope presentation 4h post HCMV infection to a similar degree (figure 3.9A). Compared to treatment with OFF-target siRNA epitope presentation was reduced about 46%. The knockdown was confirmed in Western analysis with α-PA28α and α-PA28β antibodies. Application of either siRNA resulted in knockdown of each subunit (figure 3.9B) explaining the similar effect on antigen presentation when applying PSME1 and PSME2 siRNA alone or in combination.

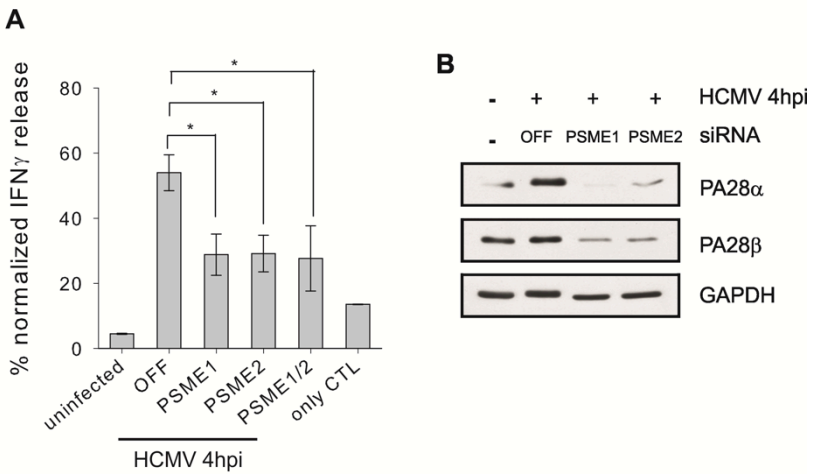

Figure 3.9 Proteasome activator PA28 supports the generation of the pp65$_{495-503}$ epitope. MRC5 cells were infected with HCMV Ad169 at moi 5 for 4hpi. 25nM OFF-target, PSME1 and PSME2 siRNA was applied 48h prior to infection. A) IFNγ release by pp65$_{495-503}$ specific CTL was measured by ELISA and displayed as percentage of the response received by loading MRC5 with 1µg/ml pp65$_{495-503}$ peptide (n = 4 of 2 independent experiments; error bars represent ±SD; ∗ $p<0.05$). B) Western analysis to confirm knockdown with α-PA28α and α-PA28β antibody. GAPDH served as loading control.

3.5 Induction of i-subunits in response to HCMV infection

In chapter 3.2.1 the induction of mixed-type proteasomes containing β5i and β1i subunits in a very early phase of infection, already 4hpi with HCMV Ad169, was shown. One aspect of this work was to shed light on the mechanisms leading to the immediate induction of i-subunit expression especially in response to HCMV infection. So far, controversial data is published about the induction of the innate immune response after HCMV entry into target cells. The investigations are complicated due to the ability of the virus to enter an extensive range of different cell types via different cell surface receptors which imposes the difficulty to identify cellular sensors. It is proposed that the initiation of the innate immune response, which comprises the induction of interferons as well as the secretion of cytokines, is directly linked to virus entry into the host cells (Compton et al., 2004). This assumption was verified in the here used model system of MRC5 infection with HCMV Ad169 by using UV-irradiated virus. A low dose of UV radiation keeps the virus particle intact, i.e. viral proteins remain functional, while the viral genome is destroyed so that no viral gene expression will occur.

HCMV particles attach to cell-type specific receptors which results either in fusion of the virus with the host cell membrane or uptake of virus particles via the endosomal pathway. At the end of the process viral components access the cytoplasm of the host cell where an unknown cellular sensor recognizes the virus particle and activates the IFN response. The recognition of viral PAMPs results amongst others in phosphorylation of the transcription factor IRF3 through Tbk1 and IKKε kinase. Activated IRF3 induces transcription of IFNβ and other ISGs. Thus, expression of IFNβ leads to further amplification via auto- and paracrin activation of the IFNα/β receptor and induction of the Jak/Stat pathway, which in turn leads to expression of further ISGs. In order to find out if this pathway is also responsible for the expression of i-subunits and PA28 in response to HCMV infection it was aimed to interfere with

this signaling cascade at different levels. Therefore, the Tbk1 and IKKε kinases, the IFNα/β receptor and the transcription factor IRF3 itself were targeted.

3.5.1 Independence of viral gene expression

Based on preliminary publications it was controlled whether transcriptional activation of i-subunits and PA28 was dependent on viral gene expression or whether the entry of the virus particle itself was sufficient to induce cellular gene expression. Therefore, viral gene expression was inactivated by UV irradiation and expression of i-subunits was analysed on mRNA as well as on protein level (figure 3.10). mRNA expression of the constitutive subunit β7, the i-subunits β5i and β1i as well as both PA28 subunits was unaltered by infection with UV-inactivated virus and no statistically significant differences were measured. Further, induction of the type I interferons IFNα and IFNβ was analysed on transcriptional level, and demonstrated for IFNβ expression in figure 3.10B. As early as 4hpi a strong increase was observed and no difference between infection with intact or UV-inactivated virus was noticed.

Protein levels were investigated by immunoblot 24h after HCMV infection (figure 3.10A). Strikingly, translation of the i-subunits as well as PA28α and PA28β was even more pronounced after infection with UV-inactivated virus, which can be explained by the missing expression of immunomodulatory HCMV gene products, so called immunevasins, which otherwise would interfere with the expression of i-subunits (Khan et al., 2004). The effectiveness of UV irradiation was proven by abolished pp65 expression 24hpi. Further, phosphorylation of Stat1 was assessed in Western analysis with αpStat1 antibody. The Jak/Stat pathway was activated in the amplification phase of the type I IFN response and was obviously also activated by infection with UV-inactivated virus.

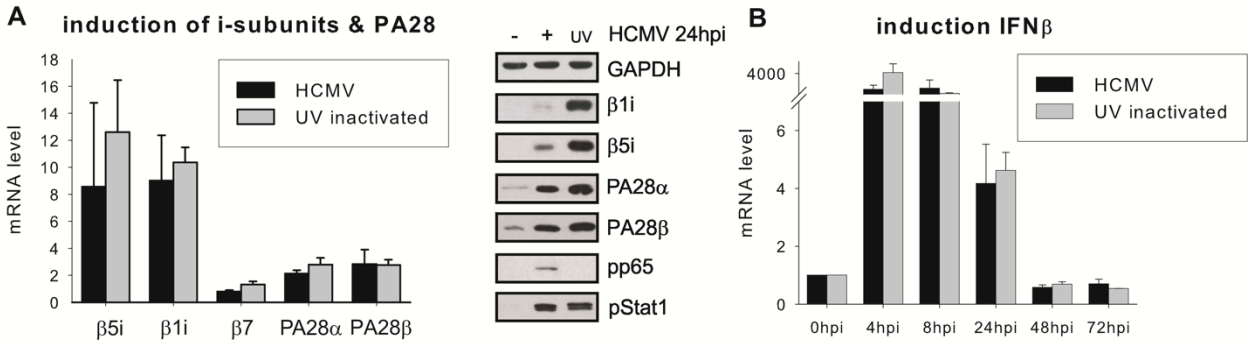

Figure 3.10 HCMV entry directly induces i-subunits. MRC5 were infected for 24h with either intact or UV-irradiated HCMV Ad169 at moi5. A) Real-time PCR analysis for the indicated genes comparing infection with intact (black bars) and UV-inactivated virus (grey bars). Results were expressed as average fold change from uninfected MRC5 (mean values of 3 experiments, normalized to HPRT1, error bars represent ±SD). Total cell lysate was subjected to immunoblot and incubated with indicated antibodies. GAPDH served as loading control. B) Real-time PCR analysis of IFNβ expression comparing infection with intact (black bars) and UV-inactivated virus (grey bars). Results were expressed as average fold change from uninfected MRC5 (mean values of 3 experiments, normalized to HPRT1, error bars represent ±SD).

In conclusion, the expression of i-proteasome and PA28 was independent of *de novo* synthesis of viral proteins, but dependent on structural components of the virion. Still it is unclear which cellular receptors or sensors are responsible for the detection of HCMV activating a pathway leading to expression of i-proteasomes.

3.5.2 Effects of kinase inhibitor BX-759 and IFNα receptor blocker

It is known that IRF3 is a key factor for the induction of ISGs and type I IFNβ during HCMV infection (DeFilippis et al., 2006). Subsequently, expression of IFNβ leads via auto- or paracrine activation of the IFNα/β receptor and the Jak/Stat pathway to expression of further ISGs. The question arose whether also the expression of i-proteasomes and PA28 was dependent on this signalling cascade.

Thus, the Tbk1 and IKKε kinases which phosphorylate the transcription factor IRF3 were inhibited by application of the kinase inhibitor BX-759. A second approach was to block the IFNα/β receptor with the monoclonal antibody MMAHR2. MMAHR2 is raised against the human interferon α/β receptor chain 2 and interacts with the extracellular domain, thereby neutralizing the receptor and blocking the biological action of type I IFNs. The cartoon in figure 3.11A shows the point of action of both inhibitors.

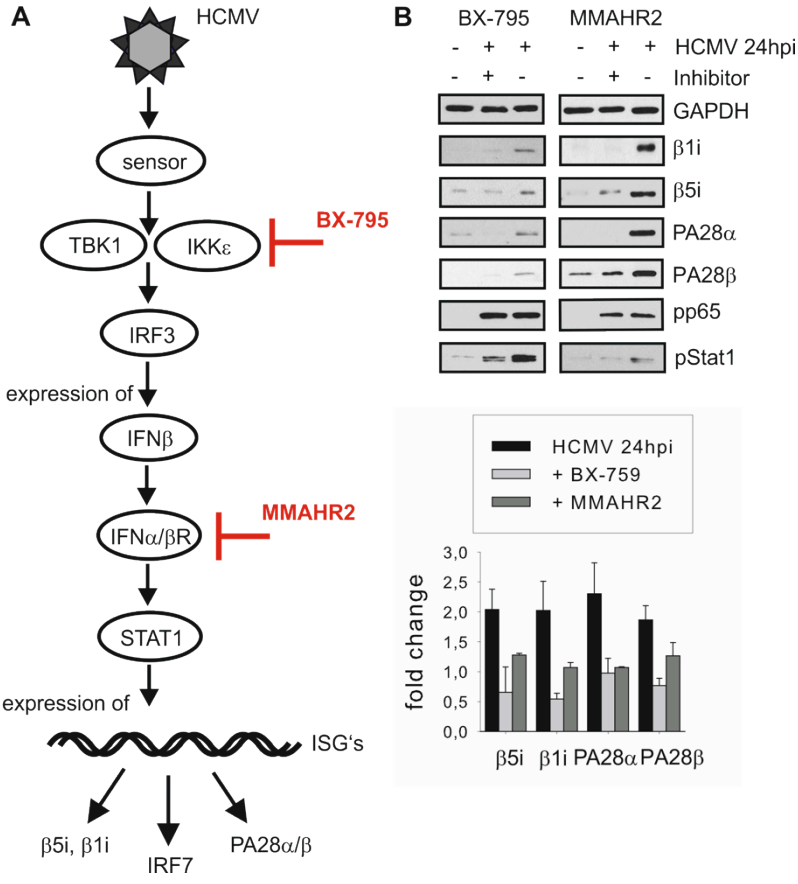

Figure 3.11 Effects of Tbk1/IKKε kinase inhibitor and IFNα/β receptor blocker on the expression of i-subunits and PA28. A) Cartoon illustrating the point of action of kinase inhibitor BX-795 and receptor blocker MMAHR2. B) MRC5 cells were incubated 1h prior to infection with 1µM BX-795 or 10µg/ml MMAHR2 and infected for 24h with HCMV Ad169 at moi 5. Total cell lysate was subjected to immunoblot with indicated antibodies. GAPDH served as loading control. Graph represents densitometric analysis of 3 experiments normalised to GAPDH (mean±SD).

When MRC5 fibroblasts were pretreated for 1h with Tbk1/IKKε kinase inhibitor or IFNα/β receptor blocker the expression of both i-subunits β5i and β1i as well as both PA28 subunits was strongly de-

creased or even abolished as measured in immunoblots 24h after HCMV infection. Moreover, Stat1 phosphorylation was downregulated in both cases, which proved that the Jak/Stat pathway downstream of the IFNα/β receptor was affected by both inhibitors (figure 3.11B).

Further, it was analysed if effects on the $pp65_{495-503}$-specific CTL response could be observed at very early time points of epitope presentation when expression of i-subunits and PA28 was downregulated by interference with this signalling cascade. Remarkably, application of 1µM BX-759 significantly decreased antigen presentation already 4hpi (figure 3.12). The effect of the neutralizing antibody MMAHR2 was slightly delayed, a significant negative effect was observed 8hpi.

Hence, the phosphorylation of IRF3 and the subsequent type I IFN response played an intriguing role for the induction of i-subunits and PA28 in response to HCMV infection and thereby also affected the processing of the immunodominant $pp65_{495-503}$ epitope.

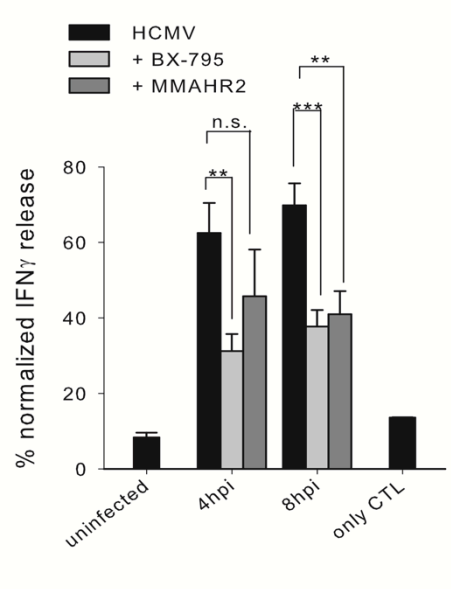

Figure 3.12 Inhibition of IRF3 phosphorylation and IFNα/β receptor activation negatively affects presentation of the $pp65_{495-503}$ epitope. MRC5 were incubated for 1h with 1µM BX-795 and 10µg/ml MMAHR2 and subsequently infected for 4 and 8h with HCMV Ad169 at moi 5. IFNγ release by $pp65_{495-503}$ specific CTL was measured by ELISA and displayed as percentage of the response received by loading MRC5 with 1µg/ml $pp65_{495-503}$ peptide (n = 6 of 3 independent experiments; error bars represent ±SD; n.s. not significant, ** $p<0.01$, *** $p<0.001$).

3.5.3 Key role for transcription factor IRF3

Due to the prominent effect of kinase inhibitor BX-795, which was supposed to block the phosphorylation of IRF3 through Tbk1 and IKKε kinase, further experiments were focused on this transcription factor. siRNA-mediated depletion of IRF3 was chosen to investigate the role of IRF3 during the innate immune response to HCMV. Real-time PCR analysis as well as Western analysis revealed that downregulation of IRF3 by siRNA was accompanied by downregulation of β5i, β1i as well as PA28α and PA28β on mRNA and protein level (figure 3.13). Also transcription of IFNβ and IRF7, known to be induced after virus infection via this pathway (Kawai and Akira, 2007), was strongly decreased as expected due to knockdown of IRF3 (figure 3.13A). Abolished IRF3 expression and subsequently reduced Stat1 phosphorylation was verified in Western analysis (figure 3.13B). Moreover, a CAT-β1i promoter construct was used to investigate whether IRF3 was essentially required to initiate expression of β1i in response to HCMV infection. MRC5 fibroblasts were therefore firstly incubated for 48h

with either 25nM OFF-target or IRF3 targeting siRNA. Subsequently, the cells were transfected with the CAT-promoter construct and a pcDNA3.1/lacZ plasmid serving as transfection control. After incubation for further 24 hours the cells were infected for 8h with HCMV Ad169. The determination of the received CAT concentrations showed a significant reduction of the β1i promoter activity after IRF3 knockdown (figure 3.13C).

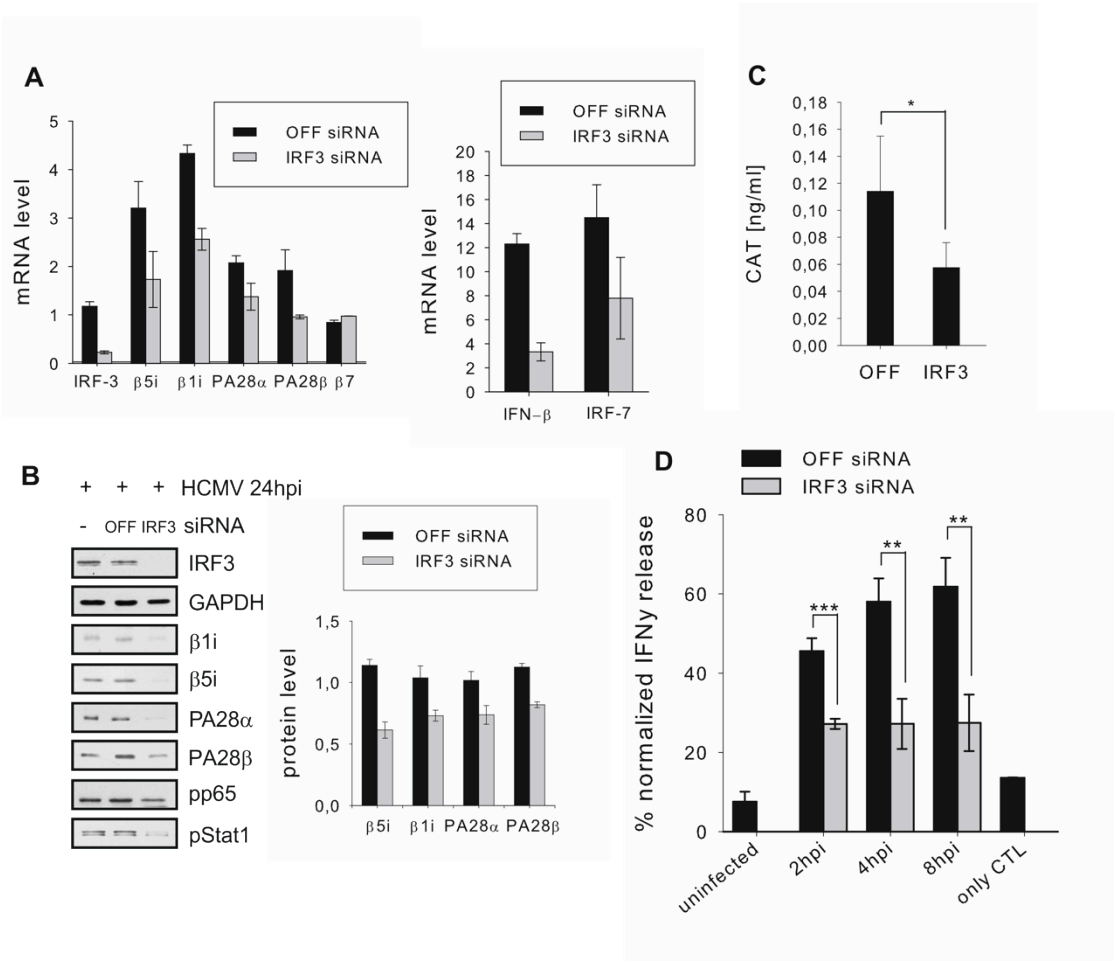

Figure 3.13 Intriguing role for IRF3 in HCMV-induced expression of i-proteasome and PA28. MRC5 were incubated for 48h with 25nM OFF-target or IRF3 siRNA and subsequently infected for indicated time points with HCMV Ad169 at moi 5. A) Real-time PCR analysis of indicated genes 24h after infection. Results were expressed as average fold change from uninfected MRC5 (mean values of 3 experiments, normalized to HPRT1, error bars represent ±SD) B) Western analysis of indicated proteins 24h after infection. GAPDH served as loading control. Graph represents densitometric analysis of 3 experiments normalized to GAPDH (mean±SD). C) CAT concentration reflects β1i promoter activity (average of 2 experiments, error bars represent ±SD; ∗ $p<0.05$). D) IFNγ release by $pp65_{495-503}$ specific CTL was measured by ELISA and displayed as percentage of the response received by loading MRC5 with 1µg/ml $pp65_{495-503}$ peptide (n = 6 of 3 independent experiments; error bars represent ±SD; ∗∗ $p<0.01$, ∗∗∗ $p<0.001$).

Finally, the impact of IRF3 siRNA knockdown on $pp65_{495-503}$ epitope presentation was analysed. As displayed in figure 3.13D abolished IRF3 expression significantly decreased the presentation of the $pp65_{495-503}$ epitope, already after 2h of infection a reduction of about 40% was measured.

Consequently, the induction of i-subunits and PA28 was based on IRF3 activation, the type I IFN response and autocrine activation of the IFNα/β receptor. The IRF-3 mediated type I IFN response thereby led to formation of i-proteasomes and subsequent, improved epitope generation.

3.6 Processing and modification of viral proteins

3.6.1 Ubiquitylation and oxidation of the viral protein pp65

Since a translation independent but still proteasome dependent generation of the $pp65_{495-503}$-epitope was shown, the question arose how non-translated pp65 is targeted for proteasomal degradation.

It is known that viral infection triggers immediate production of reactive oxygen species, as it was described for HCMV infection within minutes in infected smooth muscle cells (Speir et al., 1996). Western analysis of total cell lysate of virus-infected cells revealed a remarkably early accumulation of oxidant-damaged proteins measured 4hpi (figure 3.14A). Furthermore, 2.5-fold elevated ROS levels were observed by DCFDA staining and FACS analysis directly (30 min) after virus infection (figure 3.14B), 6h later ROS levels were reduced again to normal, uninfected levels. Concomitantly, a degradation of oxidized proteins after 8hpi was detected by oxyblot analysis.

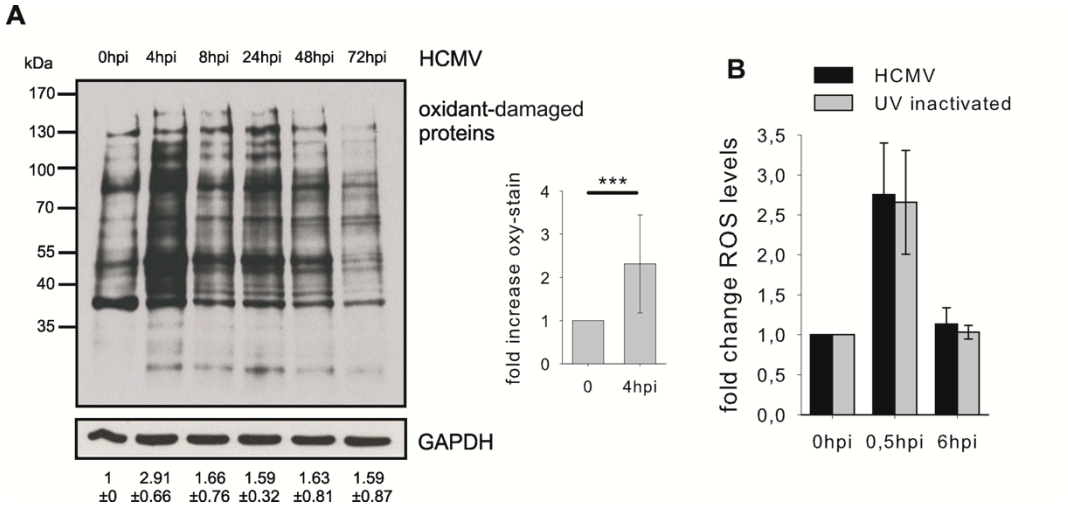

Figure 3.14 Accumulation of oxidized proteins in the course of viral infection. A) Infection of MRC5 cells with HCMV Ad169 at moi 5 for indicated time points. Carbonyl groups of oxidized proteins in total cell lysate were derivatized with DNPH and detected in immunoblot with αDNP antibody. GAPDH served as loading control. Densitometric analysis is given below (mean ± SD; normalised to GAPDH; n = 3). Comparing uninfected MRC5 to 4h HCMV-infected MRC5 a highly significant increase of oxidized proteins was measured (small graph; error bars show ±SD; *** $p<0.001$) B) Detection of ROS by DCFH-DA staining and flow cytometry in MRC5 cells infected for indicated time points with HCMV Ad169 (black bars) or with UV-irradiated HCMV (grey bars). Graph shows average of the mean fluorescence intensities (MFI) normalized to uninfected cells (n = 3, error bars show ±SD).

Moreover, transient accumulation of ubiquitin conjugates was observed in total cell lysates (figure 3.15) which was slightly delayed to the induction of oxidation reaching a peak after 4h. Accumulation of poly-ubiquitylated proteins increased till 24hpi, thereafter occurred a decrease.

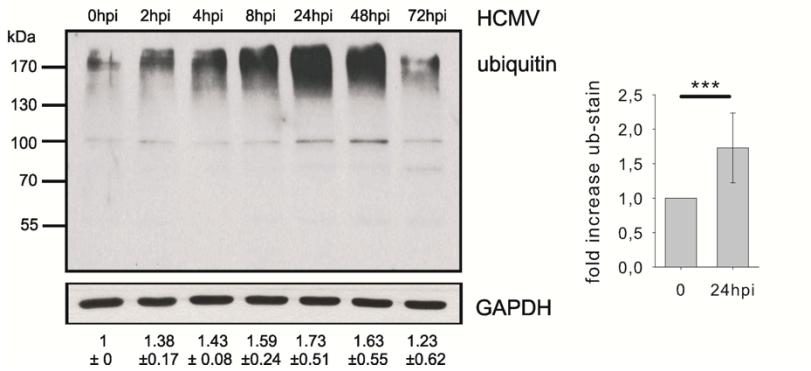

Figure 3.15 Accumulation of ubiquitylated proteins in the course of viral infection. MRC5 fibroblasts were infected with HCMV Ad169 at moi 5 for indicated time points. Total cell lysate was separated by SDS-PAGE and poly-ubiquitin conjugates were detected by staining with αubiquitin antibody. GAPDH served as loading control. Densitometric analysis of 4 blots normalised to GAPDH is given below (mean values ±SD). Comparing uninfected MRC5 to 24h HCMV-infected MRC5 a highly significant increase of poly-ubiquitylated proteins was measured (small graph; error bars show ±SD; *** $p<0.001$).

An implication for the modifications of the viral protein pp65 was tested by immunoprecipitation with αpp65 antibody from total cell lysate of HCMV-infected fibroblasts at different time points. The precipitates were stained for ubiquitylated as well as oxidized pp65 (figure 3.16). After 2, 4 and 8h of infection a significant amount of oxidized as well as ubiquitylated pp65 could be precipitated. Remarkably, after 24hpi the amount of modified pp65 was strongly reduced presumably due to proteasomal degradation.

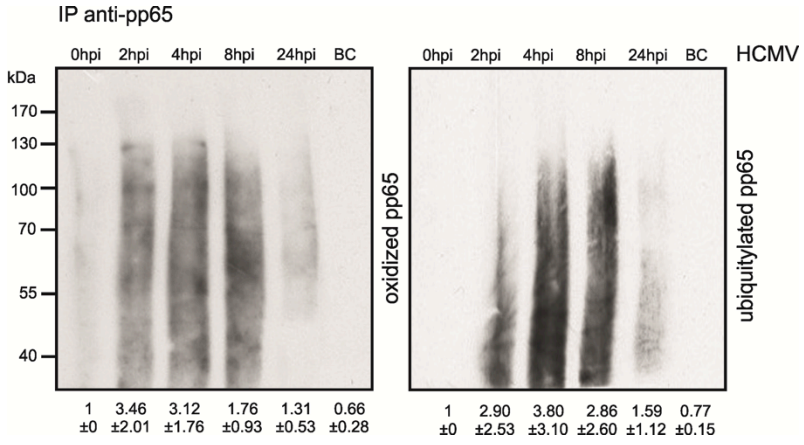

Figure 3.16 Ubiquitylation and Oxidation of the viral protein pp65. Infection of MRC5 with HCMV Ad169 at moi 5 for indicated time points. Pp65 was precipitated from total cell lysate using the αpp65 antibody MA-1569. Precipitates were either separated on SDS-PAGE and analysed by Western Blot with αubiquitin antibody (right panel) or carbonyl groups were derivatized with DNPH and then immunoblotted with αDNP antibody (left panel). Densitometric analysis of 4 blots is given below (mean values ±SD).

In conclusion, non-translated pp65 which was delivered exogenously to the cytoplasm of the host cell during the virus entry process was oxidized due to elevated ROS levels which increase within minutes after infection. Consequently, the oxidized 'defective' pp65 was rapidly ubiquitylated providing the signal for proteasomal degradation.

3.6.2 Ub-conjugation is essential for epitope generation

3.6.2.1 Involvement of the E2 enzyme UBE2L6

Concluding that the observed modifications of non-translated pp65 by oxidation and ubiquitylation might affect the generation of the immunodominant $pp65_{495-503}$ epitope, components of the ubiquitylation and oxidation pathway were analysed for their involvement in the modification of pp65. Subsequently, crucial enzymes were downregulated or inhibited in order to interfere with ubiquitylation and oxidation, respectively, and to investigate the effect on epitope presentation by CTL assay read out.

In a publication from 2010 by Seifert and colleagues an induction of the ubiquitin-conjugating enzyme UBE2L6 by more than 50-fold was observed in response to stimulation with IFNγ (Seifert et al. 2010). Further, a knockdown of UBE2L6 with siRNA abolished the accumulation poly-ub conjugates after IFNγ stimulation. Therefore, UBE2L6 was involved in IFNγ-mediated poly-ub accumulation.

In this thesis an immediate induction of UBE2L6 expression in response to HCMV infection was demonstrated on mRNA level by real-time PCR analysis as well as on protein level by Western analysis peaking 4 to 8h after HCMV infection (figure 3.17A and B). The depletion of UBE2L6 with siRNA inhibited overall ubiquitylation in total cell lysate 4h after HCMV infection significantly (figure 3.17C), comparing a 1.6-fold induction of poly-ub conjugates 4hpi under treatment with OFF-target siRNA and 0.9-fold reduction by application of UBE2L6 siRNA.

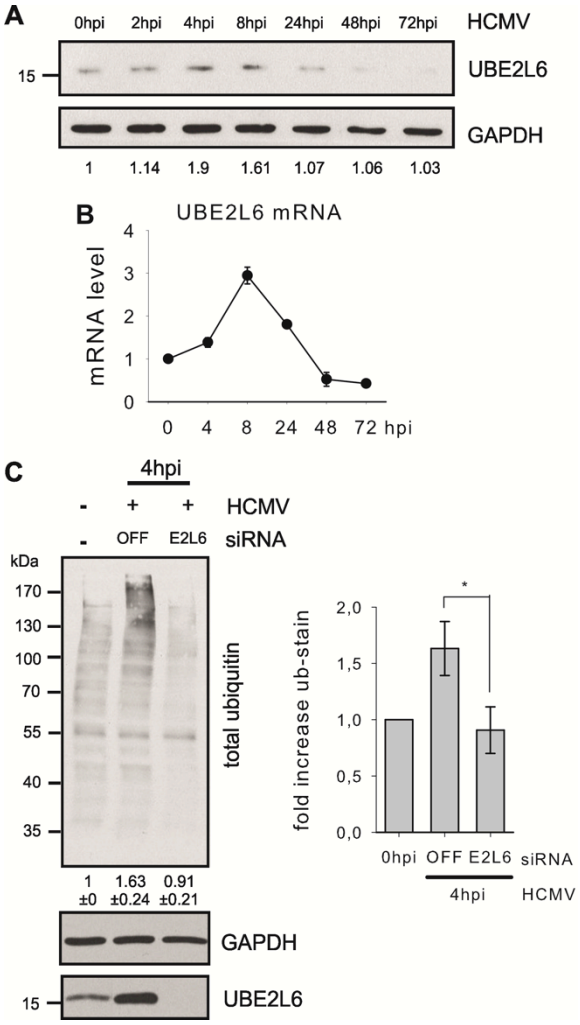

Figure 3.17 Involvement of E2 enzyme UBE2L6. MRC5 were infected with HCMV Ad169 at moi 5 for indicated time points. A) Immediate induction of UBE2L6 on protein level shown by immunoblot with αUBE2L6 antibody. GAPDH served as loading control. Densitometrical analysis of 3 experiments, mean values given below. B) Real-time PCR analysis of UBE2L6 induction. Results were expressed as average fold change from uninfected MRC5 (mean values of 3 experiments, normalized to HPRT1, error bars represent ±SD). C) MRC5 cells were treated 48h prior to HCMV infection with 25nM OFF-target or UBE2L6 siRNA. Knockdown was confirmed by immunoblot with αUBE2L6 antibody and decreased accumulation of poly-ubiquitin conjugates with αubiquitin antibody. Densitometric analysis of 3 experiments normalized to GAPDH, data shows mean values ±SD (* $p<0.05$).

Immunoprecipitation of pp65 from cell lysates of 4h HCMV-infected cells either treated with UBE2L6 siRNA or OFF-target siRNA revealed that the ubiquitylation of pp65 was decreased after knockdown of UBE2L6 (figure 3.18). Therefore, UBE2L6 seemed to play an important role for the ubiquitylation of the viral protein pp65.

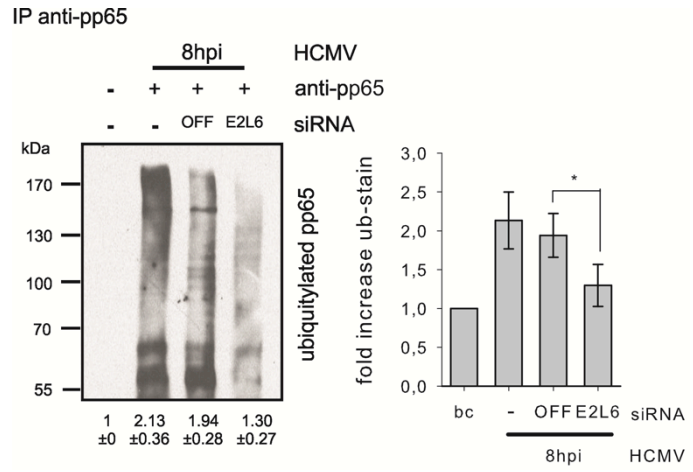

Figure 3.18 Decreased ubiquity-lation of pp65 after depletion of UBE2L6. Immunoprecipitation of pp65 after 8h infection of MRC5 with HCMV Ad169 at moi 5 and prior treatment with 25nM OFF-target or UBE2L6 siRNA. The precipitate was stained in immunoblot with αubiquitin antibody. Graph represents densitometric analysis of 3 experiments, data shows mean values ±SD (* $p<0.05$; bc – bead control).

Thus, knockdown of UBE2L6 was used to investigate the role of pp65 ubiquitylation for the processing and generation of the $pp65_{495-503}$ epitope. Comparing 48h treatment with OFF-target control siRNA to UBE2L6 siRNA, a significant negative effect on the presentation of the $pp65_{495-503}$ epitope was observed by CTL assay 2h and 4h post HCMV infection (figure 3.19A). Moreover, pp65 protein levels seemed to be stabilized due to reduced ubiquitylation. Western analysis showed increased pp65 protein levels after knockdown of UBE2L6, while the staining of high molecular weight conjugates, which appeared with longer exposure times and presumably represent ubiquitylated pp65, was decreased (figure 3.19B).

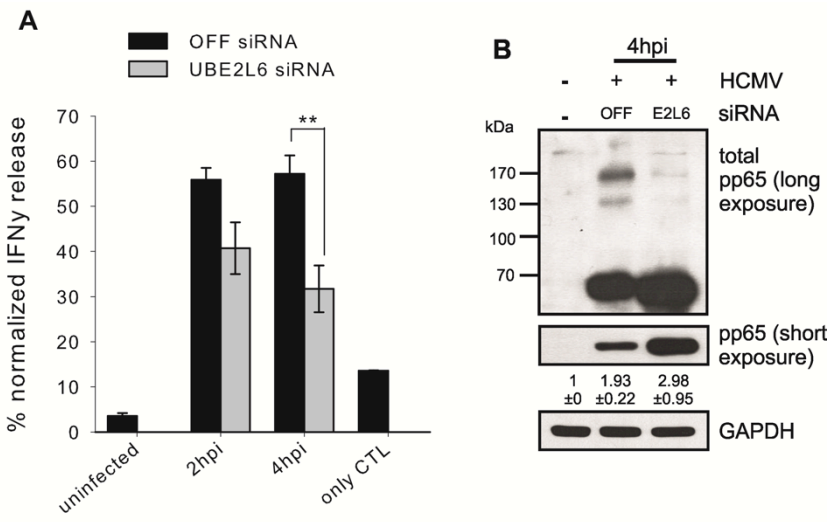

Figure 3.19 Impaired pp65495-503 epitope presentation after UBE2L6 knockdown. MRC5 cells were infected with HCMV Ad169 at moi 5 for 2h and 4h and pre-treated for 48h with 25nM OFF-target or UBE2L6 siRNA. A) IFNγ release of $pp65_{495-503}$ specific T cells was measured by ELISA and displayed as percentage of the response received by loading MRC5 with 1µg/ml $pp65_{495-503}$ peptide (n = 6 of 3 independent experiments; error bars represent ±SD; ** $p<0.01$). B) Total cell lysate was analysed in immunoblot with αpp65 antibody. GAPDH served as loading control. Densitometric analysis of 4 experiments normalised to GAPDH is given below, data shows mean values ±SD.

3.6.2.2 Knockdown of 19S subunit Rpn10 verifies the role of ubiquitylation

After observing the intriguing effect of the UBE2L6 knockdown on the ubiquitylation of the viral protein pp65, the 19S regulatory complex was addressed for further investigations. The access to the catalytical active sites within the barrel-shaped 20S core proteasome is regulated by the 19S regulator which docks at the ends of the barrel to open the channel. 19S subunits recognize ubiquitin moieties conjugated to target proteins. One of the subunits, Rpn10, contains an ubiquitin-interacting motif (UIM) that exhibits high affinity for poly-ubiquitin chains (Finley, 2009).

Thus, we silenced Rpn10 by treatment with PSMD4 siRNA which targets Rpn10. 4h post HCMV infection the accumulation of poly-ubiquitin conjugates was further increased in comparison to uninfected MRC5 and HCMV-infected MRC5 treated with OFF-target siRNA (figure 3.20A). The downregulation was verified in Western analysis with αRpn10 antibody. Moreover, pp65 protein levels were also elevated after downregulation of Rpn10 indicating an impaired degradation of poly-ubiquitylated pp65 (figure 3.20A). Subsequently, by CTL assay analysis a highly significant reduction of epitope presentation was observed after inhibiting Rpn10 expression with siRNA (figure 3.20B). As early as 2hpi a reduction of about 33% was measured which was enhanced 4hpi to more than 48%. These experiments further underline the importance of poly-ubiquitylation for the processing of the $pp65_{495\text{-}503}$ epitope.

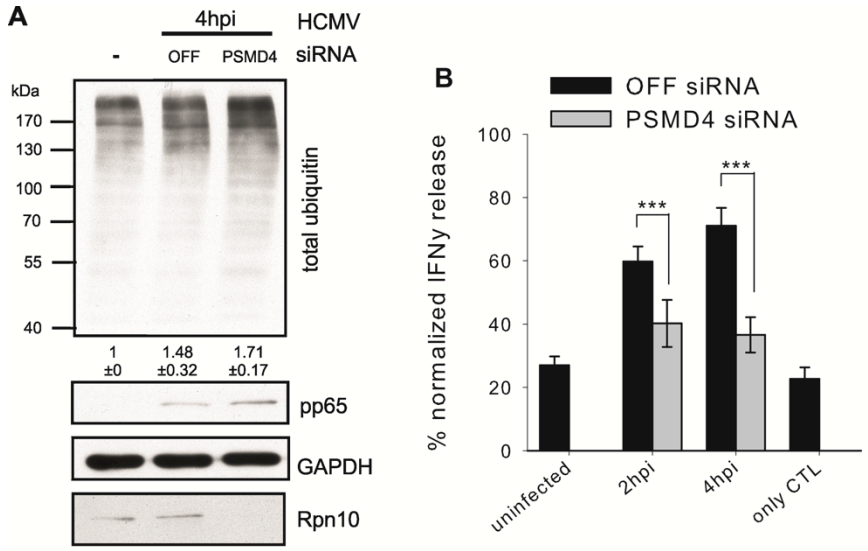

Figure 3.20 siRNA knockdown of the 19S subunit Rpn10 ablates the processing of pp65. MRC5 cells were infected with HCMV Ad169 at moi 5 for 2h and 4h. Either 50nM OFF-target or PSMD4 (Rpn10) siRNA was applied 48h prior to virus infection. A) Total cell lysate was subjected to immunoblot analysis with αubiquitin, αpp65 and αRpn10 antibodies. GAPDH served as loading control. Densitometric analysis of 3 experiments normalised to GAPDH is given below (mean values ±SD). B) IFNγ release by $pp65_{495\text{-}503}$ specific CTL was measured by ELISA and displayed as percentage of the response received by loading MRC5 with 1µg/ml $pp65_{495\text{-}503}$ peptide (n = 7 of 3 independent experiments; error bars represent ±SD; *** $p<0.001$).

3.6.3 Importance of oxidative damage for the processing of the $pp65_{495\text{-}503}$ epitope

After the discovery of the oxidation and ubiquitylation of the non-translated virus protein pp65 and the remarkable effect of the downregulation of certain components of the UPS on the generation of the immunodominant $pp65_{495\text{-}503}$ epitope, focus was laid on the oxidative damage of pp65 and its importance for the processing of the same epitope. It was assumed that the signal for the immediate ubiquitylation of non-translated pp65 represents the induction of reactive oxygen species and subsequent rapid oxidation of intracellular proteins. Accumulation of oxidized proteins also preceded the

accumulation of ubiquitin conjugates in total cell lysates of fibroblasts after infection with HCMV and in HeLa cells after influenza A infection (figure 3.14 and 3.15, IAV data not shown).

3.6.3.1 Antioxidant sulforaphane

The antioxidant sulforaphane represents an efficient inhibitor of oxidative stress due to the activation of phase II enzymes, which help to remove oxidized proteins from cells. Pre-treatment of target cells with 10µM sulforaphane for 24h reduced the induction of oxidation as well as ubiquitylation in total cell lysate significantly (figure 3.21).

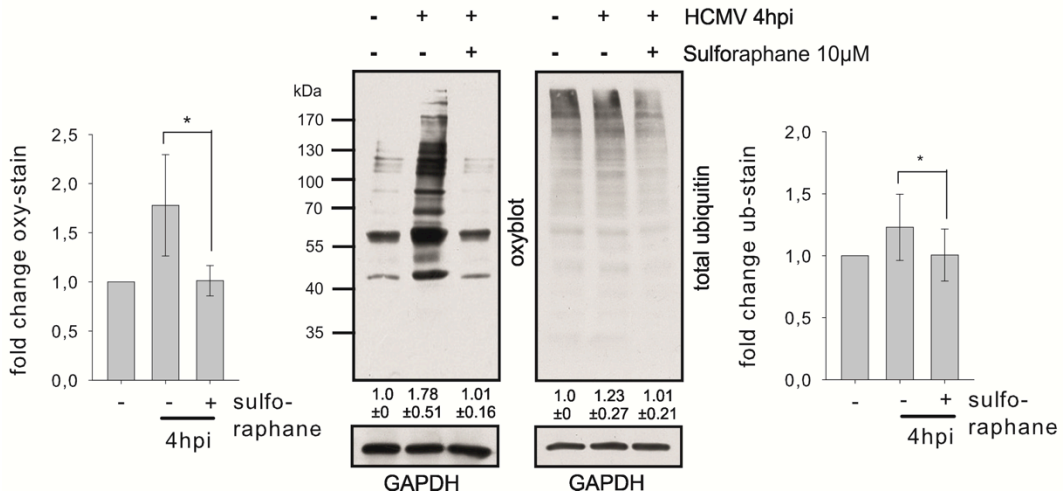

Figure 3.21 The antioxidant sulforaphane abolishes accumulation of ubiquitin conjugates as well as oxidant-damaged proteins after HCMV infection. MRC5 were pre-treated for 24h with 10µM sulforaphane and infected with HCMV Ad169 at moi 5 for 4h. Total cell lysate was subjected to immunoblot with αubiquitin antibody (right) and to oxyblot (left). GAPDH served as loading control. Graphs represent densitometric analysis of 4 experiments normalised to GAPDH (mean values ±SD; ∗ $p<0.05$).

Precipitation of the viral protein pp65 revealed that also the oxidation and ubiquitylation of pp65 is negatively affected by application of the antioxidant (figure 3.22).

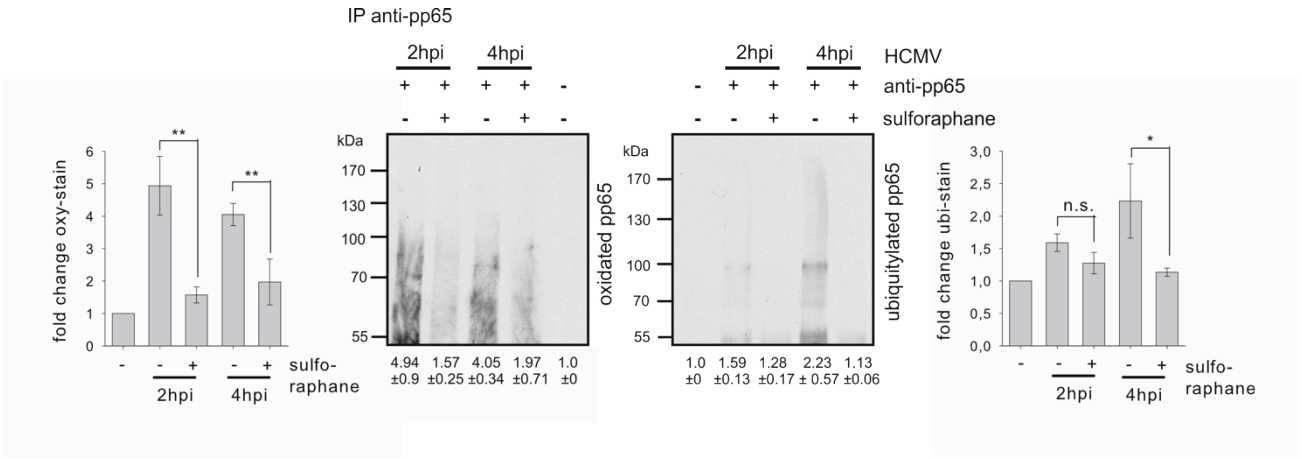

Figure 3.22 The antioxidant sulforaphane impairs the ubiquitylation and oxidation of pp65. Immunoprecipitation of pp65 from total cell lysate of MRC5 pre-treated for 24h with 10µM sulforaphane and infected with HCMV Ad169 at moi 5 for 2h and 4h. Precipitate was analysed in oxyblot and in immunoblot with αubiquitin antibody. Graphs represent densitometric analysis of 3 experiments, data shows mean values ±SD (n.s. not significant, ∗ $p<0.05$, ∗∗ $p<0.01$).

A remarkable effect of the reduced oxidation and concomitantly decreased ubiquitylation was found by CTL assay analysis 2h and 4h after HCMV infection. The antigen presentation of the $pp65_{495\text{-}503}$ epitope was significantly decreased after 24h pre-treatment with sulforaphane (figure 3.23A). Because virus infection or the induction of i-proteasomes might be itself affected by the application of antioxidant, pp65 and β5i protein levels were investigated by Western analysis. The amount of pp65 in total cell lysates at early time points after infection remained unaffected revealing unchanged infection efficiency. Even slightly elevated pp65 levels were observed probably due to impaired degradation of non-modified, more stable pp65. As well the expression of the i-subunit β5i was not significantly affected (figure 3.23B) under the influence of the applied concentration of sulforaphane. Thus, an effect on the processing of pp65 by increased i-proteasome expression in response to sulforaphane treatment, which was reported in 2007 by Kwak and colleagues (Kwak et al., 2007), was ruled out.

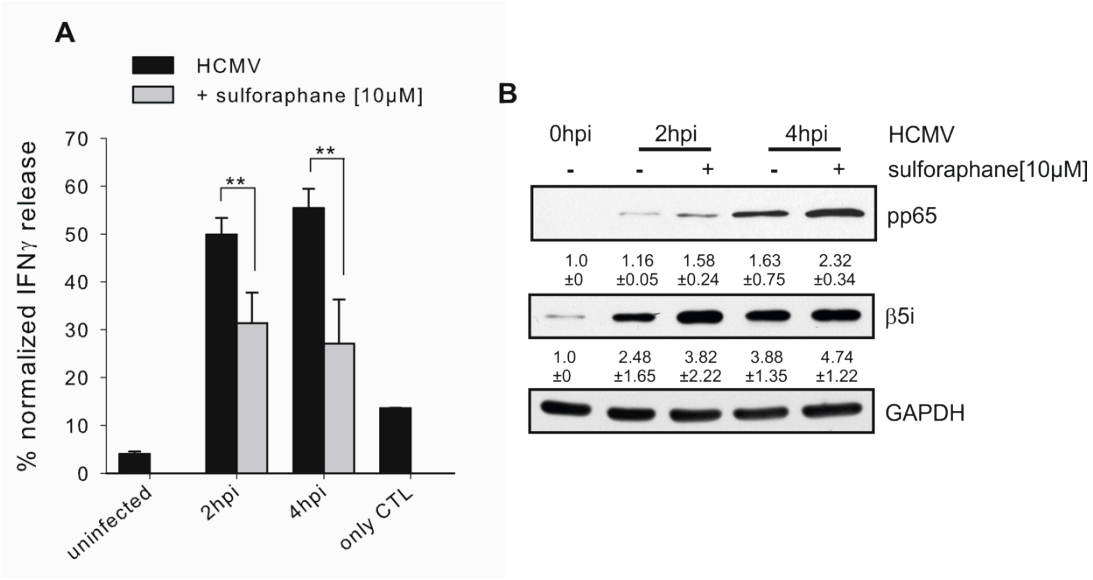

Figure 3.23 The antioxidant sulforaphane compromises the presentation of the pp65$_{495\text{-}503}$ epitope. MRC5 were treated for 24h with 10µM sulforaphane and infected with HCMV Ad169 at moi 5 for 2h and 4h. A) IFNγ release by pp65$_{495\text{-}503}$ specific CTL was measured by ELISA and displayed as percentage of the response received by loading MRC5 with 1µg/ml pp65$_{495\text{-}503}$ peptide (n = 4 of 3 independent experiments; error bars represent ±SD; ** p<0.01). B) Total cell lysate was employed for Western analysis with αpp65 and α-β5i antibody. GAPDH served as loading control. Densitometric analysis of 2 experiments normalised to GAPDH is given below (mean values ±SD).

To prove the hypothesis that oxidation as well as ubiquitylation of antigenic peptides plays a general role during the processing of viral antigens and the generation of immunodominant epitopes, the effect of sulforaphane application was analysed within another virus infection model. Permissive HeLa cells were infected with influenza A virus and incubated prior to infection with 10µM sulforaphane. Again with CTL assay the presentation of the immunodominant M1$_{58\text{-}66}$ epitope was investigated and likewise to the observed effect on the pp65$_{495\text{-}503}$ epitope a reduced presentation by around 30% was observed (figure 3.24).

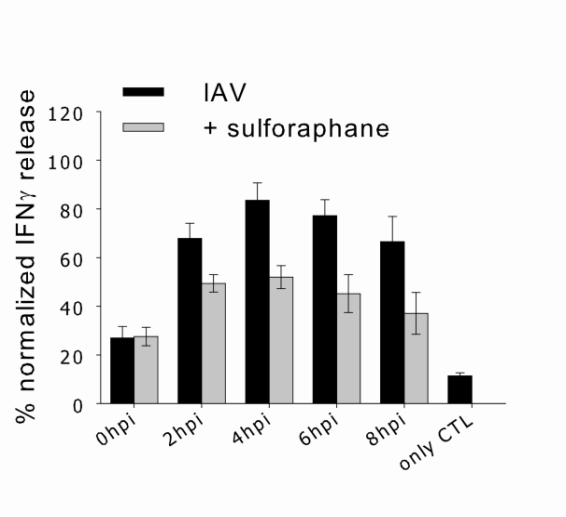

Figure 3.24 The antioxidant sulforaphane compromises the presentation of the M1$_{58\text{-}66}$ epitope. HeLa cells were treated for 24h with 10µM sulforaphane and subsequently infected with IAV at moi 5 for indicated time points. IFNγ release by M1$_{58\text{-}66}$ specific CTL was measured by ELISA and displayed as percentage of the 100% response received by loading MRC5 with 1µg/ml M1$_{58\text{-}66}$ peptide (n = 4 of 2 independent experiments; error bars represent ±SD).

3.6.3.2 NADPH oxidases

Following up the prominent effect of the antioxidant sulforaphane a search for the responsible ROS-producing enzyme or enzymes was carried out. The quest was concentrated on NADPH oxidases which are expressed in the target cells, which might mediate the immediate induction of ROS in response to virus infection and which therefore could be involved in antigen presentation. Out of the seven known members of the Nox family of NADPH oxidases, two candidates were chosen known to be expressed in fibroblasts and to play a role in innate immunity, Nox1 and Nox4 (Rada and Leto, 2008). By means of PCR analysis Nox4 expression could be detected in unstimulated fibroblasts as well as in HeLa cells with a remarkable induction after HCMV and IAV infection, respectively (figure 3.25A). Application of siRNA targeting Nox4 resulted in downregulation of Nox4 mRNA levels after virus infection (figure 3.25A). Moreover, on the Affymetrix microarray about 2-fold Nox4 induction was detected after 4h HCMV infection in fibroblasts as well as after 4h IAV infection in HeLa cells (see attachment). Further, ROS levels were significantly reduced in response to HCMV infection after Nox4 siRNA knockdown measured by DCFH-DA staining (figure 3.25B). Notably, these experiments were also repeated with similar results in IAV-infected HeLa cells (data not shown).

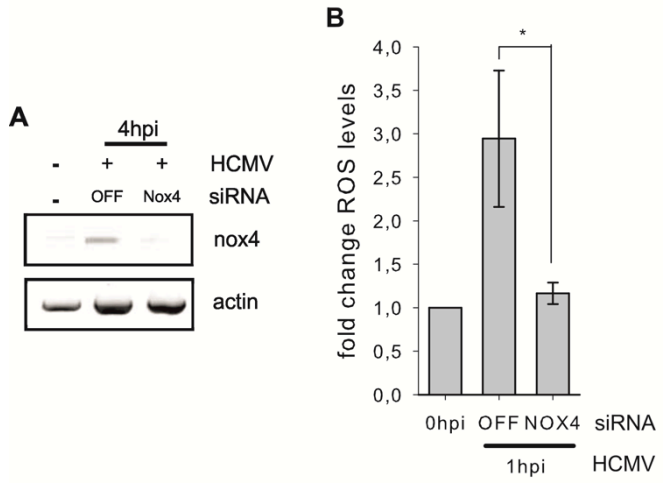

Figure 3.25 Nox4 is responsible for the induction of ROS in HCMV-infected fibroblasts. MRC5 cells were infected with HCMV Ad169 at moi 5 for indicated time points. 50nM OFF-target or Nox4 siRNA was applied 48h prior to infection. A) RT-PCR analysis of Nox4 induction and knockdown with Nox4 siRNA. B) Detection of ROS by DCFH-DA staining and FACS analysis. Data represents average of the mean fluorescence intensities (MFI) normalized to uninfected cells (mean values of 3 experiments; error bars show ±SD; * $p<0.05$).

Thus, in total cell lysates of HCMV-infected fibroblasts the accumulation of oxidized and ubiquitylated proteins was significantly reduced after Nox4 downregulation (figure 3.26).

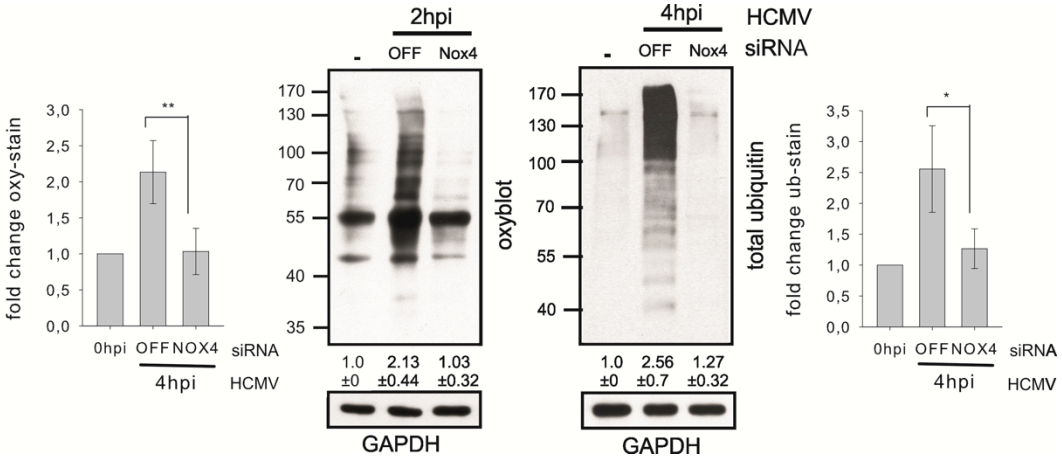

Figure 3.26 Knockdown of Nox4 decreases oxidation as well as ubiquitylation in HCMV-infected MRC5. Total cell lysate of 2h and 4h HCMV Ad169-infected fibroblasts after pre-treatment with 50nM OFF-target or Nox4 siRNA was subjected to oxyblot (left) and to immunoblot with αubiquitin antibody (right). Graphs represent densitometric analysis of 3 (oxyblot) and 4 (ub-blot) experiments normalized to GAPDH, data shows mean values ±SD (∗ $p<0.05$, ∗∗ $p<0.01$).

Further, decreased oxidation and ubiquitylation of the virus protein pp65 was verified by immunoprecipitation of pp65 and staining in immunoblot for poly-ubiquitin and carbonyl groups (figure 3.27).

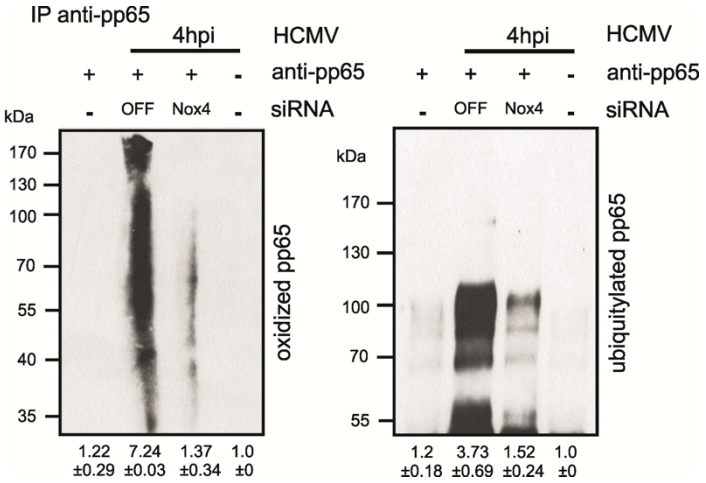

Figure 3.27 Depletion of Nox4 diminishes the oxidation and ubiquitylation of pp65. Immunoprecipitation of pp65 from lysate of MRC5 cells 4h infected with HCMV Ad169 at moi 5 and prior treatment with 50nM OFF target or Nox4 siRNA for 48h. Precipitate was analysed in oxyblot and in immunoblot with αubiquitin antibody. Densitometric analysis of 2 experiments, data shows mean values ±SD.

Finally, the presentation of the $pp65_{495\text{-}503}$ epitope was found to be remarkably reduced during the important early phase of the CTL response to HCMV infection when cells were pre-treated 48h with Nox4 siRNA (figure 3.28A). Moreover, monitoring pp65 protein levels in total cell lysate a slight accumulation of pp65 was observed following Nox4 knockdown, which might be explained by decreased oxidation and concomitantly reduced proteasomal degradation of pp65 thereby stabilizing pp65. In conclusion, the experiments suggested that Nox4 activity supported the oxidation of pp65 and thereby affected the generation of the $pp65_{495\text{-}503}$ epitope.

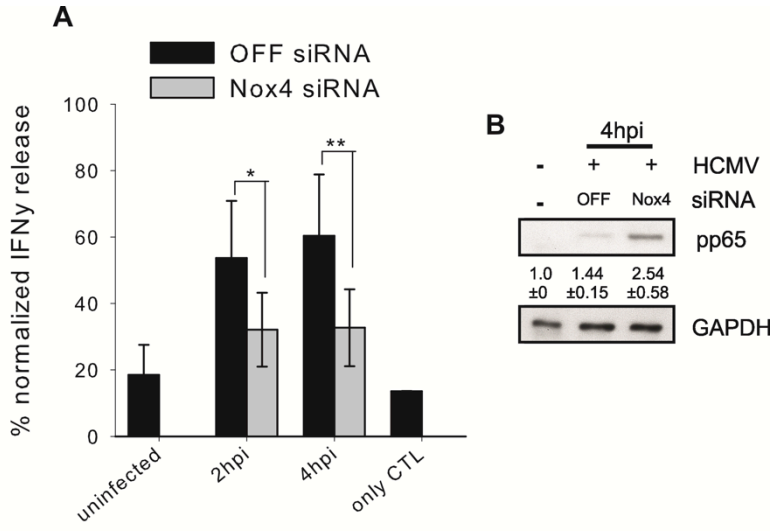

Figure 3.28 Depletion of Nox4 with siRNA impairs $pp65_{495-503}$ epitope presentation. MRC5 were incubated for 48h with 50nM OFF-target or Nox4 siRNA and subsequently infected with HCMV Ad169 at moi 5 for 2h and 4h. A) IFNγ release by $pp65_{495-503}$ specific CTL was measured by ELISA and displayed as percentage of the response received by loading MRC5 with 1µg/ml $pp65_{495-503}$ peptide (n = 7 of 3 independent experiments; error bars represent ±SD; * p<0.05, ** p<0.01). B) Total cell lysate was subjected to immunoblot with αpp65 antibody. GAPDH served as loading control. Densitometric analysis of 3 experiments normalized to GAPDH, data shows mean values ±SD.

3.6.4 A general mechanism

The previous results arose the question whether oxidation and concomitant ubiquitylation might affect antigen presentation in general. Assuming that not only the presentation of the $pp65_{495-503}$ and $M1_{58-66}$ epitopes is affected by ROS levels, MHC class I surface expression should be itself downregulated when oxidation or hence ubiquitylation is reduced.

To go to the bottom of this question HeLa cells were treated with IFNγ in order to enhance MHC class I surface expression. Additionally, siRNAs were applied to knockdown the ROS-producing NADPH oxidase Nox4 or the 19S subunit Rpn10. Subsequently, cells were labeled with an αHLA-A,B,C antibody and MHC class I surface expression was monitored by flow cytometry (figure 3.29). As expected, stimulation with IFNγ strongly induced MHC class I complexes on the cell surface in comparison to unstimulated cells (0h time point). Upon interference with oxidation by downregulation of Nox4 or with degradation of ubiquitylated proteasomal substrates via knockdown of Rpn10 the presentation of MHC class I molecules on the cell surface was significantly reduced. Therefore, a fundamental role of ROS production and concomitant ubiquitylation of oxidized proteins leading to efficient proteasomal degradation during the processing of viral antigens was assumed.

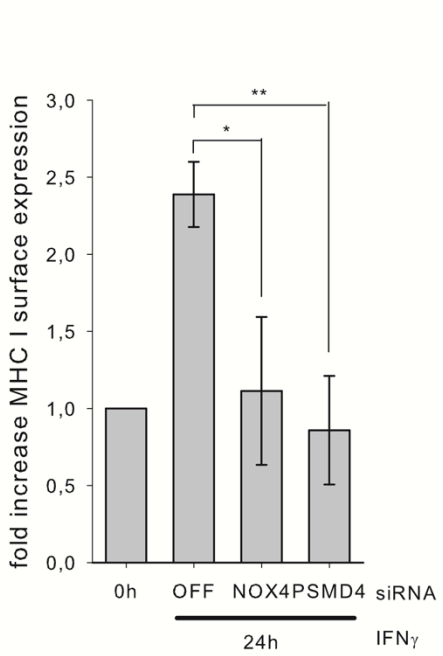

Figure 3.29 Inhibition of oxidation as well as ubiquitylation impairs MHC class I surface expression. FACS staining of MHC class I surface expression with αHLA-A,B,C-PE antibody. HeLa cells were treated for 48h with 50nM OFF-target, Nox4 or PSMD4 siRNA and subsequently stimulated for 24h with 100U/ml IFNγ. Data represents average of the mean fluorescence intensities (MFI) normalized to unstimulated cells (mean values of 3 experiments; error bars show ±SD; * $p<0.05$, ** $p<0.01$).

4. Discussion

A primary virus infection mostly occurs in non-immune cells, as for example influenza A infection is initiated in epithelial cells of the lung. Dedicated antigen-presenting cells, such as DCs and macrophages, take up pathogens to trigger the priming of naïve $CD8^+$ T cells in a process called cross-presentation (described in chapter 1.2.2). Subsequently, virus-infected target cells presenting antigens via MHC class I molecules can be eliminated by differentiated CTLs.

Indeed, the work described within this thesis shows that upon virus infection non-immune cells are able to present antigenic peptides at remarkably early time points (chapter 4.1). This very early antigen presentation appeared to occur independently of protein synthesis. Two immunodominant epitopes, the $pp65_{495\text{-}503}$ of HCMV and $M1_{58\text{-}66}$ epitope of IAV, could be shown to be presented before the viral gene expression is initiated and therefore to be generated translation-independent (chapter 4.1.1). Still their generation was dependent on proteasomal degradation and improved by the induction of i-proteasomes (chapter 4.2). Therefore, the changes imposed by viral infection on the early proteasome pool in HCMV-infected cells were scrutinized. Further, it was of interest to understand how i-proteasomes can be induced with such fast kinetics in face of viral immunoevasion strategies (chapter 4.2.1).

To answer the question how stable viral proteins are targeted for proteasomal degradation, the recently discovered ability of the i-proteasome to efficiently degrade oxidant-damaged proteins and protect cells against the accumulation of toxic protein aggregates was regarded. Posttranslational modifications of viral antigens and the impact of these modifications on the generation of immunodominant epitopes were investigated (chapter 4.3). Indeed a link between the two major functions of the i-proteasome to protect cells against inflammation-induced oxidative damage and to improve the generation of peptides for MHC class I antigen presentation could be revealed (chapter 4.3.3).

4.1 Very early antigen presentation

The replication cycles of human cytomegalovirus and influenza A virus, as described in chapter 1.5.1 (HCMV) and 1.5.2. (IAV), exhibit great differences with regard to the time course of infection. HCMV represents a rather slow progressing virus: one infection cycle from the entry of virus particles into host cells up to the assembly of new particles took around 72 hours in cell culture for infection of primary human lung fibroblasts. The IAV replication cycle was completed already after eight hours with the lysis of infected HeLa cells and the release of new virions. In this regard the observation that infection with both viruses produced a very early antigen presentation of selected immunodominant epitopes to specific cytotoxic T lymphocytes was quite surprising. Peak levels of antigen presentation of the HCMV $pp65_{495\text{-}503}$ as well as the IAV $M1_{58\text{-}66}$ epitope were observed already four hours post infection (figure 3.2 HCMV and figure 3.3 IAV). The presentation of the $M1_{58\text{-}66}$ epitope declined eight hours post infection coinciding with the lysis of infected cells, which was recognisable in cell culture in form of increasing cell death. Therefore the IAV-induced cell lysis explains the reduced antigen presentation and concomitant decreased activation of epitope-specific CTLs at later time points. The

$pp65_{495-503}$ specific CTL response to infection with the slow propagating HCMV was significantly reduced after 24 hours at the transition of early to late viral replication phase. Notably, infection with HCMV also at later time points did not result in cell lysis. Instead, the declining $pp65_{495-503}$-specific CTL response was connected to HCMV immune escape mechanisms.

Mainly the HCMV-mediated downregulation of MHC class I surface expression was responsible for reduced activation of HCMV-specific CTL after 24hpi, which is well described in the literature: Four HCMV gene products, so called immunoevasins, are acting together to abolish MHC class I antigen presentation in general: i) the glycoproteins gpUS2 and gpUS11 redirect nascent MHC class I complexes from the ER to the cytoplasm and target MHC class I for ubiquitylation and proteasomal degradation ii) gpUS3 inhibits translocation of MHC class I from ER to Golgi and iii) gpUS6 interferes with peptide loading on MHC class I by binding to TAP (Ahn et al., 1996; Hengel et al., 1996; Wiertz et al., 1996). Recently, also a transcriptional downregulation of TAP1 and TAP2 was described (Halenius et al., 2011). Further, we had the possibility to test our infection model and CTL assay read-out with the HCMV ΔUS2-11 deletion mutant obtained from Hartmut Hengel and Anne Halenius. With the mutant virus an ongoing and increasing antigen presentation was observed, since the virus causes no lysis of target cells and the expression of the MHC class I-targeting immunoevasins was abolished (see attachment figure 1).

Notably, also during infection with wild type virus epitope presentation was measured up to 72 hours post infection, although the levels were significantly reduced. Already in 2007 Besold and colleagues observed that the presentation of the $pp65_{495-503}$ epitope persists despite the expression of immunoevasins while another immunodominant epitope of the non-structural pp72 - the $pp72_{297–305}$ epitope which was described in (Gallez-Hawkins et al., 2003) - was abolished in presence of the glycoproteins gpUS2-11 (Besold et al., 2007).

Importantly, the proportion of $CD8^+$ T cells committed to the anti-HCMV response is extraordinarily large in infected humans and the most dominant antigen for the activation of CTLs represents pp65 (McLaughlin-Taylor et al., 1994). Of all HCMV-directed CTLs 70 to 90% recognise pp65 epitopes and moreover the CTL response is often focused on only one peptide (Wills et al., 1996). One of these peptides is the here studied HLA-$A2^+$-restricted $pp65_{495-503}$ epitope (Weekes et al., 1999). Ex vivo profiling of $CD8^+$ T cell responses of infected humans revealed that around 10% of $CD8^+$ T cells in the peripheral blood of healthy virus carriers and up to 40% of $CD8^+$ T cells of elderly infected individuals can be specific only for HCMV antigens (Elkington et al., 2003). Still the largest expanding CTL clone does not have to elicit the most efficient CTL response for the restriction of HCMV infection.
Moreover, the extensive expansion of HCMV-specific CTL clones could lead to the reduction of the naïve T cell pool. Further, in contrast to the immune response to other virus infections, HCMV-specific $CD8^+$ T cells accumulate with age, a phenomenon called 'memory inflation'. HCMV infection may contribute to immune senescence which is characterised by the reduction of levels of naïve T cells and the accumulation of clonally expanded memory T cells leading to a decline of the immune responsiveness of the individual. Indeed, HCMV-infected individuals show a higher rate of $CD8^+$ T cell clonal

expansions and reduced mitogen-stimulated proliferative responses which leads to the conclusion that the immunodominance of HCMV antigens may hinder responses to other pathogens (Crough and Khanna, 2009). In this regard the question arises: what makes the HCMV pp65 antigen so immunogenic to provoke such large immune responses even in the face of viral strategies to subvert the immune control (described in detail in chapter 1.5.1)? To elucidate this question during this thesis the time points of expression and processing as well as posttranslational modifications of the pp65 antigen were scrutinised.

4.1.1 The DRiP hypothesis

Surprisingly, HCMV pp65 as well as IAV M1 protein both represent late expressed proteins in the viral gene expression cascade, i.e. 24hpi for pp65 and 6hpi for M1, which was confirmed on the protein expression level with immunoblot analysis in figure 3.1. Still, presentation of epitopes derived from the respective viral proteins was measured already 2hpi (figure 3.2 for HCMV and figure 3.3 for IAV infection). A possible explanation is that both proteins represent structural components of the virus particle. Pp65 as component of the viral tegument, which is characteristic for herpesviridae, is embedded between the viral envelope and the nucleocapsid (Gibson, 1996). The M1 protein of IAV, an orthomyxovirus, constitutes the matrix, a thin layer between viral envelope and ribonucleoprotein complexes (Nayak et al., 2009).

According to the DRiP hypothesis newly synthesized defective ribosomal products serve as the major substrate for the proteasome to generate MHC class I ligands (Yewdell, 2007). Yewdell discriminates according to their half-life different pools of polypeptides: i) rapidly degraded polypeptides (RDPs), with a half-life of ten minutes on average, and ii) slowly degraded polypeptides (SDPs), which are characterised by a half-life over one hour. The generation of peptide ligands from polypeptides of the RDP as well as the SDP pool occurs within similar kinetics, which can be explained by the usage of a DRiP source (Yewdell, 2007). The DRiP hypothesis therefore delivers an explanation on how long-lived, stable and also compartmentilised viral proteins can be fed into the MHC class I antigen presentation pathway (Khan et al., 2001a). Consequently, the generation of MHC class I ligands from DRiPs is dependent on protein synthesis (Reits et al., 2000; Schubert et al., 2000).

A direct example for IAV antigenic peptides deriving from DRiPs was given by the group of Yewdell in 2010 (Dolan et al., 2010). They inserted the SIINFEKL epitope, which is derived from ovalbumin, into the stalk of IAV neuraminidase (NA) and precisely quantitated the cell surface expression of K^b-SIINFEKL complexes by flow cytometry. The epitope was generated in complete lockstep with the initiation and abrogation of NA biosynthesis. Moreover K^b-SIINFEKL presentation required proteasomal activity as well as TAP transport consistent with its generation from a cytosolic DRiP pool. The difference in the shutoff kinetics of K^b-SIINFEKL complex expression following inhibition of protein synthesis versus proteasome inhibition suggested a half-life of the biosynthetic source of NA peptides of approximately five minutes.

Within this thesis the analysis of antigen presentation was focused on early time points before DRiPs from a viral protein pool were available. Our work showed that immunodominant epitopes of HCMV as well as IAV were presented before viral gene expression started, thus independent of protein synthesis. This could be proven by application of a translation inhibitor as well as by infection with UV-irradiated virus. Antigen presentation of the $pp65_{495-503}$ epitope was unaffected by both methods in CTL assay analysis (figure 3.5). Further, in immunoblot analysis the non-structural HCMV protein pp72 could not be detected after UV irradiation or cycloheximide treatment while pp65 was still detected at early time points but not at later time points when *de novo* synthesis would occur (figure 3.4A and B). Similarily, expression of the non-structural IAV protein NS1 was abolished by translation inhibition while protein levels of M1 remained unaffected at early time points (figure 3.4C). In conclusion, both viral proteins, pp65 and M1, as components of the virus particle, appear to be delivered to the cytosol of the host cell during the virus entry process. Schmolke and colleagues observed that pp65 translocates to the nucleus of the host cell within five minutes after infection by its NLS (Schmolke et al., 1995a). Immunofluorescence analysis performed during this thesis confirmed a concentration of pp65 in the nucleus of MRC5 cells after one hour of infection and only light staining in the cytoplasm and the surrounding of the nucleus (data not shown). Likewise, the M1 protein is transported to the nucleus of the host cell, which was reported to occur after 25 minutes while an hour later M1 is evenly distributed between nucleus and cytoplasm (Martin and Helenius, 1991). Thereby the antigen processing machinery of the host cell gains access to these viral proteins immediately after infection even before viral immune escape mechanisms can set in, which has been postulated earlier for pp65 (Reddehase, 2002).

The independence of translation inhibition explains the strong and early epitope presentation and possibly contributes to the overzealous pp65-directed CTL response. The data suggests that a complementary mechanism to the DRiP hypothesis exists, which makes stable viral proteins available for proteasomal degradation and generation of antigenic peptides before defective ribosomal products can serve as substrate (see chapter 4.3.3).

4.2 Role of the i-proteasome for epitope generation

The group of Bodo Plachter had shown that despite resistance against the HCMV-mediated MHC class I downregulation the presentation of the $pp65_{495-503}$ epitope was still dependent on proteasomal activity (Besold et al., 2007). By application of the proteasome inhibitors epoxomicin or lactacystin the presentation of the $pp65_{495-503}$ epitope was significantly reduced in IFNγ ELISPOT analysis with epitope-specific CTLs. Also in this thesis by infection of MRC5 with HCMV Ad169 and application of 200nM epoxomicin the generation of the $pp65_{495-503}$ epitope was abolished almost completely at each analysed time point during the course of infection from 2 to 72hpi (figure 3.2). Likewise, the $M1_{58-66}$-specific CTL response was strongly reduced by application of 200nM epoxomicin (figure 3.3). In conclusion, the generation of both immunodominant epitopes, although translation-independent, was generally dependent on proteasomal degradation. Still, it was unclear if the processing of both viral

antigens was also ub-mediated and how non-translated stable viral proteins were targeted for proteasomal degradation (see chapter 4.3).

Firstly, attention was focused on characteristic changes of the proteasome population, such as subunit composition and association with regulatory complexes, in the respective host cells and in response to virus infection. Here, the model system of HCMV infection in MRC5 fibroblasts was chosen. In summary, an increase of proteasome expression was observed together with an additional slight induction of mixed-type proteasome complexes containing the β5i and β1i subunit (figure 3.6). Moreover, the expression of PA28 α- and β-subunits was induced which suggested an association of 26S proteasomes with the PA28 regulator possibly forming hybrid proteasomes (figure 3.6). By immunoprecipitation (figure 3.6D) and Native page analysis (figure 3.7) the incorporation of both i-subunits, though at low levels, and association with PA28 was verified.

Formation of i-proteasomes as well as induction of PA28 has been mostly associated with positive effects on the generation of viral antigenic peptides for presentation on MHC class I complexes to specific $CD8^+$ T cells. In 2000 Sijts and colleagues could show by using TET-inducible expression of i-subunits that already low levels of i-proteasomes increase the efficieny of antigenic peptide formation (Sijts et al., 2000b). Nevertheless, *in vivo* studies with knockout mice revealed that i-proteasomes can have differential effects on the generation of different epitopes from IAV (using β1i-deficient mice (Chen et al., 2001)) or LCMV (using β1i/β5i-deficient mice (Basler et al., 2004; Nussbaum et al., 2005)) probably influencing immunodominance hierarchies (Sijts and Kloetzel, 2011) (see chapter 1.4.1). Investigations by Hutchinson and colleagues with β5i knockout mice and MCMV infection revealed that $CD8^+$ T cell responses were generally affected for a range of tested immunodominant as well as subdominant MCMV-epitopes which suggested a dominant role of i-proteasomes for $CD8^+$ T cell responses to MCMV infection (Hutchinson et al., 2011).

Previously, our group could show using purified s- and i-proteasome to digest a 33mer pp65 peptide containing the $pp65_{495\text{-}503}$ epitope a proteasome-dependent processing of the same epitope (Urban et al., 2012). Moreover, *in vitro* digestion with i-proteasomes resulted in a more efficient substrate degradation as well as generation of pp65 epitopes and epitope-precursors. Thereby s- and i-proteasomes used the same cleavage sites so that identical peptide products were received but in a significantly higher amount with i-proteasomes leading to more efficient epitope generation. Possibly, the increased capacity of i-proteasomes compared to s-proteasomes to generate antigenic peptides results either from an increased chymotryptic activity following the incorporation of β5i (Strehl et al., 2008) or from conformational changes improving the substrate accessibility to the active sites (Sijts et al., 2000a). Further supporting the role for i-proteasomes were experiments in a cellular system: HLA-$A2^+$ HeLa cells constitutively expressing i-subunits were transiently transfected with a plasmid expressing a 14mer precursor peptide of the $pp65_{495\text{-}503}$ epitope. In comparison to HLA-$A2^+$ HeLa cells without expression of i-proteasomes a stronger epitope-specific CTL response was observed after six hours of transient transfection of the pp65-plasmid (Urban et al., 2012). The stability of the pp65 protein suggested that proteasomal degradation and epitope generation occurred via the DRiP pathway transla-

tion-dependent. In the context of transient transfection experiments the source for proteasomal degradation of pp65 might represent defective translation products, while this was clearly ruled out here using whole virus particles for infection because of the very early epitope presentation and independence of translation.

Nevertheless, the impact of i-proteasome induction was also analysed during infection of MRC5 fibroblasts with HCMV Ad169. Therefore, prior to infection each of the i-subunits β5i and β1i were downregulated alone or in combination with siRNA which led to a significant reduction of $pp65_{495\text{-}503}$ epitope presentation in CTL assay (figure 3.8). Thereby siRNA knockdown of the β1i, the β5i subunit and both i-subunits in combination gradually resulted in a stronger negative impact on the antigen presentation. Moreover, siRNA downregulation of PA28 similarly caused a decreased epitope generation (figure 3.9). Thus, in concert with previous *in vitro* data mixed-type proteasome complexes containing β5i and β1i as well as the proteasome activator PA28 improved the generation of the $pp65_{495\text{-}503}$ epitope.

Interestingly, the group of Hartmut Hengel carried out several investigations with MCMV and HCMV infection analysing immune escape mechanisms that abolish the induction of i-proteasomes (Khan et al., 2004; Le et al., 2008; Zimmermann et al., 2005). Already in 2000 another group had observed an inhibition of IFNγ-stimulated expression of the MHC class I antigen presentation machinery including proteasome genes peaking after 72hpi with HCMV (Miller et al., 2000). Khan et al. reported in 2004 a disturbed induction of i-proteasomes in response to MCMV as well as HCMV infection. Notably, they also analysed the expression of i-subunits 72 hours after infection with HCMV. Here, an increase of the i-subunits β5i and β1i as well as PA28 was observed on mRNA and protein level already after four hours, peaking after eight hours of infection. In agreement with previous data, a decrease was observed 48 to 72hpi (figure 3.6). For MCMV infection Khan and colleagues could show that the downregulation occurs on the level of transcription and that the MCMV protein M27 might be responsible due to its inhibition of STAT2 (Khan et al., 2004). In 2008 Le and colleagues observed that also during HCMV infection the activation of STAT2 is affected: HCMV interferes with STAT phosphorylation and further induces proteasomal degradation of STAT2 (Le et al., 2008). Possibly, STAT inhibition is based on an interaction with the HCMV immediate early protein pp72 (Paulus et al., 2006).

Nevertheless, a significant early induction of mixed-type proteasome complexes associated with PA28 was observed within the scope of this thesis. This induction further resulted in an improvement of the generation of the immunodominant $pp65_{495\text{-}503}$ epitope to elicit an efficient early HCMV-specific CTL response. In the following chapter the induction of i-proteasomes and PA28 in response to HCMV infection will be further discussed.

4.2.1 Induction of the i-proteasome in response to HCMV infection

Heink and colleagues observed a 4-fold accelerated assembly of i-proteasomes compared to s-proteasomes in response to IFNγ signalling which was essentially dependent on the induction of, and interaction between, proteasome maturation protein (POMP) and β5i (Heink et al., 2005). In the present thesis, in response to HCMV infection an immediate and transient increase of POMP and β5i was

also observed (figure 3.6C). Moreover, the immediate formation of i-proteasomes was verified by immunoprecipitation and Native page analysis (figure 3.6D and 3.7). It is known that in response to IFNγ signalling STAT1-dependent expression of all three i-subunits as well as the PA28 α- and β-subunit is increased (Ahn et al., 1995; Barton et al., 2002; Chatterjee-Kishore et al., 2000). Further, type I IFNs and pro-inflammatory cytokines are reported to induce the formation of i-proteasomes (Shin et al., 2006). Interestingly, the basal expression level of i-subunits in immune cells is unlikely to be dependent on cytokine stimulation but dependent on intracellular signaling, for example unphosphorylated STAT1 was reported to bind to IRF1 forming a complex that docks to the GAS sequences within the β1i promoter (Chatterjee-Kishore et al., 2000).

The remarkably fast kinetics of i-proteasome formation in response to viral infection, with an increase of β5i mRNA after two hours and on protein level four hours post infection (figure 3.6), were observed here for the first time in a cell culture model of HCMV infection in MRC5 fibroblasts. Thus, it was of interest to further examine the underlying innate immune mechanisms and signalling pathways leading to the expression of i-subunits and PA28. Especially in the case of HCMV infection the question arises how i-proteasome formation circumvents the multi-layered immune escape which is initiated by the virus.

Induction of the innate immune response. So far, investigations about the initiation of the innate immune response triggered by HCMV infection resulted in controversial publications. The ambiguity of the data is based on the ability of the virus to infect many different cell types utilizing different cellular receptors and sensors (Compton, 2004). Clearly, the induction of the innate immune response including the production of IFNs and the secretion of ICs is directly linked to the entry of the virus into the host cell. First evidence derived from microarray analysis of Zhu and colleagues in 1998. They compared uninfected and HCMV-infected human foreskin fibroblasts and observed the induction of many antiviral RNAs before the onset of viral gene expression (Zhu et al., 1998). Later, microarray analysis comparing HCMV infection of cycloheximide-treated host cells or infection with UV-inactivated virus revealed the upregulation of various mRNAs including those encoding for ISGs and IFNβ itself. Interestingly, the induction was independent of gene transcription, presumably triggered solely by HCMV binding and entry (Browne et al., 2001). Similarly, in this thesis the induction of i-subunits and PA28 on mRNA as well as increased protein level were observed after infection with untreated and with UV-inactivated virus (figure 3.10A). Moreover, elevated levels of β5i and β1i were observed 24 hours after infection with UV-inactivated virus, presumably due to the inhibited expression of HCMV immunomodulatory gene products which would normally interfere with the expression of i-subunits (Khan et al., 2004; Le et al., 2008). Remarkably, also the activation of STAT1 measured by staining with phospho-STAT1 antibody on immunoblots (figure 3.10A) as well as the production of IFNβ measured on transcriptional level by real-time PCR analysis (figure 3.10B) was unaltered comparing untreated and UV-inactivated virus. Hence, the type I IFN response including the activation of the Jak-Stat pathway was unaffected and probably also after infection with wild type HCMV strong enough to induce the expression of antiviral genes. Consequently, a component of the virus particle, which interacts with an as yet

unknown cellular sensor, appears to be responsible for the induction of the expression of i-subunits and PA28. Potentially, this activation occurs via the type I IFN response.

For several years scientists were searching for the key component of the HCMV particle that activates the fast innate immune response. In 2001 the HCMV envelope glycoprotein gB was proposed to be the essential factor for initiating antiviral gene expression without the need for viral gene expression (Simmen et al., 2001). Compton et al. have observed an interaction of HCMV, possibly gB, with TLR2 leading to the activation of NFκB and consequently inducing the transcription of pro-inflammatory cytokines (Compton et al., 2003). The same group later discovered a crucial role of interferon regulatory factor 3 (IRF3) for the induction of the IFN response (Boehme et al., 2004). In 2006 DeFilippis and colleagues could demonstrate by downregulation of IRF3, that indeed IRF3 is essentially required for the induction of antiviral genes (DeFilippis et al., 2006). Remarkably, in 2008 by usage of TLR2 knockout cells and further by blocking endosomal TLRs it became clear that the early type I IFN response was initiated TLR-independently by an yet unknown process (Juckem et al., 2008) and the search for the responsible virus component began anew.

Certified facts of the process of virus entry are: the initial attachment of virus particles to their target cells occurs via low-affinity tethering to cellular heparin sulfate proteoglycans (HSPGs) and interaction with viral envelope glycoproteins (Compton et al., 1993). Subsequently, virus particles dock to cellular receptors which appears to occur in a cell-type-specific manner. Further, depending on the cell type follows either the fusion with the cell membrane (Compton et al., 1992) or uptake via the endosomal pathway resulting in the deposition of virion components into the cytoplasm (Bodaghi et al., 1999). Somehow during or following this process cellular sensors activate the IFN response. After the disqualification of TLR signalling for the induction of IFNs RIG-1 came into discussion. But in 2010 a crucial observation from the group of Klaus Früh revealed that the DNA sensor ZBP1 plays an important role for the initiation of the IFN response by activating the transcription factor IRF3 (DeFilippis et al., 2010). Consequently, perhaps not glycoproteins but double stranded DNA could represent the crucial virus component. As displayed in figure 4.1 the activated IFN response is divided in two phases: an initial activation of IRF3 through phosphorylation by Tbk1 and IKKε kinase, after which hyperphosphorylated IRF3 shuttles into the nucleus where it activates target genes e.g. IFNβ itself and other ISGs. During the subsequent amplification phase the IFNα/β receptor is activated in an auto- or paracrine manner, which leads to induction of the Jak-Stat pathway and further expression of ISGs (Juckem et al., 2008).

In the present work, the described innate immune pathways were tested for their involvement in the activation of i-proteasome and PA28. It was found that both by inhibition of the IRF3 phosphorylating kinases and by blockade of the IFNα/β receptor, the expression of the i-subunits β5i and β1i was abolished. The same was true for the expression of the PA28 α- and β-subunits (figure 3.11). Moreover, this also affected the presentation of the $pp65_{495\text{-}503}$ epitope which was significantly reduced after inhibition of IRF3 phosphorylation or IFNα/β receptor activation (figure 3.12). Notably, the negative effect of blocking the IFNα/β receptor on the antigen presentation did not became significant earlier than after eight hours of virus infection. Possibly, in the very early phase of two to four hours post

infection an induction of i-subunits occured directly by IRF3-activated gene transcription, independent of the type I IFN response. Finally, treatment of the host cells with IRF3-targeting siRNA prior to virus infection reduced the induction of i-subunits and PA28 on mRNA (figure 3.13A) and protein level (figure 3.13B). Similarly, the expression of known IRF3-induced ISGs such as IRF7 and IFNβ itself was abolished (figure 3.13A). Moreover, β1i-promoter activity, which was induced in response to HCMV infection measured by CAT assay, was significantly reduced when IRF3 expression was blocked (figure 3.13C). Hence, also antigen presentation was inhibited presumably due to lower levels of i-proteasomes (figure 3.13D). In conclusion, the crucial role for IRF3 in the signalling pathways leading to the expression of i-proteasomes and PA28 in response to HCMV infection and subsequently causing an improvement of the antigen presentation could be demonstrated.

Interestingly, pp65 has been reported to act as a potent immunoevasin by interfering with antiviral gene expression (Browne and Shenk, 2003). This is possibly triggered by an interaction of pp65 with IRF3 and a subsequent reduction of the IFN response (Abate et al., 2004). Now it was demonstrated that IRF3 activation significantly improves the generation of an immunodominant epitope of the same viral protein. Still, it is unclear whether the subsequent generation of type I IFNs, which definitely leads to induction of i-proteasomes at later time points, is also responsible for the very early expression of i-subunits and the improvement of the antigen presentation at these time points. Alternatively, a short-circuit mechanism may exist which could be induced directly by IRF3. The innate signaling pathways which are activated by HCMV infection and are potentiamlly involved in i-proteasome formation are summarized in figure 4.1.

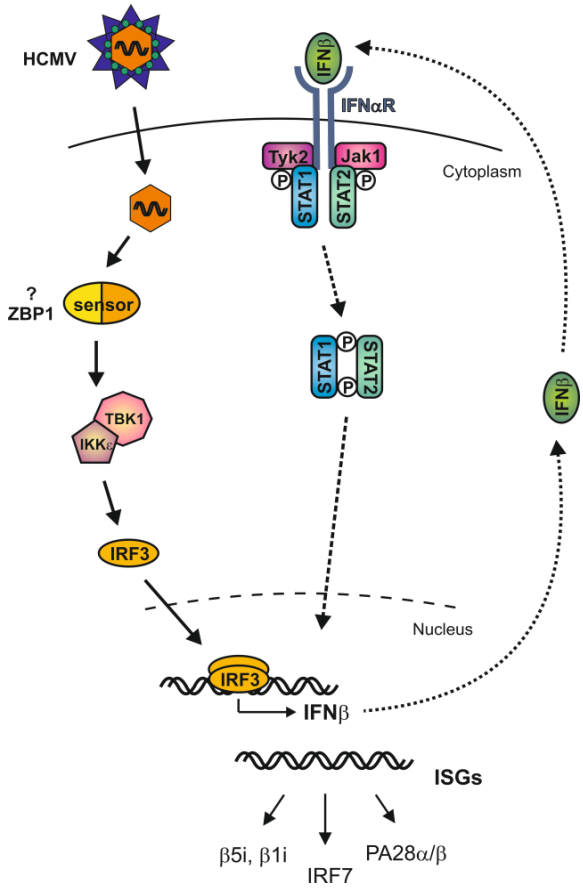

Figure 4.1 Induction of the IFN type I response by HCMV. HCMV particles enter the cell in a cell type-specific manner resulting in the release of viral components into the cytoplasm. Possibly, the DNA sensor ZBP1 recognises viral double stranded DNA and activates the kinases Tbk1 and IKKε, which in turn phosphorylate IRF3. Phosphorylated IRF3 shuttles into the nucleus and activates the transcription of ISGs and predominantly IFNβ. In an auto- or paracrine manner IFNβ binds to IFNα/β receptors on the cell surface and activates the Jak-Stat pathway. Phosphorylated Stat1 and Stat2 heterodimerise and activate the transcription of further ISGs thereto the i-subunits β5i and β1i as well as both PA28 subunits.

4.3 The i-proteasome at the interface of innate and adaptive immune responses to viral infection

4.3.1 Modifications of non-translated pp65

Remarkably, the very early epitope presentation essentially required proteasomal degradation of non-translated viral antigens which was further improved by the induction and incorporation of i-subunits into proteasome complexes. In this chapter the question how non-translated proteins were targeted for proteasomal degradation will be clarified. Therefore, posttranslational modifications which might label virus proteins for degradation were considered.

In a publication from 2010 by our group it was shown that after stimulation of cells with IFNγ the generation of reactive oxygen species (ROS) caused a transient accumulation of oxidized as well as ubiquitylated proteins (Seifert et al., 2010). Earlier, it has been demonstrated that pro-inflammatory cytokines trigger the formation of ROS which consequently cause oxidative stress (Sasaki et al., 2008; Watanabe et al., 2003). It could be monitored that IFN-induced oxidative stress mainly affected newly synthesized proteins. Nascent proteins seemed to be particularly sensitive to oxidative stress, thus cytokine stimulation caused an enhanced formation of oxidized and ubiquitylated DRiPs (Seifert et al., 2010). The subsequent IFNγ-mediated induction of i-proteasomes induced an efficient and rapid degradation of the poly-ubiquitylated DRiPs, thus providing the removal of potentially toxic oxidant-damaged proteins (Seifert et al., 2010).

The data discussed above excluded that the $pp65_{495-503}$ epitope is generated from a DRiP at the analysed early time points and instead derives independently of its translation from the virus particle itself. Still, it was important to check the oxidation and ubiquitylation levels in the virus-infected cells, since also during viral infection ROS are generated as part of the innate host response. It has been reported that in response to HCMV infection intracellular ROS levels increase significantly within five minutes, as was measured by DCFDA staining in smooth muscle cells (Speir et al., 1996). Likewise, infection of MRC5 fibroblasts with HCMV Ad169 elicited a strong increase of ROS levels immediately after infection (figure 3.14B). Moreover, the innate ROS response was also initiated by infection with UV-irradiated virus, thus directly by entry of virus particles into the host cell. For example, activation of TLR signaling triggered by virus-cell contact could lead to the production of ROS and RNS (Orient et al., 2007; Rada and Leto, 2008). Consequently, also the amount of oxidant-damaged protein increased almost three-fold within a short time span of four hours inside HCMV-infected fibroblasts (figure 3.14A). This was also reported in response to influenza A infection in HeLa cells (personal communication with Theresa Bergann). Moreover, in agreement with the data published in (Seifert et al., 2010), poly-ub conjugates transiently accumulated after viral infection (figure 3.15) indicating ubiquitylation of oxidant-damaged proteins, which will be discussed further.

During ageing or age-related neurodegenerative diseases dysfunctional proteins tend to aggregate in large ub-positive structures (Mishto et al., 2006). Further, in response to physiological stress conditions, such as starvation and cytokine stimulation as well as oxidative stress, protein aggregation is

enhanced leading to the formation of aggresome-like induced structures (ALISs) (Szeto et al., 2006). Moreover, in phagocytic cells such as DCs and macrophages the recognition of PAMPs entails the formation of so-called dendritic cell aggresome-like induced structures (DALISs) (Lelouard et al., 2002). Under inflammatory conditions these structures are believed to occur when the accumulation of aberrant and oxidant-damaged proteins temporarily exceeds the degradation capacity of the proteasome. Notably, the formation of ALIS in response to oxidative stress has been shown to be dependent on protein synthesis, while during starvation ALIS occurred translation-independent. At least under oxidative stress conditions ALIS and DALIS are believed to result from excess DRiP levels and to require protein synthesis (Szeto et al., 2006).

In this regard it was of great interest to analyse whether in case of viral infection besides newly-synthesized cellular proteins also non-translated and completely folded viral proteins might be affected by ROS. As displayed in figure 3.16 this could be verified through immunoprecipitation studies for the HCMV antigen pp65. Already two hours after infection the oxidized as well as ubiquitylated forms of pp65 could be precipitated with pp65-specific antibody (figure 3.16). Due to this observation at very early time points as well as after infection with UV-irradiated virus it has to be concluded that non-translated virus proteins are subjected to oxidation and subsequent ubiquitylation. While the investigations described before concentrated on oxidative damage of newly synthesized proteins, in this thesis normally stable virus proteins were shown to be sensitive to oxidative stress, too. The mechanisms for targeting virus-delivered pp65 to oxidation remain unclear. The unmodified pp65 could be targeted directly by ROS-producing enzymes. Alternatively, the high abundance of pp65 in the virus tegument, representing a major constituent of HCMV particles, leads to accordingly high levels of pp65 that are distributed immediately inside infected cells upon virus entry, and this could promote oxidation. Possible sources of ROS in response to viral infection will be discussed later in chapter 4.3.3.

Further investigations that were applied on the proteasomal degradation of oxidized pp65, an implication of i-proteasomes and their potential impact on epitope generation will be discussed in the following chapter.

4.3.2 Proteasomal degradation of oxidant-damaged viral proteins

The role of the proteasome in the removal of oxidized proteins has been accepted for a long time. Already in 1985 Jennifer Rivett isolated a large protease complex from liver which preferentially degraded oxidatively modified model substrates in comparison to unmodified substrates (Rivett, 1985). Independently another group purified a 670kDa protease complex from red blood cells which degraded oxidatively damaged proteins (Pacifici et al., 1989). Later, these proteases were shown to be identical to the proteasome. Through knockdown of proteasome subunits and proteasome inhibitors the proteasomal degradation of oxidized model substrates has been verified (Grune et al., 1997; Sitte et al., 1998), still the contribution of free 20S, 26S proteasome complexes and ubiquitylation has since been subject to controversial discussions.

In vitro, most unfolded proteins including oxidatively damaged proteins could be degraded by purified 20S proteasomes alone (Davies, 2001; Grune et al., 1998; Pacifici et al., 1989; Rivett, 1985) and indeed increasing oxidative damage of model proteins could also reduce the ubiquitylation efficiency (Shringarpure et al., 2003). Further, in mammalian cells expressing a temperature-sensitive E1 mutant, oxidant-damaged proteins were still degraded efficiently (Shringarpure et al., 2003). Mechanistically, the exposure of hydrophobic areas which could occur due to oxidation and unfolding of proteins may cause the binding of oxidized substrates directly to α-subunits of the 20S proteasome, which could promote the gating process (Kisselev et al., 2002).

Interestingly, evidence for the ub-mediated degradation of oxidized proteins by the 26S proteasome is increasing. Already in 2001 Shang and colleagues observed upon induction of oxidative stress an increase in oxidized and concomitantly ubiquitylated proteins in lens cells (Shang et al., 2001). Ubiquitin conjugates isolated from oxidatively stressed mammalian cells were highly enriched in oxidized proteins and blocking of the UPS increased the susceptibility of cells to oxidative stress and induced cytotoxicity (Dudek et al., 2005). Further, it has been demonstrated in β5i knockout mice that i-proteasome deficiency rendered retina cells more susceptible to oxidation-induced cell death (Hussong et al., 2010). An inhibitor of the mammalian deubiquitylation enzyme Usp14, which has been shown to associate with the 19S regulator, accelerated the degradation of oxidized proteins suggesting a role for 26S proteasomes (Lee et al., 2011). Though Pickering et al. discuss that a knockdown of the 26S proteasome exerts only a minor effect, they observed in mammalian cells that siRNA-mediated knockdown of the 19S particle by targeting the Rpt2 subunit resulted in stabilization of oxidized proteins, further pointing out a role for the 26S proteasome (Pickering et al., 2010). Medicherla and Goldberg observed in budding yeast that the degradation of newly synthesized proteins was enhanced two- to three-fold by induction of oxidative stress and that this degradation was dependent on ATP and ubiquitin. Knockdown of E2 enzymes and 26S components like Rpn10 revealed that all these UPS components were essentially required for the efficient removal of oxidant-damaged proteins (Medicherla and Goldberg, 2008). In this regard also the connection of age and oxidative stress with the proteasome activity (Abd El Mohsen et al., 2005) and the observation that proteasome inhibitors cause senescence are of importance (Chondrogianni and Gonos, 2004; Chondrogianni et al., 2003).

Within this thesis, application of the potent antioxidant sulforaphane prior to viral infection was able to reduce the overall amount of oxidized proteins significantly (figure 3.21). Sulforaphane acts indirectly by activation of phase II enzymes such as glutathione-S-transferase or UDP-glucuronyl transferase which detoxify oxidant-damaged proteins by conjugation reactions. By immunoprecipitation analysis the treatment with antioxidant also revealed reduced levels of oxidant-damaged pp65 (figure 3.22). Interestingly, decreased oxidation of pp65 also resulted in decreased ubiquitylation of pp65, which further verified a model in which oxidation precedes the subsequent ubiquitylation of a virus-delivered antigen.

The slight delay of pp65 ubiquitylation to oxidation - peak levels of oxidant-damaged pp65 were measured after two hours and poly-ubiquitylated pp65 after four hours of HCMV infection (figure 3.16

and 3.22) - again indicates that pp65 is first subjected to oxidation caused by virus-induced oxidative stress before it is subsequently ubiquitylated. Hence, it is likely that the oxidation of pp65 gives the signal for its ubiquitylation. Possibly, oxidant-damaged pp65 may be ubiquitylated by a specific E3 ligase, as it is reported for the iron regulatory protein 2 which has been shown to be specifically ubiquitylated after oxidative damage by the E3 ligase HOIL-1 (Yamanaka et al., 2003). Further, the oxidation of pp65 causes unfolding of the protein and this might induce the activation of chaperones. When refolding of oxidant-damaged proteins fails, these chaperones are reported to recruit E3 ligases which then target irreversibly misfolded proteins to proteasomal degradation (Kriegenburg et al., 2012). In this regard it could also be of interest to further analyse the sites of oxidation and ubiquitylation within the pp65 protein sequence by means of mass spectrometry-based approaches.

The presented data approve the ubiquitylation of oxidant-damaged pp65 and suggest an implication of 26S proteasomal degradation. By application of proteasome inhibitor epoxomicin subsequent to HCMV infection not only poly-ub conjugates in total cell lysate accumulated, but also the degradation of pp65 was inhibited (figure 3.2B). Without proteasome inhibitor 24hpi a significant decrease of oxidized and ubiquitylated pp65 was measured by precipitation with pp65-specific antibody (figure 3.16) presumably due to degradation by the proteasome.

Notably, at 24hpi reduced levels of pp65 were observed in Western analysis after treatment with epoxomicin when compared to untreated cells. At this time point another effect of proteasome inhibition was exerted. The expression of pp65, and viral gene expression in general, is dependent on proteasomal activity to eliminate transcriptional repressors (Kaspari et al., 2008; Tran et al., 2010). At 24hpi *de novo* synthesis of pp65 would occur which might be blocked by proteasome inhibition therefore leading to decreased pp65 levels, while at earlier time points the degradation of non-translated pp65 might be inhibited thereby leading to increased pp65 levels.

Recently, Seifert and colleagues have shown the upregulation of several components of the UPS including the ub-conjugating enzyme UBE2L6 in response to stimulation with IFNs. Moreover, they could verify the involvement of UBE2L6 during IFN-mediated accumulation of oxidized poly-ub conjugates (Seifert et al., 2010). Also in response to virus infection an upregulation of UBE2L6 was observed. Microarray analysis revealed an induction of UBE2L6 four hours post infection with HCMV as well as IAV (see attachment table 1). This was confirmed by real-time PCR and immunoblot analysis (figure 3.17A and B). By means of siRNA knockdown it could be verified that UBE2L6 was indeed involved in the induction of poly-ub conjugates in infected target cells (figure 3.17C) and moreover affected poly-ubiquitylation of pp65 (figure 3.18).

Further underlining the proteasomal degradation of ubiquitylated pp65 was the effect of siRNA-mediated knockdown of the 19S subunit Rpn10. The access to the catalytical active sites within the barrel-shaped 20S core proteasome is regulated by the 19S regulator which docks at the ends of the barrel to open gated channels (Finley, 2009). 19S subunits recognize ubiquitin moieties conjugated to target proteins. One of the subunits, Rpn10, contains an ub-interacting motif (UIM) that exhibits high affinity for poly-ub chains. Mutation of the UIM domain of Rpn10 significantly impaired the proteolytic

capacity of the 26S proteasome and led to accumulation of poly-ubiquitylated proteins (Finley, 2009). Also after HCMV infection knockdown of Rpn10 caused an accumulation of poly-ub conjugates and moreover of pp65 (figure 3.20A) which suggested proteasomal degradation of non-translated ubiquitylated pp65 by the 26S proteasome.

Role of the i-proteasome for efficient degradation of oxidant-damaged viral proteins. Only recently evidence has been increasing that i-proteasomes are more efficient in eliminating damaged proteins than s-proteasomes. In 2010 our group had observed in response to stimulation with IFNγ a significantly increased accumulation of poly-ub conjugates in β5i knockout mouse embryonic fibroblasts (MEFs) compared to wild type MEFs (Seifert et al., 2010). At time points when the wild type cells were already cleared the formation of ALISs was observed in β5i knockout MEFs. Further, they demonstrated *in vivo* in LPS-challenged liver as well as in EAE-induced brains of i-proteasome-deficient mice an increased formation of ALIS compared to wild type mice (Seifert et al., 2010). Thus, they could show a so far unknown function of i-proteasomes in the maintenance of protein homeostasis upon inflammation-induced oxidative stress. Already earlier, Yewdell had proposed other cellular functions of i-proteasomes besides the processing of MHC class I ligands since during the inflammation process in pathogen-challenged tissue not only infected but also non-infected cells induce i-proteasomes in response to secreted cytokines (Yewdell, 2005). Uninfected cells have no need to form i-proteasomes to improve antigen processing. Therefore, it seemed unlikely that the induction represents a side effect of cytokine stimulation. Further evidence was delivered by the observation that the induction of i-proteasomes is linked to cell stress (Hussong et al., 2010). I-proteasomes are not only induced in response to cytokine stimulation and infection but also for example due to heat stress (Callahan et al., 2006), arsenite treatment (Zheng et al., 2005) or nitric oxide (Kotamraju et al., 2006) supporting a more general physiological function of i-proteasomes besides its role in antigen processing. Moreover, i-proteasome deficiency has been associated with inflammatory diseases. In humans a missense mutation in the β5i gene PSMB8 has been shown to cause the auto-inflammatory immune disease Nakajo-Nishimura syndrome (NNS) which is associated with impaired formation of i-proteasomes and concomitant increased accumulation of poly-ubiquitylated proteins (Arima et al., 2011; Kitamura et al., 2011). Furthermore, the brain and liver of β1i knockout mice are threatened by higher levels of protein carbonyls upon ageing compared to wild type littermates (Ding et al., 2006). Also in a viral infection model the function of i-proteasomes to protect against oxidative protein damage has been shown: during acute coxsackievirus B3 (CVB3)-induced myocarditis, i-proteasome-deficient mice showed exacerbated tissue damage due to increased levels of oxidant-damaged proteins. This led to the conclusion that indeed infection-induced formation of i-proteasomes can protect against inflammation- and oxidation-mediated protein damage (Opitz et al., 2011). Consequently, an important, newly discovered function of the i-proteasome is to control the innate immune reaction and to protect against overshooting inflammatory responses.

As discussed above, in this thesis also an increase of oxidative damage in response to viral infection was observed and moreover viral antigens were affected as well. Concomitantly, the almost immediate induction of i-proteasomes revealed an improvement of the presentation of an immunodominant

epitope processed from the same viral antigen. Further, by siRNA knockdown of the i-subunits β5i and β1i pp65 protein levels were increased in HCMV-infected fibroblasts (figure 3.8B) presumably due to less efficient degradation of pp65 by inhibition of i-proteasome formation.

4.3.3 The DrOP hypothesis

The observed effect of oxidation and ubiquitylation on the degradation of viral antigens, e.g. the HCMV protein pp65, implied an impact of oxidative stress on the generation of immunodominant epitopes from viral proteins, which could be confirmed clearly here.

Indeed, the observed downregulation of pp65 ubiquitylation by siRNA knockdown of the ub-conjugating enzyme UBE2L6 resulted also in reduced presentation of the immunodominant $pp65_{495-503}$ epitope to specific CTLs (figure 3.19A). In concert with the reduced epitope presentation, also the degradation of pp65 was inhibited and unlabelled pp65 accumulated after siRNA knockdown of UBE2L6 (figure 3.19B). Thus, content of ubiquitylated pp65 was correlated with the degradation efficiency by the proteasome and consequently with epitope generation. Moreover, the siRNA-mediated depletion of Rpn10 impairing degradation of pp65 by the 26S proteasome also caused an accumulation of pp65 (figure 3.20A) and subsequently affected the generation of the $pp65_{495-503}$ epitope (figure 3.20B). Hence, the epitope generation was dependent on ub-mediated proteasomal degradation.

To test whether also the observed oxidation of pp65 was a prerequisite for the efficient processing of the immunodominant epitope the impact of antioxidant treatment was monitored. Sulforaphane application lowered the amount of oxidized and concomitantly ubiquitylated pp65 (figure 3.22), in turn the degradation rate of unlabelled pp65 was reduced, as observed by accumulating pp65 levels in immunoblot (figure 3.23B), and consequently the generation of the $pp65_{495-503}$ epitope was negatively affected (figure 3.23A). Notably, the effect of sulforaphane on the antigen presentation could be reproduced in another model system by infection of HeLa cells with IAV and analysis of the presentation of the immunodominant $M1_{58-66}$ epitope (figure 3.24). In summary, reduction of oxidative damage in virus-infected cells decreases also ubiquitylation. This consequently affects the degradation of viral antigens by the 26S proteasome and the processing and presentation of viral epitopes.

I-proteasomes protect cells against the accumulation of dysfunctional proteins during the innate immune response (Seifert et al., 2010). Here, this function could be linked to the induction of an efficient adaptive immune response. The induction of ROS and consequently oxidant-damaged proteins in virus-infected cells together with the ability of i-proteasomes to efficiently degrade oxidant-damaged proteins improved the processing of viral antigens. This mechanism might play an important role during the early phase of a virus infection in infected target cells. Before virus replication is initiated DRiPs are not available for the generation of viral antigenic peptides. As a complementation to the DRiP hypothesis we introduce another protein pool: the DrOPs, directly oxidized proteins. DrOPs might provide proteasomal substrates for the generation of MHC class I ligands before the viral gene expression starts and do not require protein synthesis but the generation of oxygen radicals.

4.3.4 Oxidation of viral antigens – NADPH oxidase Nox4

A central question raised was how pp65 was oxidized so fast besides being a stable virus-delivered, non–translated viral protein. As already discussed, the observed fast production of ROS in response to HCMV infection (figure 3.14B) is also reported from the literature to occur with minutes in HCMV-infected SMCs (Speir et al., 1996). Further, ROS induction seems to play a role for the initiation of HCMV gene expression via NFκB (Speir et al., 1996). Interestingly, HCMV also induces an anti-ROS response by different virus-specific mechanisms for example the induction of antioxidant glutathione (Tilton et al., 2011). Still, the observed accumulation of oxidant-damaged proteins by immunoblot (figure 3.14A) and oxidative modification of pp65 (figure 3.16) in response to HCMV infection was strong despite ROS-detoxifying viral mechanisms.

It was tempting to analyse the source of ROS in response to virus infection inside the infected target cells. From the literature it is described that ROS as part of the host defense are not only produced by the well-known phagocytic NADPH oxidase Nox2 but also by enzymes present in many other cell types and tissues (Orient et al., 2007). Nox1 and Nox4 represent the two most prominent NADPH oxidases in the target cells. While Nox1 is described to be induced in fibroblasts and epithelial cells in response to IFN stimulation, Nox4 is reported to be expressed in almost every cell type (Orient et al., 2007; Rada and Leto, 2008).

Both enzymes, Nox1 and Nox4, were analysed for their expression and induction in response to HCMV- and IAV-infection in MRC5 fibroblasts and HeLa cells, respectively. Nox4 was found to be transcriptionally induced in HCMV-infected fibroblasts already after four hours of infection (figure 3.25A) and as reported from Theresa Bergann also in IAV-infected HeLa cells (personal communication). Further, Nox4 has been proven to contribute to ROS production in HCMV-infected fibroblasts. Depletion of Nox4 by siRNA treatment caused significantly reduced ROS levels in response to HCMV infection (figure 3.25B). Consequently, siRNA-mediated Nox4 knockdown also affected overall levels of oxidized and concomitantly ubiquitylated cellular proteins (figure 3.26) as well as levels of oxidized and ubiquitylated pp65 (figure 3.27). Hence, also the epitope presentation measured with $pp65_{495\text{-}593}$-specific CTLs was drastically impaired (figure 3.28A). In concert, due to impaired degradation of pp65 levels of unlabelled pp65 accumulated (figure 3.28B). Notably, also expression of Nox1 was found by real-time PCR analysis in MRC5 fibroblasts as well as in HeLa cells (personal communication with Theresa Bergann). Furthermore, siRNA knockdown of Nox1 also had minor effects on the presentation of the $pp65_{495\text{-}503}$ epitope in CTL assays (data not shown). Due to the possible different effectiveness of siRNAs the effects of Nox1 and Nox4 downregulation cannot be compared directly. In the future a possible involvement of Nox1 should be further elucidated.

The NADPH oxidase Nox1, likewise Nox2, is regulated differently compared to Nox4. While Nox1 and 2 are mostly regulated by posttranslational modifications such as phosphorylation of regulatory subunits or by association with other regulatory proteins like $p22^{phox}$, Nox4 represents a constitutively active NADPH oxidase (Katsuyama, 2010; Rada and Leto, 2008). Nox4 does not require agonist stimulation or association with regulatory proteins. In fact, its activity is rather dependent on its level of protein

expression and gene transcription. While Nox enzymes in general are reported to be located on the apical cell surface, Nox4 has been observed also intracellularly, associated to the ER, and within perinuclear localization (Katsuyama, 2010). Manea and colleagues performed investigations about the transcriptional activation of Nox1 and Nox4. They found that Nox1 and 4 are induced by IFNγ via the Jak-STAT pathway and also could show a physical interaction of STAT1/STAT3 proteins with GAS elements in the promoter of Nox1 and 4 in SMCs (Manea et al., 2010a). Further they observed that TNFα-induced NFκB signaling induced the transcription of both Nox1 and Nox4 (Manea et al., 2010b). Certainly, also TLR signaling activates the production of ROS via NADPH oxidases and in this way direct virus–cell contact could trigger Nox activation (Orient et al., 2007; Rada and Leto, 2008).

Notably, also independently of NADPH oxidases mitochondrial ROS occur in response to TLR stimulation. It is reported that signaling from TLR1, 2 and 4 leads to translocation of TRAF6 to mitochondria where it induces ubiquitylation of ECSIT (evolutionarily conserved signalling intermediate in Toll pathways) which is implicated in the mitochondrial respiratory chain leading to increased production of mitochondrial and cellular ROS (West et al., 2011). These TLRs are known as bacterial TLRs, but for example for TLR2 an interaction with HCMV is well described (Compton et al., 2003). Other possible sources for ROS in response to HCMV or viral infection in general cannot be excluded.

Besides other mechanisms than Nox4-induced ROS production, in future, further investigations on how Nox4 is induced by virus infection could be performed. *In vivo* analyses with Nox4-deficient mice were so far mostly concentrated on cardiovascular and neuronal pathologies (Kuroda et al., 2010; Sedwick, 2010). Under normal conditions Nox4 knockout mice appear to be healthy without any signs of dysfunction in areas where Nox4 is normally expressed. Interestingly, Nox4 activation has been associated with the exacerbation of chronic obstructive pulmonary disease (COPD). Apparently Nox4-mediated ROS generation leads to the release of pro-inflammatory cytokines and tissue damage (Michaeloudes et al., 2011; Ngkelo et al., 2012). Further, it has been shown that Nox4 upregulation in response to lung injury causes pulmonary fibrosis (Hecker et al., 2009).

However, the consequences of viral infection have not been analysed in Nox4-deficient mice. In figure 4.2 a model for HCMV infection, that summarises the mechanisms leading to very early antigen presentation in non-immune cells by i-proteasome-improved generation of peptides from oxidized and ubiquitylated viral antigens, is displayed.

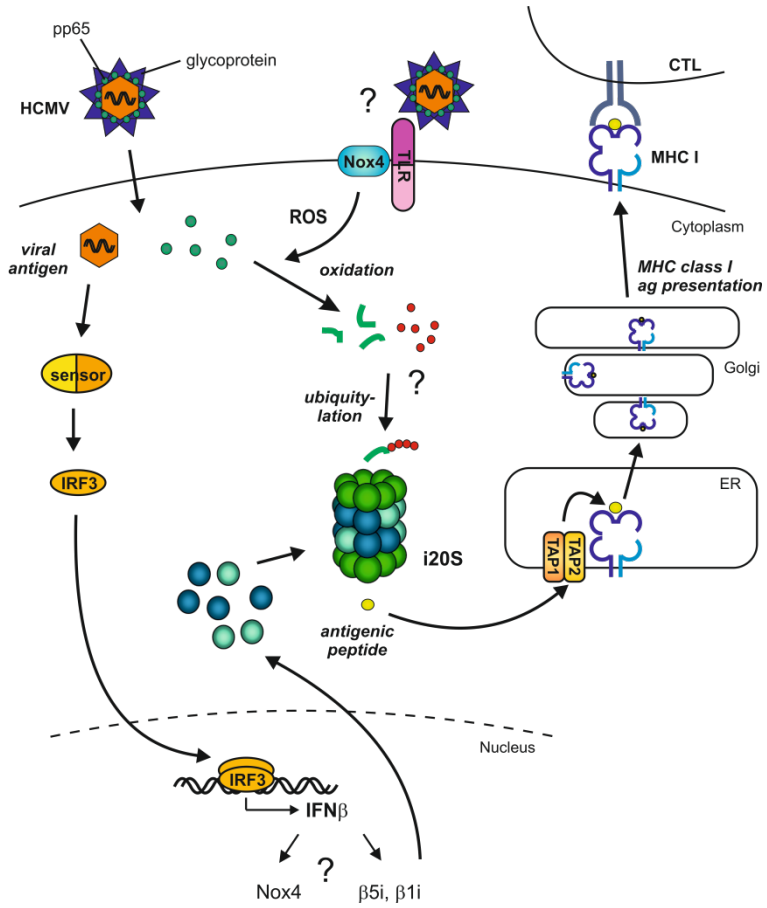

Figure 4.2 Model of HCMV infection in non-immune cells. With the entry of HCMV particles viral components are released into the cytoplasm of the host cell. Probably viral dsDNA is recognised by a certain sensor which induces transcription factor IRF3 to shuttle into the nucleus and activate the transcription of IFNβ and further ISGs. Either directly or via IFNβ feedback signalling (?) the expression of i-subunits is induced. Consequently, i-proteasomes which are probably associated with 19S on one and PA28 on the other side (not shown) are formed. Next, by secretion of type I IFN or possibly via an interaction of HCMV with TLRs (?), expression of the NADPH oxidase Nox4 is activated. The production of ROS by Nox4 affects viral antigens, such as the HCMV tegument protein pp65. Oxidized pp65 is targeted by an unknown mechanism (?) for ubiquitylation and hence degradation by the proteasome. The virus-dependent induction of i26S complexes improves the generation of antigenic peptides. The resulting peptides are transported via TAP into the lumen of the ER where they are loaded on MHC class I molecules. Peptide-MHC class I complexes are transported via the Golgi apparatus to the cell surface where they are presented to specific CTLs. In the text mentioned open questions suggesting future investigations were labelled with question marks.

4.3.5 A new role for ROS production

Finally, a general mechanism for the production of ROS in response to viral infection could be pointed out. As reported earlier also stimulation with inflammatory cytokines such as IFNγ elicits the production of ROS and increases the amount of oxidant-damaged and ubiquitylated proteins in cells (Seifert et al., 2010). By induction of the i-proteasome and DRiPs IFNγ treatment also enhances the peptide supply for MHC class I molecules and upregulates the surface expression of MHC class I (Strehl et al.,

2005). Here, the upregulation of MHC class I surface expression on IFNγ-treated HeLa cells was verified, in which an induction by almost 2.5-fold was observed after 24 hours (figure 3.29). Remarkably, the downregulation of either Nox4, to diminish the production of ROS, or of Rpn10, to inhibit the degradation of ubiquitylated proteins, strongly affected surface expression levels of MHC class I complexes (figure 3.29). In conclusion, the oxidative damage caused by ROS production plays an important general role to ensure the peptide supply for the MHC class I antigen presentation pathway in general. Supporting this finding is the reduction of total levels of oxidized as well as ubiquitylated proteins upon Nox4 knockdown in infected cells (figure 3.26). In conclusion, Nox4-generated radicals affect the degradation of newly translated as well as short- and long-lived cellular proteins in the same way as exogenously delivered proteins.

Within this thesis an exciting new role for the production of ROS in response to viral infection has been uncovered. A link between innate immune mechanisms and the induction of an efficient adaptive immune response has been provided in infected target cells. Presumably, ROS-induced oxidative damage of proteins is able to accelerate the protein turnover by concomitantly induced i-proteasomes which in turn more efficiently degrade the oxidized and ubiquitylated protein substrates to generate antigenic peptides for the presentation via MHC class I molecules. So far the acknowledged functions of ROS were restricted to the direct antimicrobial activity against pathogens, the production of hydrogen peroxide (H_2O_2) for peroxidases and the regulation of gene expression, such as the induction of pro-inflammatory genes by NFκB activation (Gloire et al., 2006). Here, ROS-induced oxidation of intracellular viral antigens leads to ubiquitylation and rapid degradation by the i-proteasome thereby supporting epitope generation and presentation to specific CTLs.

In the future, certain viral infections could be analysed in this regard. For example, during HCMV infection where overshooting $CD8^+$ T cell responses are problematic the role of ROS could be investigated from a new point of view. Also ROS production is known to play a role in inflammatory autoimmune diseases causing tissue damage and affecting gene expression. Maybe inflammation-induced ROS during autoimmune diseases also play a role for the presentation of auto-antigens.

The presented results in this thesis shed new light on the recently discovered link between oxidative stress and the induction of i-proteasomes. The ability of the i-proteasome to efficiently degrade oxidized proteins and to protect cells from accumulating toxic aggregates under stress and inflammation could be connected again to the initiation of adaptive immunity to fight and control virus infection.

Literature

Abate, D.A., Watanabe, S., and Mocarski, E.S. (2004). Major Human Cytomegalovirus Structural Protein pp65 (ppUL83) Prevents Interferon Response Factor 3 Activation in the Interferon Response. J Virol *78*, 10995-11006.

Abd El Mohsen, M.M., Iravani, M.M., Spencer, J.P.E., Rose, S., Fahim, A.T., Motawi, T.M.K., Ismail, N.A.F., and Jenner, P. (2005). Age-associated changes in protein oxidation and proteasome activities in rat brain: Modulation by antioxidants. Biochem Biophys Res Commun *336*, 386 - 391.

Ahn, J.Y., Tanahashi, N., Akiyama, K.-y., Hisamatsu, H., Noda, C., Tanaka, K., Chung, C.H., Shibmara, N., Willy, P.J., Mott, J.D.*, et al.* (1995). Primary structures of two homologous subunits of PA28, a γ-interferon-inducible protein activator of the 20S proteasome. FEBS Letters *366*, 37-42.

Ahn, K., Angulo, A., Ghazal, P., Peterson, P.A., Yang, Y., and Früh, K. (1996). Human cytomegalovirus inhibits antigen presentation by a sequential multistep process. Proceedings of the National Academy of Sciences *93*, 10990-10995.

Ahn, K., Gruhler, A., Galocha, B., Jones, T.R., Wiertz, E.J.H.J., Ploegh, H.L., Peterson, P.A., Yang, Y., and Früh, K. (1997). The ER-Luminal Domain of the HCMV Glycoprotein US6 Inhibits Peptide Translocation by TAP. Immunity *6*, 613-621.

Aki, M., Shimbara, N., Takashina, M., Akiyama, K., Kagawa, S., Tamura, T., Tanahashi, N., Yoshimura, T., Tanaka, K., and Ichihara, A. (1994). Interferon-gamma Induces Different Subunit Organizations and Functional Diversity of Proteasomes. Journal of Biochemistry *115*, 257-269.

Akira, S., Takeda, K., and Kaisho, T. (2001). Toll-like receptors: critical proteins linking innate and acquired immunity. Nat Immunol *2*, 675-680.

Akira, S., Uematsu, S., and Takeuchi, O. (2006). Pathogen Recognition and Innate Immunity. Cell *124*, 783-801.

Al-hakim, A.K., Zagorska, A., Chapman, L., Deak, M., Peggie, M., and Alessi, D.R. (2008). Control of AMPK-related kinases by USP9X and atypical Lys29/Lys33-linked polyubiquitin chains. Biochem J *411*, 249-260.

Alexopoulou, L., Holt, A.C., Medzhitov, R., and Flavell, R.A. (2001). Recognition of double-stranded RNA and activation of NF-[kappa]B by Toll-like receptor 3. Nature *413*, 732-738.

Alford, C.A., Stagno, S., Pass, R.F., and Britt, W.J. (1990). Congenital and perinatal cytomegalovirus infections. Rev Infect Dis *12*, 745-753.

Ardley, H.C., and Robinson, P.A. (2005). E3 ubiquitin ligases. Essays Biochem *41*, 15-30.

Arima, K., Kinoshita, A., Mishima, H., Kanazawa, N., Kaneko, T., Mizushima, T., Ichinose, K., Nakamura, H., Tsujino, A., Kawakami, A.*, et al.* (2011). Proteasome assembly defect due to a proteasome subunit beta type 8 (PSMB8) mutation causes the autoinflammatory disorder, Nakajo-Nishimura syndrome. Proceedings of the National Academy of Sciences *108*, 14914-14919.

Arnon, T.I., Achdout, H., Levi, O., Markel, G., Saleh, N., Katz, G., Gazit, R., Gonen-Gross, T., Hanna, J., Nahari, E.*, et al.* (2005). Inhibition of the NKp30 activating receptor by pp65 of human cytomegalovirus. Nat Immunol *6*, 515-523.

Arrode, G., and Davrinche, C. (2003). Dendritic cells and HCMV cross-presentation. Curr Top Microbiol Immunol *276*, 277-294.

Baker, R.T., and Board, P.G. (1987). The human ubiquitin gene family: structure of a gene and pseudogenes from the Ub B subfamily. Nucleic Acids Research *15*, 443-463.

Barton, L.F., Cruz, M., Rangwala, R., Deepe, G.S., and Monaco, J.J. (2002). Regulation of Immunoproteasome Subunit Expression In Vivo Following Pathogenic Fungal Infection. The Journal of Immunology *169*, 3046-3052.

Basler, M., Moebius, J., Elenich, L., Groettrup, M., and Monaco, J.J. (2006). An Altered T Cell Repertoire in MECL-1-Deficient Mice. The Journal of Immunology *176*, 6665-6672.

Basler, M., Youhnovski, N., van den Broek, M., Przybylski, M., and Groettrup, M. (2004). Immunoproteasomes Down-Regulate Presentation of a Subdominant T Cell Epitope from Lymphocytic Choriomeningitis Virus. The Journal of Immunology *173*, 3925-3934.

Baumeister, W., Walz, J., Zühl, F., and Seemüller, E. (1998). The Proteasome: Paradigm of a Self-Compartmentalizing Protease. Cell *92*, 367-380.

Bednarek, M.A., Sauma, S.Y., Gammon, M.C., Porter, G., Tamhankar, S., Williamson, A.R., and Zweerink, H.J. (1991). The minimum peptide epitope from the influenza virus matrix protein. Extra and intracellular loading of HLA-A2. The Journal of Immunology *147*, 4047-4053.

Benham, A., and Neefjes, J. (1997). Proteasome activity limits the assembly of MHC class I molecules after IFN-gamma stimulation. The Journal of Immunology *159*, 5896-5904.

Besold, K., Frankenberg, N., Pepperl-Klindworth, S., Kuball, J., Theobald, M., Hahn, G., and Plachter, B. (2007). Processing and MHC class I presentation of human cytomegalovirus pp65-derived peptides persist despite gpUS2-11-mediated immune evasion. J Gen Virol *88*, 1429-1439.

Bochtler, M., Ditzel, L., Groll, M., Hartmann, C., and Huber, R. (1999). THE PROTEASOME. Annual Review of Biophysics and Biomolecular Structure *28*, 295-317.

Bodaghi, B., Slobbe–vanDrunen, M.E.P., Topilko, A., Perret, E., Vossen, R.C.R.M., van Dam–Mieras, M.C.E., Zipeto, D., Virelizier, J.-L., LeHoang, P., Bruggeman, C.A.*, et al.* (1999). Entry of Human Cytomegalovirus into Retinal Pigment Epithelial and Endothelial Cells by Endocytosis. Investigative Ophthalmology & Visual Science *40*, 2598-2607.

Boehme, K.W., Singh, J., Perry, S.T., and Compton, T. (2004). Human Cytomegalovirus Elicits a Coordinated Cellular Antiviral Response via Envelope Glycoprotein B. J Virol *78*, 1202-1211.

Boes, B., Hengel, H., Ruppert, T., Multhaup, G., Koszinowski, U.H., and Kloetzel, P.M. (1994). Interferon gamma stimulation modulates the proteolytic activity and cleavage site preference of 20S mouse proteasomes. J Exp Med *179*, 901-909.

Boname, J.M., Thomas, M., Stagg, H.R., Xu, P., Peng, J., and Lehner, P.J. (2010). Efficient Internalization of MHC I Requires Lysine-11 and Lysine-63 Mixed Linkage Polyubiquitin Chains. Traffic *11*, 210-220.

Boo, K.-H., and Yang, J.-S. (2010). Intrinsic Cellular Defenses against Virus Infection by Antiviral Type I Interferon. Yonsei Med J *51*, 9-17.

Boppana, S.B., and Britt, W.J. (1995). Antiviral Antibody Responses and Intrauterine Transmission after Primary Maternal Cytomegalovirus Infection. Journal of Infectious Diseases *171*, 1115-1121.

Boulo, S., Akarsu, H., Ruigrok, R.W.H., and Baudin, F. (2007). Nuclear traffic of influenza virus proteins and ribonucleoprotein complexes. Virus Research *124*, 12-21.

Bouvier, N.M., and Palese, P. (2008). The Biology of Influenza viruses. Vaccine *26*, D49-D53.

Bowerman, B., and Kurz, T. (2006). Degrade to create: developmental requirements for ubiquitin-mediated proteolysis during early C. elegans embryogenesis. Development *133*, 773-784.

Britt, W.J., and Mach, M. (1996). Human cytomegalovirus glycoproteins. Intervirology *39*, 401-412.

Britt, W.J., Vugler, L., Butfiloski, E.J., and Stephens, E.B. (1990). Cell surface expression of human cytomegalovirus (HCMV) gp55-116 (gB): use of HCMV-recombinant vaccinia virus-infected cells in analysis of the human neutralizing antibody response. Journal of Virology *64*, 1079-1085.

Browne, E.P., and Shenk, T. (2003). Human cytomegalovirus UL83-coded pp65 virion protein inhibits antiviral gene expression in infected cells. Proceedings of the National Academy of Sciences of the United States of America *100*, 11439-11444.

Browne, E.P., Wing, B., Coleman, D., and Shenk, T. (2001). Altered Cellular mRNA Levels in Human Cytomegalovirus-Infected Fibroblasts: Viral Block to the Accumulation of Antiviral mRNAs. Journal of Virology *75*, 12319-12330.

Bui, M., Whittaker, G., and Helenius, A. (1996). Effect of M1 protein and low pH on nuclear transport of influenza virus ribonucleoproteins. Journal of Virology *70*, 8391-8401.

Bunde, T., Kirchner, A., Hoffmeister, B., Habedank, D., Hetzer, R., Cherepnev, G., Proesch, S., Reinke, P., Volk, H.-D., Lehmkuhl, H.*, et al.* (2005). Protection from cytomegalovirus after transplantation is correlated with immediate early 1–specific CD8 T cells. The Journal of Experimental Medicine *201*, 1031-1036.

Burri, L., Höckendorff, J., Boehm, U., Klamp, T., Dohmen, R.J., and Lévy, F. (2000). Identification and characterization of a mammalian protein interacting with 20S proteasome precursors. Proc Natl Acad Sci USA *97*, 10348-10353.

Callahan, M.K., Wohlfert, E.A., Ménoret, A., and Srivastava, P.K. (2006). Heat Shock Up-Regulates lmp2 and lmp7 and Enhances Presentation of Immunoproteasome-Dependent Epitopes. The Journal of Immunology *177*, 8393-8399.

Callan, M.F.C., Fazou, C., Yang, H., Rostron, T., Poon, K., Hatton, C., and McMichael, A.J. (2000). CD8+ T-cell selection, function, and death in the primary immune response in vivo. The Journal of Clinical Investigation *106*, 1251-1261.

Cardozo, C. (1993). Catalytic components of the bovine pituitary multicatalytic proteinase complex (proteasome). Enzyme Protein *47*, 296-305.

Cascio, P., Call, M., Petre, B.M., Walz, T., and Goldberg, A.L. (2002). Properties of the hybrid form of the 26S proteasome containing both 19S and PA28 complexes. EMBO J *21*, 2636-2645.

Castillo, J.P., and Kowalik, T.F. (2002). Human cytomegalovirus immediate early proteins and cell growth control. Gene *290*, 19-34.

Cerundolo, V., Kelly, A., Elliott, T., Trowsdale, J., and Townsend, A. (1995). Genes encoded in the major histocompatibility complex affecting the generation of peptides for TAP transport. European Journal of Immunology *25*, 554-562.

Cha, T.A., Tom, E., Kemble, G.W., Duke, G.M., Mocarski, E.S., and Spaete, R.R. (1996). Human cytomegalovirus clinical isolates carry at least 19 genes not found in laboratory strains. Journal of Virology *70*, 78-83.

Chatterjee-Kishore, M., Wright, K.L., Ting, J.P.Y., and Stark, G.R. (2000). How Stat1 mediates constitutive gene expression: a complex of unphosphorylated Stat1 and IRF1 supports transcription of the LMP2 gene. EMBO J *19*, 4111 - 4122.

Chau, V., Tobias, J., Bachmair, A., Marriott, D., Ecker, D., Gonda, D., and Varshavsky, A. (1989). A multiubiquitin chain is confined to specific lysine in a targeted short-lived protein. Science *243*, 1576-1583.

Chen, W., Norbury, C.C., Cho, Y., Yewdell, J.W., and Bennink, J.R. (2001). Immunoproteasomes Shape Immunodominance Hierarchies of Antiviral CD8+ T Cells at the Levels of T Cell Repertoire and Presentation of Viral Antigens. J Exp Med *193*, 1319-1326.

Chevillotte, M., Landwehr, S., Linta, L., Frascaroli, G., Luske, A., Buser, C., Mertens, T., and von Einem, J. (2009). Major Tegument Protein pp65 of Human Cytomegalovirus Is Required for the Incorporation of pUL69 and pUL97 into the Virus Particle and for Viral Growth in Macrophages. J Virol *83*, 2480-2490.

Chondrogianni, N., and Gonos, E. (2004). Proteasome inhibition induces senescence-like phenotype in primary human fibroblasts cultures. Biogerontoloy *5*, 55-61.

Chondrogianni, N., Stratford, F.L.L., Trougakos, I.P., Friguet, B., Rivett, A.J., and Gonos, E.S. (2003). Central role of the proteasome in senescence and survival of human fibroblasts. J Biol Chem *278*, 28026-28037.

Ciechanover, A., Finley, D., and A., V. (1984). The ubiquitin-mediated proteolytic pathway and mechanisms of energy-dependent intracellular protein degradation. J Cell Biochem *24*, 27-53.

Coffino, P. (2001). Antizyme, a mediator of ubiquitin-independent proteasomal degradation. Biochimie *83*, 319-323.

Collins, G.A., and Tansey, W.P. (2006). The proteasome: a utility tool for transcription? Current Opinion in Genetics & Development *16*, 197-202.

Compton, T. (2004). Receptors and immune sensors: the complex entry path of human cytomegalovirus. Trends in Cell Biology *14*, 5-8.

Compton, T., Kurt-Jones, E.A., Boehme, K.W., Belko, J., Latz, E., Golenbock, D.T., and Finberg, R.W. (2003). Human Cytomegalovirus Activates Inflammatory Cytokine Responses via CD14 and Toll-Like Receptor 2. J Virol *77*, 4588-4596.

Compton, T., Nepomuceno, R.R., and Nowlin, D.M. (1992). Human cytomegalovirus penetrates host cells by pH-independent fusion at the cell surface. Virology *191*, 387-395.

Compton, T., Nowlin, D.M., and Cooper, N.R. (1993). Initiation of Human Cytomegalovirus Infection Requires Initial Interaction with Cell Surface Heparan Sulfate. Virology *193*, 834-841.

Coux, O., Tanaka, K., and Goldberg, A.L. (1996). Structure and functions of the 20S and 26S proteasomes. Annu Rev Biochem *65*, 801-847.

Cox, N.J., and Subbarao, K. (2000). Global epidemiology of influenza: past and present. Annu Rev Med *51*, 407-421.

Cresswell, P., Ackerman, A.L., Giodini, A., Peaper, D.R., and Wearsch, P.A. (2005). Mechanisms of MHC class I-restricted antigen processing and cross-presentation. Immunological Reviews *207*, 145-157.

Crough, T., and Khanna, R. (2009). Immunobiology of Human Cytomegalovirus: from Bench to Bedside. Clin Microbiol Rev *22*, 76-98.

Dahlmann, B. (2007). Role of proteasomes in disease. BMC Biochemistry *8*, S3.

Dahlmann, B., Kopp, F., Kuehn, L., Reinauer, H., and Schwenen, M. (1986). Studies on the multicatalytic proteinase from rat skeletal muscle. Biomed Biochim Acta *45*, 1493-1501.

Dahlmann, B., Ruppert, T., Kuehn, L., Merforth, S., and Kloetzel, P.-M. (2000). Different proteasome subtypes in a single tissue exhibit different enzymatic properties. Journal of Molecular Biology *303*, 643-653.

Daniels, P.S., Jeffries, S., Yates, P., Schild, G.C., Rogers, G.N., Paulson, J.C., Wharton, S.A., Douglas, A.R., Skehel, J.J., and Wiley, D.C. (1987). The receptor-binding and membrane-fusion properties of influenza virus variants selected using anti-haemagglutinin monoclonal antibodies. EMBO J *6*, 1459-1465.

Davies, K.J.A. (2001). Degradation of oxidized proteins by the 20S proteasome. Biochimie *83*, 301-310.

Davignon, J.L., Castanié, P., Yorke, J.A., Gautier, N., Clément, D., and Davrinche, C. (1996). Anti-human cytomegalovirus activity of cytokines produced by CD4+ T-cell clones specifically activated by IE1 peptides in vitro. Journal of Virology *70*, 2162-2169.

de Jong, M.D., Galasso, G.J., Gazzard, B., Griffiths, P.D., Jabs, D.A., Kern, E.R., and Spector, S.A. (1998). Summary of the II International Symposium on Cytomegalovirus. Antiviral Research *39*, 141-162.

DeFilippis, V.R., Alvarado, D., Sali, T., Rothenburg, S., and Fruh, K. (2010). Human Cytomegalovirus Induces the Interferon Response via the DNA Sensor ZBP1. J Virol *84*, 585-598.

DeFilippis, V.R., Robinson, B., Keck, T.M., Hansen, S.G., Nelson, J.A., and Fruh, K.J. (2006). Interferon Regulatory Factor 3 Is Necessary for Induction of Antiviral Genes during Human Cytomegalovirus Infection. J Virol *80*, 1032-1037.

Deng, L., Wang, C., Spencer, E., Yang, L., Braun, A., You, J., Slaughter, C., Pickart, C., and Chen, Z.J. (2000). Activation of the IkappaB Kinase Complex by TRAF6 Requires a Dimeric Ubiquitin-Conjugating Enzyme Complex and a Unique Polyubiquitin Chain. Cell *103*, 351-361.

Deol, P., Zaiss, D.M.W., Monaco, J.J., and Sijts, A.J.A.M. (2007). Rates of Processing Determine the Immunogenicity of Immunoproteasome-Generated Epitopes. The Journal of Immunology *178*, 7557-7562.

Diamond, D.J., York, J., Sun, J.-Y., Wright, C.L., and Forman, S.J. (1997). Development of a Candidate HLA A*0201 Restricted Peptide-Based Vaccine Against Human Cytomegalovirus Infection. Blood *90*, 1751-1767.

Dick, T.P., Nussbaum, A.K., Deeg, M., Heinemeyer, W., Groll, M., Schirle, M., Keilholz, W., Stevanovic, S., Wolf, D.H., Huber, R.*, et al.* (1998). Contribution of proteasomal beta-subunits to the cleavage of peptide substrates analysed with yeast mutants. J Biol Chem *273*, 25637-25646.

Ding, Q., Martin, S., Dimayuga, E., Bruce-Keller, A.J., and Keller, J.N. (2006). LMP2 Knock-Out Mice Have Reduced Proteasome Activities and Increased Levels of Oxidatively Damaged Proteins. Antioxidants & Redox Signaling *8*, 130-135.

Dolan, B.P., Li, L., Takeda, K., Bennink, J.R., and Yewdell, J.W. (2010). Defective Ribosomal Products Are the Major Source of Antigenic Peptides Endogenously Generated from Influenza A Virus Neuraminidase. The Journal of Immunology *184*, 1419-1424.

Driscoll, J., Brown, M.G., Finley, D., and Monaco, J.J. (1993). MHC-linked LMP gene products specifically alter peptidase activities of the proteasome. Nature *365*, 262-264.

Dudek, E.J., Shang, F., Liu, Q., Valverde, P., Hobbs, M., and Taylor, A. (2005). Selectivity of the ubiquitin pathway for oxidatively modified proteins: relevance to protein precipitation diseases. The FASEB Journal *19*, 1707 - 1709.

Ebstein, F., Kloetzel, P.-M., Krüger, E., and Seifert, U. (2012). Emerging roles of immunoproteasomes beyond MHC class I antigen processing. Cellular and Molecular Life Sciences, 1-16.

Ebstein, F., Lange, N., Urban, S., Seifert, U., Krüger, E., and Kloetzel, P.-M. (2009). Maturation of human dendritic cells is accompanied by functional remodelling of the ubiquitin-proteasome system. The International Journal of Biochemistry & Cell Biology *41*, 1205-1215.

Elkington, R., Walker, S., Crough, T., Menzies, M., Tellam, J., Bharadwaj, M., and Khanna, R. (2003). Ex Vivo Profiling of CD8+-T-Cell Responses to Human Cytomegalovirus Reveals Broad and Multispecific Reactivities in Healthy Virus Carriers. J Virol *77*, 5226-5240.

Emery, V.C., Cope, A.V., Bowen, E.F., Gor, D., and Griffiths, P.D. (1999). The Dynamics of Human Cytomegalovirus Replication in Vivo. The Journal of Experimental Medicine *190*, 177-182.

Falk, K., and Rötzschke, O. (1993). Consensus motifs and peptide ligands of MHC class I molecules. Seminars in Immunology *5*, 81-94.

Fehling, H.J., Swat, W., Laplace, C., Kühn, R., Rajewsky, K., Müller, U., and von Boehmer, H. (1994). MHC class I expression in mice lacking the proteasome subunit LMP-7. Science *265*, 1234-1237.

Ferrell, K., Wilkinson, C.R.M., Dubiel, W., and Gordon, C. (2000). Regulatory subunit interactions of the 26S proteasome, a complex problem. Trends in Biochemical Sciences *25*, 83-88.

Finley, D. (2009). Recognition and Processing of Ubiquitin-Protein Conjugates by the Proteasome. Annual Review of Biochemistry *78*, 477-513.

Fonteneau, J.-F., Larsson, M., Somersan, S., Sanders, C., Münz, C., Kwok, W.W., Bhardwaj, N., and Jotereau, F. (2001). Generation of high quantities of viral and tumor-specific human CD4+ and CD8+ T-cell clones using peptide pulsed mature dendritic cells. Journal of Immunological Methods *258*, 111-126.

Fortunato, E.A., and Spector, D.H. (1998). p53 and RPA Are Sequestered in Viral Replication Centers in the Nuclei of Cells Infected with Human Cytomegalovirus. J Virol *72*, 2033-2039.

Frentzel, S., Pesold-Hurt, B., Seelig, A., and Kloetzel, P.-M. (1994). 20S proteasomes are assembled via distinct precursor complexes processing of LMP2 and LMP7 proproteins takes place in 13-16S preproteasome complexes. Journal of Molecular Biology *236*, 975-981.

Fricke, B., Heink, S., Steffen, J., Kloetzel, P.-M., and Krüger, E. (2007). The proteasome maturation protein POMP facilitates major steps of 20S proteasome formation at the endoplasmic reticulum. Nature Publishing Group *8*, 1170-1175.

Fujita, K.-I., and Srinivasula, S.M. (2011). TLR4-mediated autophagy in macrophages is a p62-dependent type of selective autophagy of aggresome-like induced structures (ALIS). Autophagy *7*, 552-554.

Gaczynska, M., Rock, K.L., and Goldberg, A.L. (1993). Gamma-Interferon and expression of MHC genes regulate peptide hydrolysis by proteasomes. *365*, 264-267.

Gallez-Hawkins, G., Villacres, M.C., Li, X., Sanborn, M.C., Lomeli, N.A., and Zaia, J.A. (2003). Use of transgenic HLA A*0201/Kb and HHD II mice to evaluate frequency of cytomegalovirus IE1-derived peptide usage in eliciting human CD8 cytokine response. J Virol *77*, 4457–4462.

Geraghty, D.E., Daza, R., Williams, L.M., Vu, Q., and Ishitani, A. (2002). Genetics of the immune response: identifying immune variation within the MHC and throughout the genome. Immunological Reviews *190*, 69-85.

Gerna, G., Zipeto, D., Percivalle, E., Parea, M., Revello, M.G., Maccario, R., Peri, G., and Milanesi, G. (1992). Human Cytomegalovirus Infection of the Major Leukocyte Subpopulations and Evidence for Initial Viral Replication in Polymorphonuclear Leukocytes from Viremic Patients. Journal of Infectious Diseases *166*, 1236-1244.

Gibson, W. (1996). Structure and assembly of the virion. Intervirology *39*, 389-400.

Gilbert, M.J., Riddell, S.R., Plachter, B., and Greenberg, P.D. (1996). Cytomegalovirus selectively blocks antigen processing and presentation of its immediate-early gene product. Nature *383*, 720-722.

Giles, J. (2004). Chemistry Nobel for trio who revealed molecular death-tag. Nature *431*, 729-729.

Glickman, M.H., and Ciechanover, A. (2002). The Ubiquitin-Proteasome Proteolytic Pathway: Destruction for the Sake of Construction. Physiol Rev *82*, 373-428.

Glickman, M.H., Rubin, D.M., Coux, O., Wefes, I., Pfeifer, G., Cjeka, Z., Baumeister, W., Fried, V.A., and Finley, D. (1998). A subcomplex of the regulatory particle required for ubiquitin-conjugate degradation and related to the COP9-signalosome and eIF3. Cell *94*, 615 - 623.

Glickman, M.H., Rubin, D.M., Fu, H., Larsen, C.N., Coux, O., Wefes, I., Pfeifer, G., Cjeka, Z., Vierstra, R., Baumeister, W., *et al.* (1999). Functional analysis of the proteasome regulatory particle. Molecular Biology Reports *26*, 21-28.

Gloire, G., Legrand-Poels, S., and Piette, J. (2006). NF-κB activation by reactive oxygen species: Fifteen years later. Biochemical Pharmacology *72*, 1493-1505.

Golab, J., Bauer, T.M., Daniel, V., and Naujokat, C. (2004). Role of the ubiquitin-proteasome pathway in the diagnosis of human diseases. Clinica Chimica Acta *340*, 27-40.

Goldberg, A.L. (2007). Functions of the proteasome: from protein degradation and immune surveillance to cancer therapy. Biochem Soc Trans *35*, 12-17.

Goldberg, A.L., Cascio, P., Saric, T., and Rock, K.L. (2002). The importance of the proteasome and subsequent proteolytic steps in the generation of antigenic peptides. Molecular Immunology *39*, 147-164.

Goldberg, A.L., and Rock, K.L. (1992). Proteolysis, proteasomes and antigen presentation. Nature *357*, 375-379.

Goldstein, G., Scheid, M., Hammerling, U., Schlesinger, D.H., Niall, H.D., and Boyse, E.A. (1975). Isolation of a polypeptide that has lymphocyte-differentiating properties and is probably represented universally in living cells. Proc Natl Acad Sci U S A *72*, 11-15.

Gotch, F., McMichael, A., Smith, G., and Moss, B. (1987). Identification of viral molecules recognized by influenza-specific human cytotoxic T lymphocytes. J Exp Med *165*, 408-416.

Gottschalk, A. (1958). The influenza virus neuraminidase. Nature *181*, 377-378.

Grefte, A., Harmsen, M.C., van der Giessen, M., Knollema, S., van Son, W.J., and The, T.H. (1994). Presence of human cytomegalovirus (HCMV) immediate early mRNA but not ppUL83 (lower matrix protein pp65) mRNA in polymorphonuclear and mononuclear leukocytes during active HCMV infection. Journal of General Virology *75*, 1989-1998.

Grefte, J.M., van der Giessen, M., Blom, N., The, T.H., and van Son, W.J. (1995). Circulating cytomegalovirus-infected endothelial cells after renal transplantation: possible clue to pathophysiology? Transplant Proc *27*, 939-942.

Griffin, T.A., Nandi, D., Cruz, M., Fehling, H.J., Kaer, L.V., Monaco, J.J., and Colbert, R.A. (1998). Immunoproteasome Assembly: Cooperative Incorporation of Interferon gamma (IFN-gamma)-inducible Subunits. J Exp Med *187*, 97-104.

Groettrup, M., Kirk, C.J., and Basler, M. (2010). Proteasomes in immune cells: more than peptide producers? Nat Rev Immunol *10*, 73-78.

Groettrup, M., Kraft, R., Kostka, S., Standera, S., Stohwasser, R., and Kloetzel, P.-M. (1996a). A third interferon-γ-induced subunit exchange in the 20S proteasome. European Journal of Immunology *26*, 863-869.

Groettrup, M., Soza, A., Kuckelkorn, U., and Kloetzel, P.-M. (1996b). Peptide antigen production by the proteasome: complexity provides efficiency. Immunology Today *17*, 429-435.

Groettrup, M., Standera, S., Stohwasser, R., and Kloetzel, P.-M. (1997). The subunits MECL-1 and LMP2 are mutually required for incorporation into the 20S proteasome. Proc Natl Acad Sci USA *94*, 8970-8975.

Groll, M., Bajorek, M., Kohler, A., Moroder, L., Rubin, D.M., Huber, R., Glickman, M.H., and Finley, D. (2000). A gated channel into the proteasome core particle. Nat Struct Mol Biol *7*, 1062-1067.

Groll, M., Ditzel, L., Lowe, J., Stock, D., Bochtler, M., Bartunik, H.D., and Huber, R. (1997). Structure of 20S proteasome from yeast at 2.4A resolution. *386*, 463-471.

Grune, T., Blasig, I.E., Sitte, N., Roloff, B., Haseloff, R., and Davies, K.J.A. (1998). Peroxynitrite Increases the Degradation of Aconitase and Other Cellular Proteins by Proteasome. Journal of Biological Chemistry *273*, 10857-10862.

Grune, T., Reinheckel, T., and Davies, K. (1997). Degradation of oxidized proteins in mammalian cells. The FASEB Journal *11*, 526-534.

Guillot, L., Le Goffic, R., Bloch, S., Escriou, N., Akira, S., Chignard, M., and Si-Tahar, M. (2005). Involvement of Toll-like Receptor 3 in the Immune Response of Lung Epithelial Cells to Double-stranded RNA and Influenza A Virus. Journal of Biological Chemistry *280*, 5571-5580.

Haas, A.L., Warms, J.V., Hershko, A., and Rose, I.A. (1982). Ubiquitin-activating enzyme. Mechanism and role in protein-ubiquitin conjugation. Journal of Biological Chemistry *257*, 2543-2548.

Halenius, A., Hauka, S., Dölken, L., Stindt, J., Reinhard, H., Wiek, C., Hanenberg, H., Koszinowski, U.H., Momburg, F., and Hengel, H. (2011). Human Cytomegalovirus Disrupts the Major Histocompatibility Complex Class I Peptide-Loading Complex and Inhibits Tapasin Gene Transcription. Journal of Virology *85*, 3473-3485.

Heath, W.R., Belz, G.T., Behrens, G.M.N., Smith, C.M., Forehan, S.P., Parish, I.A., Davey, G.M., Wilson, N.S., Carbone, F.R., and Villadangos, J.A. (2004). Cross-presentation, dendritic cell subsets, and the generation of immunity to cellular antigens. Immunological Reviews *199*, 9-26.

Hecker, L., Vittal, R., Jones, T., Jagirdar, R., Luckhardt, T.R., Horowitz, J.C., Pennathur, S., Martinez, F.J., and Thannickal, V.J. (2009). NADPH oxidase-4 mediates myofibroblast activation and fibrogenic responses to lung injury. Nat Med *15*, 1077-1081.

Heil, F., Hemmi, H., Hochrein, H., Ampenberger, F., Kirschning, C., Akira, S., Lipford, G., Wagner, H., and Bauer, S. (2004). Species-specific recognition of single-stranded RNA via toll-like receptor 7 and 8. Science *303*, 1526-1529.

Heink, S., Ludwig, D., Kloetzel, P.M., and Krüger, E. (2005). IFN-gamma-induced immune adaptation of the proteasome system is an accelerated and transient response. Proc Natl Acad Sci USA *102*, 9241-9246.

Hendil, K.B., Khan, S., and Tanaka, K. (1998). Simultaneous binding of PA28 and PA700 activators to 20 S proteasomes. Biochem J *3*, 749-754.

Hengel, H., Flohr, T., Hämmerling, G.J., Koszinowski, U.H., and Momburg, F. (1996). Human Cytomegalovirus Inhibits Peptide Translocation into the Endoplasmic Reticulum for MHC Class I Assembly. Journal of General Virology *77*, 2287-2296.

Henkart, P. (1994). Lymphocyte-mediated cytotoxicity: Two pathways and multiple effector molecules. Immunity *1*, 343-346.

Hensley, S.E., Das, S.R., Bailey, A.L., Schmidt, L.M., Hickman, H.D., Jayaraman, A., Viswanathan, K., Raman, R., Sasisekharan, R., Bennink, J.R.*, et al.* (2009). Hemagglutinin Receptor Binding Avidity Drives Influenza A Virus Antigenic Drift. Science *326*, 734-736.

Hensley, S.E., Zanker, D., Dolan, B.P., David, A., Hickman, H.D., Embry, A.C., Skon, C.N., Grebe, K.M., Griffin, T.A., Chen, W.*, et al.* (2010). Unexpected Role for the Immunoproteasome Subunit LMP2 in Antiviral Humoral and Innate Immune Responses. J Immunol *184*, 4115-4122.

Hershko, A., and Ciechanover, A. (1998). THE UBIQUITIN SYSTEM. Annual Review of Biochemistry *67*, 425-479.

Hershko, A., Ciechanover, A., Heller, H., Haas, A.L., and Rose, I.A. (1980). Proposed role of ATP in protein breakdown: conjugation of protein with multiple chains of the polypeptide of ATP-dependent proteolysis. Proc Natl Acad Sci U S A *77*, 1783-1786.

Hershko, A., Ganoth, D., Pehrson, J., Palazzo, R.E., and Cohen, L.H. (1991). Methylated ubiquitin inhibits cyclin degradation in clam embryo extracts. Journal of Biological Chemistry *266*, 16376-16379.

Hershko, A., Heller, H., Elias, S., and Ciechanover, A. (1983). Components of ubiquitin-protein ligase system. Resolution, affinity purification, and role in protein breakdown. Journal of Biological Chemistry *258*, 8206-8214.

Hirano, Y., Hendil, K.B., Yashiroda, H., Iemura, S.-i., Nagane, R., Hioki, Y., Natsume, T., Tanaka, K., and Murata, S. (2005). A heterodimeric complex that promotes the assembly of mammalian 20S proteasomes. Nature *437*, 1381-1385.

Hirano, Y., Kaneko, T., Okamoto, K., Bai, M., Yashiroda, H., Furuyama, K., Kato, K., Tanaka, K., and Murata, S. (2008). Dissecting beta-ring assembly pathway of the mammalian 20S proteasome. EMBO J *27*, 2204-2213.

Horimoto, T., and Kawaoka, Y. (2005). Influenza: lessons from past pandemics, warnings from current incidents. Nat Rev Microbiol *3*, 591-600.

Hough, R., Pratt, G., and Rechsteiner, M. (1986). Ubiquitin-lysozyme conjugates. Identification and characterization of an ATP-dependent protease from rabbit reticulocyte lysates. Journal of Biological Chemistry *261*, 2400-2408.

Hussong, S.A., Kapphahn, R.J., Phillips, S.L., Maldonado, M., and Ferrington, D.A. (2010). Immunoproteasome deficiency alters retinal proteasome's response to stress. Journal of Neurochemistry *113*, 1481-1490.

Hutchinson, S., Sims, S., O'Hara, G., Silk, J., Gileadi, U., Cerundolo, V., and Klenerman, P. (2011). A Dominant Role for the Immunoproteasome in CD8+ T Cell Responses to Murine Cytomegalovirus. PLoS ONE *6*, e14646.

Jahn, G., and Mach, M. (1990). Human cytomegalovirus phosphoproteins and glycoproteins and their coding regions. Curr Top Microbiol Immunol *154*, 171-185.

Jahn, G., Pohl, W., Plachter, B., and v. Hintzenstern, J. (1988). Congenital cytomegalovirus infection with fatal outcome. Dtsch med Wochenschr *113*, 424-427.

Jäkel, S., Kuckelkorn, U., Szalay, G., Plötz, M., Textoris-Taube, K., Opitz, E., Klingel, K., Stevanovic, S., Kandolf, R., Kotsch, K.*, et al.* (2009). Differential Interferon Responses Enhance Viral Epitope Generation by Myocardial Immunoproteasomes in Murine Enterovirus Myocarditis. The American Journal of Pathology *175*, 510-518.

Jamaluddin, M., Wang, S., Garofalo, R.P., Elliott, T., Casola, A., Baron, S., and Brasier, A.R. (2001). IFN-beta mediates coordinate expression of antigen-processing genes in RSV-infected pulmonary epithelial cells. Am J Physiol Lung Cell Mol Physiol *280*, L248-257.

Janeway, C.A.J. (1989). Approaching the asymptote? Evolution and revolution in immunology. Cold Spring Harbor Symp Quant Biol *54*, 1-13.

Jin, J., Li, X., Gygi, S.P., and Harper, J.W. (2007). Dual E1 activation systems for ubiquitin differentially regulate E2 enzyme charging. Nature *447*, 1135-1138.

Jin, L., Williamson, A., Banerjee, S., Philipp, I., and Rape, M. (2008). Mechanism of Ubiquitin-Chain Formation by the Human Anaphase-Promoting Complex. Cell *133*, 653-665.

Johnson, N.P., and Mueller, J. (2002). Updating the accounts: global mortality of the 1918-1920 "Spanish" influenza pandemic. Bull Hist Med, 2002 *76*, 105-115.

Juckem, L.K., Boehme, K.W., Feire, A.L., and Compton, T. (2008). Differential Initiation of Innate Immune Responses Induced by Human Cytomegalovirus Entry into Fibroblast Cells. J Immunol *180*, 4965-4977.

Kagan, J.C., Su, T., Horng, T., Chow, A., Akira, S., and Medzhitov, R. (2008). TRAM couples endocytosis of Toll-like receptor 4 to the induction of interferon-beta. Nat Immunol *9*, 361-368.

Karabinova, P., Kubelka, M., and Susor, A. (2011). Proteasomal degradation of ubiquitinated proteins in oocyte meiosis and fertilization in mammals. Cell and Tissue Research *346*, 1-9.

Karin, M., and Ben-Neriah, Y. (2000). Phosphorylation meets ubiquitination: the control of NF-kappaB activity. Annu Rev Immunol *18*, 621-663.

Kaspari, M., Tavalai, N., Stamminger, T., Zimmermann, A., Schilf, R., and Bogner, E. (2008). Proteasome inhibitor MG132 blocks viral DNA replication and assembly of human cytomegalovirus. FEBS Letters *582*, 666-672.

Katsuyama, M. (2010). NOX/NADPH Oxidase, the Superoxide-Generating Enzyme: Its Transcriptional Regulation and Physiological Roles. Journal of Pharmacological Sciences *114*, 134-146.

Kawai, T., and Akira, S. (2006). Innate immune recognition of viral infection. Nat Immunol *7*, 131-137.

Kawai, T., and Akira, S. (2007). Antiviral Signaling Through Pattern Recognition Receptors. Journal of Biochemistry *141*, 137-145.

Kawai, T., and Akira, S. (2010). The role of pattern-recognition receptors in innate immunity: update on Toll-like receptors. Nat Immunol *11*, 373-384.

Kawai, T., Takahashi, K., Sato, S., Coban, C., Kumar, H., Kato, H., Ishii, K.J., Takeuchi, O., and Akira, S. (2005). IPS-1, an adaptor triggering RIG-I- and Mda5-mediated type I interferon induction. Nat Immunol *6*, 981-988.

Keller, J.N., Dimayuga, E., Chen, Q., Thorpe, J., Gee, J., and Ding, Q. (2004). Autophagy, proteasomes, lipofuscin, and oxidative stress in the aging brain. The International Journal of Biochemistry and Cell Biology *36*, 2376-2391.

Kern, F., Surel, I.P., Faulhaber, N., Frömmel, C., Schneider-Mergener, J., Schönemann, C., Reinke, P., and Volk, H.-D. (1999). Target Structures of the CD8+-T-Cell Response to Human Cytomegalovirus: the 72-Kilodalton Major Immediate-Early Protein Revisited. Journal of Virology *73*, 8179-8184.

Khan, S., de Giuli, R., Schmidtke, G., Bruns, M., Buchmeier, M., van den Broek, M., and Groettrup, M. (2001a). Cutting Edge: Neosynthesis Is Required for the Presentation of a T Cell Epitope from a Long-Lived Viral Protein. The Journal of Immunology *167*, 4801-4804.

Khan, S., van den Broek, M., Schwarz, K., de Giuli, R., Diener, P.-A., and Groettrup, M. (2001b). Immunoproteasomes Largely Replace Constitutive Proteasomes During an Antiviral and Antibacterial Immune Response in the Liver. J Immunol *167*, 6859-6868.

Khan, S., Zimmermann, A., Basler, M., Groettrup, M., and Hengel, H. (2004). A Cytomegalovirus Inhibitor of Gamma Interferon Signaling Controls Immunoproteasome Induction. J Virol *78*, 1831-1842.

Kim, H.T., Kim, K.P., Lledias, F., Kisselev, A.F., Scaglione, K.M., Skowyra, D., Gygi, S.P., and Goldberg, A.L. (2007). Certain Pairs of Ubiquitin-conjugating Enzymes (E2s) and Ubiquitin-Protein Ligases (E3s) Synthesize Nondegradable Forked Ubiquitin Chains Containing All Possible Isopeptide Linkages. Journal of Biological Chemistry *282*, 17375-17386.

Kim, H.T., Kim, K.P., Uchiki, T., Gygi, S.P., and Goldberg, A.L. (2009). S5a promotes protein degradation by blocking synthesis of nondegradable forked ubiquitin chains. EMBO J *28*, 1867-1877.

Kimura, Y., and Tanaka, K. (2010). Regulatory mechanisms involved in the control of ubiquitin homeostasis. Journal of Biochemistry *147*, 793-798.

Kisselev, A.F., Kaganovich, D., and Goldberg, A.L. (2002). Binding of hydrophobic peptides to several non-catalytic sites promotes peptide hydrolysis by all active sites of 20S proteasomes. Evidence for peptide induced channel opening in the alpha-rings. J Biol Chem *277*, 22260 - 22270.

Kitamura, A., Maekawa, Y., Uehara, H., Izumi, K., Kawachi, I., Nishizawa, M., Toyoshima, Y., Takahashi, H., Standley, D.M., Tanaka, K.*, et al.* (2011). A mutation in the immunoproteasome subunit PSMB8 causes autoinflammation and lipodystrophy in humans. J Clin Invest *121*, 4150-4160.

Kloetzel, P.-M. (2001). Antigen processing by the proteasome. Nat Rev Mol Cell Biol *2*, 179-188.

Kloetzel, P.-M. (2004). The proteasome and MHC class I antigen processing. Biochimica et Biophysica Acta (BBA) - Molecular Cell Research *1695*, 225-233.

Klumpp, K., Ruigrok, R.W., and Baudin, F. (1997). Roles of the influenza virus polymerase and nucleoprotein in forming a functional RNP structure. EMBO J *16*, 1248-1257.

Komander, D. (2009). The emerging complexity of protein ubiquitination. Biochem Soc Trans *37*, 937-953.

Kotamraju, S., Matalon, S., Matsunaga, T., Shang, T., Hickman-Davis, J.M., and Kalyanaraman, B. (2006). Upregulation of immunoproteasomes by nitric oxide: Potential antioxidative mechanism in endothelial cells. Free Radical Biol Med *40*, 1034 - 1044.

Kreijtz, J.H.C.M., Fouchier, R.A.M., and Rimmelzwaan, G.F. (2011). Immune responses to influenza virus infection. Virus Research *162*, 19-30.

Kriegenburg, F., Ellgaard, L., and Hartmann-Petersen, R. (2012). Molecular chaperones in targeting misfolded proteins for ubiquitin-dependent degradation. FEBS Journal *279*, 532-542.

Kriegenburg, F., Poulsen, E.G., Koch, A., Krueger, E., and Hartmann-Petersen, R. (2011). Redox Control of the Ubiquitin-Proteasome System: From Molecular Mechanisms to Functional Significance. Antioxidants & Redox Signaling.

Krüger, E., and Kloetzel, P.-M. (2012). Immunoproteasomes at the interface of innate and adaptive immune responses: two faces of one enzyme. Current Opinion in Immunology *24*, 77-83.

Kruger, E., Kloetzel, P.-M., and Enenkel, C. (2001). 20S proteasome biogenesis. Biochimie *83*, 289-293.

Kuckelkorn, U., Frentzel, S., Kraft, R., Kostka, S., Groettrup, M., and Kloetzel, P.-M. (1995). Incorporation of major histocompatibility complex – encoded subunits LMP2 and LMP7 changes the quality of the 20S proteasome polypeptide processing products independent of interferon-γ. European Journal of Immunology *25*, 2605-2611.

Kuehn, L., Dahlmann, B., and Reinauer, H. (1986). Tissue distribution of the multicatalytic proteinase in rat: An immunological and enzymic study. Cienc Biol (Portugal) *11*, 101 - 107.

Kuroda, J., Ago, T., Matsushima, S., Zhai, P., Schneider, M.D., and Sadoshima, J. (2010). NADPH oxidase 4 (Nox4) is a major source of oxidative stress in the failing heart. Proceedings of the National Academy of Sciences *107*, 15565-15570.

Kurt-Jones, E.A., Popova, L., Kwinn, L., Haynes, L.M., Jones, L.P., Tripp, R.A., Walsh, E.E., Freeman, M.W., Golenbock, D.T., Anderson, L.J.*, et al.* (2000). Pattern recognition receptors TLR4 and CD14 mediate response to respiratory syncytial virus. Nat Immunol *1*, 398-401.

Kwak, M.-K., Cho, J.-M., Huang, B., Shin, S., and Kensler, T.W. (2007). Role of increased expression of the proteasome in the protective effects of sulforaphane against hydrogen peroxide-mediated cytotoxicity in murine neuroblastoma cells. Free Radical Biology and Medicine *43*, 809-817.

Le, V.T.K., Trilling, M., Wilborn, M., Hengel, H., and Zimmermann, A. (2008). Human cytomegalovirus interferes with signal transducer and activator of transcription (STAT) 2 protein stability and tyrosine phosphorylation. J Gen Virol *89*, 2416-2426.

Lee, M.J., Lee, B.-H., Hanna, J., King, R.W., and Finley, D. (2011). Trimming of Ubiquitin Chains by Proteasome-associated Deubiquitinating Enzymes. Molecular & Cellular Proteomics *10*.

Lelouard, H., Gatti, E., Cappello, F., Gresser, O., Camosseto, V., and Pierre, P. (2002). Transient aggregation of ubiquitinated proteins during dendritic cell maturation. Nature *417*, 177-182.

Lemaitre, B., Nicolas, E., Michaut, L., Reichhart, J.-M., and Hoffmann, J.A. (1996). The Dorsoventral Regulatory Gene Cassette spätzle/Toll/cactus Controls the Potent Antifungal Response in Drosophila Adults. Cell *86*, 973-983.

Li, J., Schuler-Thurner, B., Schuler, G., Huber, C., and Seliger, B. (2001). Bipartite regulation of different components of the MHC class I antigen-processing machinery during dendritic cell maturation. Int Immunol *13*, 1515-1523.

Li, S., Min, J.-Y., Krug, R.M., and Sen, G.C. (2006). Binding of the influenza A virus NS1 protein to PKR mediates the inhibition of its activation by either PACT or double-stranded RNA. Virology *349*, 13-21.

Li, W., Tu, D., Brunger, A.T., and Ye, Y. (2007). A ubiquitin ligase transfers preformed polyubiquitin chains from a conjugating enzyme to a substrate. Nature *446*, 333-337.

Lu, G., Reinert, J.T., Pitha-Rowe, I., Okumura, A., Kellum, M., Knobeloch, K.P., Hassel, B., and Pitha, P.M. (2006). ISG15 enhances the innate antiviral response by inhibition of IRF-3 degradation. Cell Mol Biol *52*, 29-41.

Macagno, A., Gilliet, M., Sallusto, F., Lanzavecchia, A., Nestle, F.O., and Groettrup, M. (1999). Dendritic cells up-regulate immunoproteasomes and the proteasome regulator PA28 during maturation. European Journal of Immunology *29*, 4037-4042.

Majde, J.A. (2000). Viral double-stranded RNA, cytokines, and the flu. J Interferon Cytokine Res *20*, 259-272.

Manea, A., Tanase, L.I., Raicu, M., and Simionescu, M. (2010a). JAK/STAT Signaling Pathway Regulates Nox1 and Nox4-Based NADPH Oxidase in Human Aortic Smooth Muscle Cells. Arteriosclerosis, Thrombosis, and Vascular Biology *30*, 105-112.

Manea, A., Tanase, L.I., Raicu, M., and Simionescu, M. (2010b). Transcriptional regulation of NADPH oxidase isoforms, Nox1 and Nox4, by nuclear factor-κB in human aortic smooth muscle cells. Biochemical and Biophysical Research Communications *396*, 901-907.

Marchal, C., Haguenauer-Tsapis, R., and Urban-Grimal, D. (2000). Casein Kinase I-dependent Phosphorylation within a PEST Sequence and Ubiquitination at Nearby Lysines Signal Endocytosis of Yeast Uracil Permease. Journal of Biological Chemistry *275*, 23608-23614.

Martin, K., and Helenius, A. (1991). Transport of incoming influenza virus nucleocapsids into the nucleus. Journal of Virology *65*, 232-244.

McLaughlin-Taylor, E., Pande, H., Forman, S.J., Tanamachi, B., Li, C.R., Zaia, J.A., Greenberg, P.D., and Riddell, S.R. (1994). Identification of the major late human cytomegalovirus matrix protein pp65 as a target antigen for CD8+ virus-specific cytotoxic T lymphocytes. J Med Virol *43*, 103-110.

Medd, P.G., and Chain, B.M. (2000). Protein degradation in MHC class II antigen presentation: opportunities for immunomodulation. Seminars in Cell and Developmental Biology *11*, 203-210.

Medicherla, B., and Goldberg, A.L. (2008). Heat shock and oxygen radicals stimulate ubiquitin-dependent degradation mainly of newly synthesized proteins. The Journal of Cell Biology *182*, 663-673.

Medzhitov, R., Preston-Hurlburt, P., and Janeway, C.A.J. (1997). A human homologue of the Drosophila Toll protein signals activation of adaptive immunity. Nature *388*, 394-397.

Meng, L., Mohan, R., Kwok, B.H.B., Elofsson, M., Sin, N., and Crews, C.M. (1999). Epoxomicin, a potent and selective proteasome inhibitor, exhibits in vivo antiinflammatory activity. Proceedings of the National Academy of Sciences *96*, 10403-10408.

Meylan, E., Curran, J., Hofmann, K., Moradpour, D., Binder, M., Bartenschlager, R., and Tschopp, J. (2005). Cardif is an adaptor protein in the RIG-I antiviral pathway and is targeted by hepatitis C virus. Nature *437*, 1167-1172.

Michaeloudes, C., Sukkar, M.B., Khorasani, N.M., Bhavsar, P.K., and Chung, K.F. (2011). TGF-β regulates Nox4, MnSOD and catalase expression, and IL-6 release in airway smooth muscle cells. American Journal of Physiology - Lung Cellular and Molecular Physiology *300*, L295-L304.

Miller, D.M., Zhang, Y., Rahill, B.M., Kazor, K., Rofagha, S., Eckel, J.J., and Sedmark, D.D. (2000). Human cytomegalovirus blocks interferon-gamma stimulated up-regulation of major histocompatibility complex class I expression and the class I antigen processing machinery. Transplantation *69*, 687-690.

Min, J.-Y., and Krug, R.M. (2006). The primary function of RNA binding by the influenza A virus NS1 protein in infected cells: Inhibiting the 2′-5′ oligo (A) synthetase/RNase L pathway. Proceedings of the National Academy of Sciences *103*, 7100-7105.

Mishto, M., Bellavista, E., Santoro, A., Stolzing, A., Ligorio, C., Nacmias, B., Spazzafumo, L., Chiappelli, M., Licastro, F., Sorbi, S.*, et al.* (2006). Immunoproteasome and LMP2 polymorphism in aged and Alzheimer's disease brains. Neurobiology of Aging *27*, 54-66.

Mocarski, E.S. (2002). Immunomodulation by cytomegaloviruses: manipulative strategies beyond evasion. Trends in Microbiology *10*, 332-339.

Mocarski, E.S. (2004). Immune escape and exploitation strategies of cytomegaloviruses: impact on and imitation of the major histocompatibility system. Cellular Microbiology *6*, 707-717.

Moebius, J., van den Broek, M., Groettrup, M., and Basler, M. (2010). Immunoproteasomes are essential for survival and expansion of T cells in virus-infected mice. European Journal of Immunology *40*, 3439-3449.

Morrison, J., Elvin, J., Latron, F., Gotch, F., Moots, R., Strominger, J.L., and McMichael, A. (1992). Identification of the nonamer peptide from influenza A matrix protein and the role of pockets of HLA-A2 in its recognition by cytotoxic T lymphocytes. European Journal of Immunology *22*, 903-907.

Muchamuel, T., Basler, M., Aujay, M.A., Suzuki, E., Kalim, K.W., Lauer, C., Sylvain, C., Ring, E.R., Shields, J., Jiang, J.*, et al.* (2009). A selective inhibitor of the immunoproteasome subunit LMP7 blocks cytokine production and attenuates progression of experimental arthritis. Nat Med *15*, 781-787.

Murakami, Y., Matsufuji, S., Kameji, T., Hayashi, S.-i., Igarashi, K., Tamura, T., Tanaka, K., and Ichihara, A. (1992). Ornithine decarboxylase is degraded by the 26S proteasome without ubiquitination. Nature *360*, 597-599.

Murata, S., Sasaki, K., Kishimoto, T., Niwa, S.-i., Hayashi, H., Takahama, Y., and Tanaka, K. (2007). Regulation of CD8+ T Cell Development by Thymus-Specific Proteasomes. Science *316*, 1349-1353.

Murata, S., Yashiroda, H., and Tanaka, K. (2009). Molecular mechanisms of proteasome assembly. Nat Rev Mol Cell Biol *10*, 104-115.

Murphy, K. (2011). Janeway's Immunobiology, 8th edn (Taylor & Francis, Garland Science).

Nandi, D., Jiang, H., and Monaco, J. (1996). Identification of MECL-1 (LMP-10) as the third IFN-gamma-inducible proteasome subunit. The Journal of Immunology *156*, 2361-2364.

Nandi, D., Woodward, E., Ginsburg, D.B., and Monaco, J.J. (1997). Intermediates in the formation of mouse 20S proteasomes: implications for the assembly of precursor beta subunits. EMBO J *16*, 5363-5375.

Naujokat, C., and Hoffmann, S. (2002). Role and function of the 26S proteasome in proliferation and apoptosis. Lab Invest *82*, 965 - 980.

Nayak, D.P., Balogun, R.A., Yamada, H., Hong Zhou, Z., and Barman, S. (2009). Influenza virus morphogenesis and budding. Virus Res *143*, 147-161.

Nayak, D.P., Hui, E.K., and Barman, S. (2004). Assembly and budding of influenzavirus. Virus Research *106*, 147-165.

Neefjes, J., Gottfried, E., Roelse, J., Grommé, M., Obst, R., Hämmerling, G.J., and Momburg, F. (1995). Analysis of the fine specificity of rat, mouse and human TAP peptide transporters. European Journal of Immunology *25*, 1133-1136.

Neumann, L., and Tampé, R. (1999). Kinetic analysis of peptide binding to the TAP transport complex: evidence for structural rearrangements induced by substrate binding. Journal of Molecular Biology *294*, 1203-1213.

Ngkelo, A., Meja, K., Yeadon, M., Adcock, I., and Kirkham, P. (2012). LPS induced inflammatory responses in human peripheral blood mononuclear cells is mediated through NOX4 and Gialpha dependent PI-3kinase signalling. Journal of Inflammation *9*, 1.

Noda, C., Tanahashi, N., Shimbara, N., Hendil, K.B., and Tanaka, K. (2000). Tissue Distribution of Constitutive Proteasomes, Immunoproteasomes, and PA28 in Rats. Biochemical and Biophysical Research Communications *277*, 348-354.

Nussbaum, A.K., Rodriguez-Carreno, M.P., Benning, N., Botten, J., and Whitton, J.L. (2005). Immunoproteasome-Deficient Mice Mount Largely Normal CD8+ T Cell Responses to Lymphocytic Choriomeningitis Virus Infection and DNA Vaccination. The Journal of Immunology *175*, 1153-1160.

Odeberg, J., Plachter, B., Brandén, L., and Söderberg-Nauclér, C. (2003). Human cytomegalovirus protein pp65 mediates accumulation of HLA-DR in lysosomes and destruction of the HLA-DR alpha-chain. Blood *101*, 4870-4877.

Opitz, E., Koch, A., Klingel, K., Schmidt, F., Prokop, S., Rahnefeld, A., Sauter, M., Heppner, F.L., Völker, U., Kandolf, R.*, et al.* (2011). Impairment of Immunoproteasome Function by β5i/LMP7 Subunit Deficiency Results in Severe Enterovirus Myocarditis. PLoS Pathog *7*, e1002233.

Orient, A., Donkó, Á., Szabó, A., Leto, T.L., and Geiszt, M. (2007). Novel sources of reactive oxygen species in the human body. Nephrology Dialysis Transplantation *22*, 1281-1288.

Orlowski, M., and Wilk, S. (2000). Catalytic Activities of the 20 S Proteasome, a Multicatalytic Proteinase Complex. Archives of Biochemistry and Biophysics *383*, 1-16.

Oslund, K.L., and Baumgarth, N. (2011). Influenza-induced innate immunity: regulators of viral replication, respiratory tract pathology & adaptive immunity. Future Virol *6*, 951-962.

Ossendorp, F., Fu, N., Camps, M., Granucci, F., Gobin, S.J.P., van den Elsen, P.J., Schuurhuis, D., Adema, G.J., Lipford, G.B., Chiba, T.*, et al.* (2005). Differential Expression Regulation of the alpha and beta Subunits of the PA28 Proteasome Activator in Mature Dendritic Cells. The Journal of Immunology *174*, 7815-7822.

Ozkaynak, E., Finley, D., Solomon, M.J., and Varshavsky, A. (1987). The yeast ubiquitin genes: a family of natural gene fusions. EMBO J *6*, 1429-1439.

Pacifici, R.E., Salo, D.C., and Davies, K.J. (1989). Macroxyproteinase (M.O.P.): a 670 kDa proteinase complex that degrades oxidatively denatured proteins in red blood cells. Free Radic Biol Med *7*, 521-536.

Palese, P., and García-Sastre, A. (1999). INFLUENZA VIRUSES (ORTHOMYXOVIRIDAE) | Molecular Biology. In Encyclopedia of Virology (Second Edition), G. Editors-in-Chief: Allan, and G.W. Robert, eds. (Oxford, Elsevier), pp. 830-836.

Palese, P., and Shaw, M.L. (2007). Orthomyxoviridae: The Viruses and Their Replication. In Fields Virology, e.a. D.M. Knipe, ed. (Philadelphia, Lippincott Williams & Wilkins), pp. 1647-1677.

Palombella, V.J., Rando, O.J., Goldberg, A.L., and Maniatis, T. (1994). The ubiquitinproteasome pathway is required for processing the NF-kappaB1 precursor protein and the activation of NF-kappaB. Cell *78*, 773-785.

Pass, R.F. (1985). Epidemiology and Transmission of Cytomegalovirus. Journal of Infectious Diseases *152*, 243-248.

Paulus, C., Krauss, S., and Nevels, M. (2006). A human cytomegalovirus antagonist of type I IFN-dependent signal transducer and activator of transcription signaling. Proceedings of the National Academy of Sciences of the United States of America *103*, 3840-3845.

Pichlmair, A., Schulz, O., Tan, C.P., Näslund, T.I., Liljeström, P., Weber, F., and Reis e Sousa, C. (2006). RIG-I-Mediated Antiviral Responses to Single-Stranded RNA Bearing 5'-Phosphates. Science *314*, 997-1001.

Pickart, C.M., and Eddins, M.J. (2004). Ubiquitin: structures, functions, mechanisms. Biochimica et Biophysica Acta (BBA) - Molecular Cell Research *1695*, 55-72.

Pickering, A.M., Koop, A.L., Teoh, C.Y., Ermak, G., Grune, T., and Davies, K.J.A. (2010). The immunoproteasome, the 20S proteasome and the PA28alpha/beta proteasome regulator are oxidative-stress-adaptive proteolytic complexes. Biochemical Journal *432*, 585-594.

Plachter, B., Sinzger, C., and Jahn, G. (1996). Cell types involved in replication and distribution of human cytomegalovirus. Adv Virus Res *46*, 195-261.

Qian, S.-B., Princiotta, M.F., Bennink, J.R., and Yewdell, J.W. (2006). Characterization of Rapidly Degraded Polypeptides in Mammalian Cells Reveals a Novel Layer of Nascent Protein Quality Control. J Biol Chem *281*, 392-400.

Quinnan, G.V.J., Delery, M., Rook, A.H., Frederick, W.R., Epstein, J.S., Manischewitz, J.F., Jackson, L., Ramsey, K.M., Mittal, K., Plotkin, S.A.*, et al.* (1984). Comparative virulence and immunogenicity of the Towne strain and a nonattenuated strain of cytomegalovirus. Ann Intern Med *101*, 478-483.

Rada, B., and Leto, T.L. (2008). Oxidative innate immune defenses by Nox/Duox family NADPH Oxidases. Contrib Microbiol *15*, 164-187.

Ramachandra, L., Noss, E., Boom, and Harding, C.V. (1999). Phagocytic processing of antigens for presentation by class II major histocompatibility complex molecules. Cellular Microbiology *1*, 205-214.

Rammensee, H.G., Falk, K., and RÃ¶tzschke, O. (1993). Peptides Naturally Presented by MHC Class I Molecules. Annual Review of Immunology *11*, 213-244.

Ramos, P.C., Höckendorff, J., Johnson, E.S., Varshavsky, A., and Dohmen, R.J. (1998). Ump1p Is Required for Proper Maturation of the 20S Proteasome and Becomes Its Substrate upon Completion of the Assembly. Cell *92*, 489-499.

Reddehase, M.J. (2000). The immunogenicity of human and murine cytomegaloviruses. Current Opinion in Immunology *12*, 738.

Reddehase, M.J. (2002). Antigens and immunoevasins: opponents in cytomegalovirus immune surveillance. *2*, 831-844.

Rehwinkel, J., and Reis e Sousa, C. (2010). RIGorous Detection: Exposing Virus Through RNA Sensing. Science *327*, 284-286.

Reid, A.H., and Taubenberger, J.K. (2003). The origin of the 1918 pandemic influenza virus: a continuing enigma. J Gen Virol *84*, 2285-2292.

Reits, E.A.J., Vos, J.C., Gromme, M., and Neefjes, J. (2000). The major substrates for TAP invivo are derived from newly synthesized proteins. *404*, 774-778.

Reusser, P., Riddell, S.R., Meyers, J.D., and Greenberg, P.D. (1991). Cytotoxic T-lymphocyte response to cytomegalovirus after human allogeneic bone marrow transplantation: pattern of recovery and correlation with cytomegalovirus infection and disease. Blood *78*, 1373-1380.

Reyes-Turcu, F.E., and Wilkinson, K.D. (2009). Polyubiquitin Binding and Disassembly By Deubiquitinating Enzymes. Chemical Reviews *109*, 1495-1508.

Riddell, S.R., Watanabe, K.S., Goodrich, J.M., Li, C.R., Agha, M.E., and Greenberg, P.D. (1992). Restoration of viral immunity in immunodeficient humans by the adoptive transfer of T cell clones. Science *257*, 238-241.

Rivett, A.J. (1985). Preferential degradation of the oxidatively modified form of glutamine synthetase by intracellular mammalian proteases. Journal of Biological Chemistry *260*, 300-305.

Rock, K.L., Farfán-Arribas, D.J., and Shen, L. (2010). Proteases in MHC Class I Presentation and Cross-Presentation. The Journal of Immunology *184*, 9-15.

Rock, K.L., and Goldberg, A.L. (1999). Degradation of cell proteins and the generation of MHC class I-presented peptides. Annual Review of Immunology *17*, 739-779.

Rock, K.L., Gramm, C., Rothstein, L., Clark, K., Stein, R., Dick, L.R., Hwang, D., and Goldberg, A.L. (1994). Inhibitors of the proteasome block the degradation of most cell proteins and the generation of peptides presented on MHC class I molecules. Cell *78*, 761-771.

Roizman, B., and Baines, J. (1991). The diversity and unity of herpesviridae. Comparative Immunology, Microbiology and Infectious Diseases *14*, 63-79.

Roizman, B., Carmichael, L.E., Deinhardt, F., de-The, G., Nahmias, A.J., Plowright, W., Rapp, F., Sheldrick, P., Takahashi, M., and Wolf, K. (1981). Herpesviridae. Definition, provisional nomenclature, and taxonomy. The Herpesvirus Study Group, the International Committee on Taxonomy of Viruses. Intervirology *16*, 201-217.

Saeki, Y., Kudo, T., Sone, T., Kikuchi, Y., Yokosawa, H., Toh-e, A., and Tanaka, K. (2009). Lysine 63-linked polyubiquitin chain may serve as a targeting signal for the 26S proteasome. EMBO J *28*, 359-371.

Sakai, N., Sawada, M.T., and Sawada, H. (2004). Non-traditional roles of ubiquitin-proteasome system in fertilization and gametogenesis. Int J Biochem Cell Biol *36*, 776 - 784.

Sasaki, M., Ikeda, H., Sato, Y., and Nakanuma, Y. (2008). Proinflammatory cytokine-induced cellular senescence of biliary epithelial cells is mediated via oxidative stress and activation of ATM pathway: A culture study. Free Radical Research *42*, 625-632.

Schmidt, N., Gonzalez, E., Visekruna, A., Kühl, A.A., Loddenkemper, C., Mollenkopf, H., Kaufmann, S.H.E., Steinhoff, U., and Joeris, T. (2010). Targeting the proteasome: partial inhibition of the proteasome by bortezomib or deletion of the immunosubunit LMP7 attenuates experimental colitis. Gut *59*, 896-906.

Schmidtke, G., Kraft, R., Kostka, S., Henklein, P., Frömmel, C., Löwe, J., Huber, R., Kloetzel, P.-M., and Schmidt, M. (1996). Analysis of mammalian 20S proteasome biogenesis: the maturation of beta-subunits is an ordered two-step mechanism involving autocatalysis. EMBO J *15*, 6887-6898.

Schmidtke, G., Schmidt, M., and Kloetzel, P.M. (1997). Maturation of mammalian 20 S proteasome: purification and characterization of 13 S and 16 S proteasome precursor complexes. Journal of Molecular Biology *268*, 95-106.

Schmolke, S., Drescher, P., Jahn, G., and Plachter, B. (1995a). Nuclear targeting of the tegument protein pp65 (UL83) of human cytomegalovirus: an unusual bipartite nuclear localization signal functions with other portions of the protein to mediate its efficient nuclear transport. J Virol *69*, 1071-1078.

Schmolke, S., Kern, H., Drescher, P., Jahn, G., and Plachter, B. (1995b). The dominant phosphoprotein pp65 (UL83) of human cytomegalovirus is dispensable for growth in cell culture. J Virol *69*, 5959-5968.

Schoenhals, G.J., Krishna, R.M., Grandea, A.G., Spies, T., Peterson, P.A., Yang, Y., and Fruh, K. (1999). Retention of empty MHC class I molecules by tapasin is essential to reconstitute antigen presentation in invertebrate cells. EMBO J *18*, 743-753.

Schubert, U., Anton, L.C., Gibbs, J., Norbury, C.C., Yewdell, J.W., and Bennink, J.R. (2000). Rapid degradation of a large fraction of newly synthesized proteins by proteasomes. *404*, 770-774.

Schwartz, D.C., and Hochstrasser, M. (2003). A superfamily of protein tags ubiquitin, SUMO and related modifiers. Trends in Biochemical Sciences *28*, 321-328.

Schwarz, K., van den Broek, M., Kostka, S., Kraft, R., Soza, A., Schmidtke, G., Kloetzel, P.-M., and Groettrup, M. (2000). Overexpression of the Proteasome Subunits LMP2, LMP7, and MECL-1, But Not PA28alpha/beta, Enhances the Presentation of an Immunodominant Lymphocytic Choriomeningitis Virus T Cell Epitope. J Immunol *165*, 768-778.

Sedwick, C. (2010). NOX4: A Guilty Party in Stroke Damage. PLoS Biol *8*, e1000478.

Seifert, U., Bialy, L.P., Ebstein, F., Bech-Otschir, D., Voigt, A., Schröter, F., Prozorovski, T., Lange, N., Steffen, J., Rieger, M.*, et al.* (2010). Immunoproteasomes Preserve Protein Homeostasis upon Interferon-Induced Oxidative Stress. Cell *142*, 613-624.

Seth, R.B., Sun, L., Ea, C.-K., and Chen, Z.J. (2005). Identification and Characterization of MAVS, a Mitochondrial Antiviral Signaling Protein that Activates NF-kappaB and IRF3. Cell *122*, 669-682.

Shang, F., Nowell, T.R., and Taylor, A. (2001). Removal of Oxidatively Damaged Proteins from Lens Cells by the Ubiquitin-Proteasome Pathway. Experimental Eye Research *73*, 229-238.

Shin, E.C., Seifert, U., Kato, T., Rice, C.M., Feinstone, S.M., Kloetzel, P.-M., and Rehermann, B. (2006). Virus-induced type I IFN stimulates generation of immunoproteasomes at the site of infection. J Clin Invest *116*, 3006-3014.

Shringarpure, R., Grune, T., Mehlhase, J., and Davies, K.J.A. (2003). Ubiquitin Conjugation Is Not Required for the Degradation of Oxidized Proteins by Proteasome. Journal of Biological Chemistry *278* 311-318

Sibille, C., Gould, K.G., Gallo, K.W., Thomson, S., Rivett, A.J., Powis, S., Butcher, G.W., and Baetselier, P.D. (1995). LMP2+ proteasomes are required for the presentation of specific antigens to cytotoxic T lymphocytes. Current Biology *5*, 923-930.

Sijts, A.J.A.M., Ruppert, T., Rehermann, B., Schmidt, M., Koszinowski, U., and Kloetzel, P.-M. (2000a). Efficient Generation of a Hepatitis B Virus Cytotoxic T Lymphocyte Epitope Requires the Structural Features of Immunoproteasomes. J Exp Med *191*, 503-514.

Sijts, A.J.A.M., Standera, S., Toes, R.E.M., Ruppert, T., Beekman, N.J.C.M., van Veelen, P.A., Ossendorp, F.A., Melief, C.J.M., and Kloetzel, P.M. (2000b). MHC Class I Antigen Processing of an

Adenovirus CTL Epitope Is Linked to the Levels of Immunoproteasomes in Infected Cells. J Immunol *164*, 4500-4506.

Sijts, E.J., and Kloetzel, P.-M. (2011). The role of the proteasome in the generation of MHC class I ligands and immune responses. Cell Mol Life Sci *68*, 1491-1502.

Simmen, K.A., Singh, J., Luukkonen, B.G.M., Lopper, M., Bittner, A., Miller, N.E., Jackson, M.R., Compton, T., and Früh, K. (2001). Global modulation of cellular transcription by human cytomegalovirus is initiated by viral glycoprotein B. Proceedings of the National Academy of Sciences *98*, 7140-7145.

Sinclair, J., and Sissons, P. (2006). Latency and reactivation of human cytomegalovirus. Journal of General Virology *87*, 1763-1779.

Singer, A., Adoro, S., and Park, J.-H. (2008). Lineage fate and intense debate: myths, models and mechanisms of CD4- versus CD8-lineage choice. Nat Rev Immunol *8*, 788-801.

Sinzger, C., Digel, M., and Jahn, G. (2008). Cytomegalovirus cell tropism. Curr Top Microbiol Immunol *325*, 63-83.

Sinzger, C., Grefte, A., Plachter, B., Gouw, A.S.H., The, T.H., and Jahn, G. (1995). Fibroblasts, epithelial cells, endothelial cells and smooth muscle cells are major targets of human cytomegalovirus infection in lung and gastrointestinal tissues. Journal of General Virology *76*, 741-750.

Sitte, N., Merker, K., and Grune, T. (1998). Proteasome-dependent degradation of oxidized proteins in MRC-5 fibroblasts. FEBS Letters *440*, 399-402.

Skaug, B., Jiang, X., and Chen, Z.J. (2009). The Role of Ubiquitin in NF-κB Regulatory Pathways. Annual Review of Biochemistry *78*, 769-796.

Smith, M.H., Ploegh, H.L., and Weissman, J.S. (2011). Road to Ruin: Targeting Proteins for Degradation in the Endoplasmic Reticulum. Science *334*, 1086-1090.

Speir, E., Shibutani, T., Yu, Z.-X., Ferrans, V., and Epstein, S.E. (1996). Role of Reactive Oxygen Intermediates in Cytomegalovirus Gene Expression and in the Response of Human Smooth Muscle Cells to Viral Infection. Circ Res *79*, 1143-1152.

Spence, J., Sadis, S., Haas, A.L., and Finley, D. (1995). A ubiquitin mutant with specific defects in DNA repair and multiubiquitination. Molecular and Cellular Biology *15*, 1265-1273.

Spies, T., Cerundolo, V., Colonna, M., Cresswell, P., Townsend, A., and DeMars, R. (1992). Presentation of viral antigen by MHC class I molecules is dependent on a putative peptide transporter heterodimer. Nature *355*, 644-646.

Stark, G.R., Kerr, I.M., Williams, B.R.G., Silverman, R.H., and Schreiber, R.D. (1998). HOW CELLS RESPOND TO INTERFERONS. Annual Review of Biochemistry *67*, 227-264.

Stinski, M.F. (1978). Sequence of protein synthesis in cells infected by human cytomegalovirus: early and late virus-induced polypeptides. J Virol *26*, 686–701.

Stohwasser, R., Salzmann, U., Giesebrecht, J., Kloetzel, P.-M., and Holzhütter, H.-G. (2000). Kinetic evidences for facilitation of peptide channelling by the proteasome activator PA28. European Journal of Biochemistry *267*, 6221-6230.

Strehl, B., Joeris, T., Rieger, M., Visekruna, A., Textoris-Taube, K., Kaufmann, S.H.E., Kloetzel, P.-M., Kuckelkorn, U., and Steinhoff, U. (2006). Immunoproteasomes Are Essential for Clearance of Listeria monocytogenes in Nonlymphoid Tissues but Not for Induction of Bacteria-Specific CD8+ T Cells. The Journal of Immunology *177*, 6238-6244.

Strehl, B., Seifert, U., Kruger, E., Heink, S., Kuckelkorn, U., and Kloetzel, P.-M. (2005). Interferon-gamma, the functional plasticity of the ubiquitin-proteasome system, and MHC class I antigen processing. Immunological Reviews *207*, 19-30.

Strehl, B., Textoris-Taube, K., Jäkel, S., Voigt, A., Henklein, P., Steinhoff, U., Kloetzel, P.-M., and Kuckelkorn, U. (2008). Antitopes Define Preferential Proteasomal Cleavage Site Usage. Journal of Biological Chemistry *283*, 17891-17897.

Szeto, J., Kaniuk, N.A., Canadien, V., Nisman, R., Mizushima, N., Yoshimori, T., Bazett-Jones, D.P., and Brumell, J.H. (2006). ALIS are Stress-Induced Protein Storage Compartments for Substrates of the Proteasome and Autophagy. Autophagy *2*, 189-199.

Tabeta, K., Georgel, P., Janssen, E., Du, X., Hoebe, K., Crozat, K., Mudd, S., Shamel, L., Sovath, S., Goode, J.*, et al.* (2004). Toll-like receptors 9 and 3 as essential components of innate immune defense

against mouse cytomegalovirus infection. Proceedings of the National Academy of Sciences of the United States of America *101*, 3516-3521.

Tanahashi, N., Murakami, Y., Minami, Y., Shimbara, N., Hendil, K.B., and Tanaka, K. (2000). Hybrid Proteasomes. Journal of Biological Chemistry *275*, 14336-14345.

Tanaka, K. (2009). The proteasome: Overview of structure and functions. Proceedings of the Japan Academy, Series B *85*, 12-36.

Tanaka, K., Ii, K., Ichihara, A., Waxman, L., and Goldberg, A.L. (1986). A high molecular weight protease in the cytosol of rat liver. I. Purification, enzymological properties, and tissue distribution. Journal of Biological Chemistry *261*, 15197-15203.

Taylor, C., and Jobin, C. (2005). Ubiquitin protein modification and signal transduction: implications for inflammatory bowel diseases. Inflamm Bowel Dis *11*, 1097-1107.

Thompson, A.J.V., and Locarnini, S.A. (2007). Toll-like receptors, RIG-I-like RNA helicases and the antiviral innate immune response. *85*, 435-445.

Thrower, J.S., Hoffman, L., Rechsteiner, M., and Pickart, C.M. (2000). Recognition of the polyubiquitin proteolytic signal. EMBO J *19*, 94-102.

Tilton, C., Clippinger, A.J., Maguire, T., and Alwine, J.C. (2011). Human Cytomegalovirus Induces Multiple Means To Combat Reactive Oxygen Species. J Virol *85*, 12585-12593.

Toes, R.E.M., Nussbaum, A.K., Degermann, S., Schirle, M., Emmerich, N.P.N., Kraft, M., Laplace, C., Zwinderman, A., Dick, T.P., Muller, J.*, et al.* (2001). Discrete Cleavage Motifs of Constitutive and Immunoproteasomes Revealed by Quantitative Analysis of Cleavage Products. J Exp Med *194*, 1-12.

Tomaru, U., Ishizu, A., Murata, S., Miyatake, Y., Suzuki, S., Takahashi, S., Kazamaki, T., Ohara, J., Baba, T., Iwasaki, S.*, et al.* (2009). Exclusive expression of proteasome subunit beta5t in the human thymic cortex. Blood *113*, 5186-5191.

Tran, K., Mahr, J.A., and Spector, D.H. (2010). Proteasome Subunits Relocalize during Human Cytomegalovirus Infection, and Proteasome Activity Is Necessary for Efficient Viral Gene Transcription. J Virol *84*, 3079-3093.

Tu, L., Moriya, C., Imai, T., Ishida, H., Tetsutani, K., Duan, X., Murata, S., Tanaka, K., Shimokawa, C., Hisaeda, H.*, et al.* (2009). Critical role for the immunoproteasome subunit LMP7 in the resistance of mice to Toxoplasma gondii infection. European Journal of Immunology *39*, 3385-3394.

Unno, M., Mizushima, T., Morimoto, Y., Tomisugi, Y., Tanaka, K., Yasuoka, N., and Tsukihara, T. (2002). The Structure of the Mammalian 20S Proteasome at 2.75 Å Resolution. Structure (London, England : 1993) *10*, 609-618.

Urban, S., Textoris-Taube, K., Reimann, B., Janek, K., Dannenberg, T., Ebstein, F., Seifert, C., Zhao, F., Kessler, J.H., Halenius, A.*, et al.* (2012). The Efficiency of Human Cytomegalovirus pp65495–503 CD8+ T Cell Epitope Generation Is Determined by the Balanced Activities of Cytosolic and Endoplasmic Reticulum-Resident Peptidases. The Journal of Immunology *189*, 529-538.

Ustrell, V., Pratt, G., and Rechsteiner, M. (1995). Effects of interferon gamma and major histocompatibility complex-encoded subunits on peptidase activities of human multicatalytic proteases. Proceedings of the National Academy of Sciences *92*, 584-588.

Van Endert, P.M., Riganelli, D., Greco, G., Fleischhauer, K., Sidney, J., Sette, A., and Bach, J.-F. (1995). The peptide-binding motif for the human transporter associated with antigen processing. J Exp Med *182*, 1883-1895.

van Kaer, L., Ashton-Rickardt, P.G., Eichelberger, M., Gaczynska, M., Nagashima, K., Rock, K.L., Goldberg, A.L., Doherty, P.C., and Tonegawa, S. (1994). Altered peptidase and viral-specific T cell response in LMP2 mutant mice. Immunity *1*, 533-541.

van Kaer, L., Ashton-Rickardt, P.G., Ploegh, H.L., and Tonegawa, S. (1992). TAP1 mutant mice are deficient in antigen presentation, surface class I molecules, and $CD4^{-}8^{+}$ T cells. Cell *71*, 1205-1214.

van Wijk, S.J.L., and Timmers, H.T.M. (2010). The family of ubiquitin-conjugating enzymes (E2s): deciding between life and death of proteins. The FASEB Journal *24*, 981-993.

Visekruna, A., Joeris, T., Seidel, D., Kroesen, A., Loddenkemper, C., Zeitz, M., Kaufmann, S.H.E., Schmidt-Ullrich, R., and Steinhoff, U. (2006). Proteasome-mediated degradation of IκBα and processing of p105 in Crohn disease and ulcerative colitis. The Journal of Clinical Investigation *116*, 3195-3203.

von Boehmer, H., Karjalainen, K., Pelkonen, J., Borgulya, P., and Rammensee, H.G. (1988). The T-cell receptor for antigen in T-cell development and repertoire selection. Immunol Rev *101*, 21-37.

Walter, E.A., Greenberg, P.D., Gilbert, M.J., Finch, R.J., Watanabe, K.S., Thomas, E.D., and Riddell, S.R. (1995). Reconstitution of Cellular Immunity against Cytomegalovirus in Recipients of Allogeneic Bone Marrow by Transfer of T-Cell Clones from the Donor. New England Journal of Medicine *333*, 1038-1044.

Wang, J., and Maldonado, M.A. (2006). The ubiquitin-proteasome system and its role in inflammatory and autoimmune diseases. Cell Mol Immunol *3*, 255-261.

Watanabe, Y., Suzuki, O., Haruyama, T., and Akaike, T. (2003). Interferon-γ induces reactive oxygen species and endoplasmic reticulum stress at the hepatic apoptosis. Journal of Cellular Biochemistry *89*, 244-253.

Weekes, M.P., Wills, M.R., Mynard, K., Carmichael, A.J., and Sissons, J.G.P. (1999). The Memory Cytotoxic T-Lymphocyte (CTL) Response to Human Cytomegalovirus Infection Contains Individual Peptide-Specific CTL Clones That Have Undergone Extensive Expansion In Vivo. J Virol *73*, 2099-2108.

Weissman, A.M. (2001). Themes and variations on ubiquitylation. Nat Rev Mol Cell Biol *2*, 169-178.

West, A.P., Brodsky, I.E., Rahner, C., Woo, D.K., Erdjument-Bromage, H., Tempst, P., Walsh, M.C., Choi, Y., Shadel, G.S., and Ghosh, S. (2011). TLR signalling augments macrophage bactericidal activity through mitochondrial ROS. Nature *472*, 476-480.

Whitby, F.G., Masters, E.I., Kramer, L., Knowlton, J.R., Yao, Y., Wang, C.C., and Hill, C.P. (2000). Structural basis for the activation of 20S proteasomes by 11S regulators. Nature *408*, 115-120.

Wiborg, O., Pedersen, M.S., Wind, A., Berglund, L.E., Marcker, K.A., and Vuust, J. (1985). The human ubiquitin multigene family: some genes contain multiple directly repeated ubiquitin coding sequences. EMBO J *4*, 755-759.

Wiertz, E.J.H.J., Jones, T.R., Sun, L., Bogyo, M., Geuze, H.J., and Ploegh, H.L. (1996). The Human Cytomegalovirus US11 Gene Product Dislocates MHC Class I Heavy Chains from the Endoplasmic Reticulum to the Cytosol. Cell *84*, 769-779.

Wilkinson, K.D. (2000). Ubiquitination and deubiquitination: Targeting of proteins for degradation by the proteasome. Seminars in Cell and Developmental Biology *11*, 141-148.

Wilkinson, K.D., Urban, M.K., and Haas, A.L. (1980). Ubiquitin is the ATP-dependent proteolysis factor I of rabbit reticulocytes. Journal of Biological Chemistry *255*, 7529-7532.

Wills, M., Carmichael, A., Mynard, K., Jin, X., Weekes, M., Plachter, B., and Sissons, J. (1996). The human cytotoxic T-lymphocyte (CTL) response to cytomegalovirus is dominated by structural protein pp65: frequency, specificity, and T- cell receptor usage of pp65-specific CTL. J Virol *70*, 7569-7579.

Witt, E., Zantopf, D., Schmidt, M., Kraft, R., Kloetzel, P.-M., and Krüger, E. (2000). Characterisation of the newly identified human Ump1 homologue POMP and analysis of LMP7([beta]5i) incorporation into 20 S proteasomes. Journal of Molecular Biology *301*, 1-9.

Woelk, T., Sigismund, S., Penengo, L., and Polo, S. (2007). The ubiquitination code: a signalling problem. Cell Division *2*.

Wójcik, C., and DeMartino, G.N. (2003). Intracellular localization of proteasomes. The International Journal of Biochemistry & Cell Biology *35*, 579-589.

Wójcik, C., Tanaka, K., Paweletz, N., Naab, U., and Wilk, S. (1998). Proteasome activator (PA28) subunits, alpha, beta and gamma (Ki antigen) in NT2 neuronal precursor cells and HeLa S3 cells. Eur J Cell Biol *77*, 151-160.

Wright, P.F., Neumann, G., and Kawaoka, Y. (2007). Orthomyxoviruses. In Fields Virology, e.a. D.M. Knipe, ed. (Philadelphia, Lippincott Williams & Wilkins), pp. 1692-1731.

Xu, L.-G., Wang, Y.-Y., Han, K.-J., Li, L.-Y., Zhai, Z., and Shu, H.-B. (2005). VISA Is an Adapter Protein Required for Virus-Triggered IFN-beta Signaling. Molecular Cell *19*, 727-740.

Xu, P., Duong, D.M., Seyfried, N.T., Cheng, D., Xie, Y., Robert, J., Rush, J., Hochstrasser, M., Finley, D., and Peng, J. (2009). Quantitative Proteomics Reveals the Function of Unconventional Ubiquitin Chains in Proteasomal Degradation. Cell *137*, 133-145.

Yamanaka, K., Ishikawa, H., Megumi, Y., Tokunaga, F., Kanie, M., Rouault, T.A., Morishima, I., Minato, N., Ishimori, K., and Iwai, K. (2003). Identification of the ubiquitin-protein ligase that recognizes oxidized IRP2. Nat Cell Biol *5*, 336-340.

Yewdell, J. (2002). To DRiP or not to DRiP: generating peptide ligands for MHC class I molecules from biosynthesized proteins. Molecular Immunology *39*, 139-146.

Yewdell, J.W. (2005). The seven dirty little secrets of major histocompatibility complex class I antigen processing. Immunological Reviews *207*, 8-18.

Yewdell, J.W. (2007). Plumbing the sources of endogenous MHC class I peptide ligands. Current Opinion in Immunology *19*, 79-86.

Yoneyama, M., Kikuchi, M., Natsukawa, T., Shinobu, N., Imaizumi, T., Miyagishi, M., Taira, K., Akira, S., and Fujita, T. (2004). The RNA helicase RIG-I has an essential function in double-stranded RNA-induced innate antiviral responses. Nat Immunol *5*, 730-737.

Zaia, J.A. (1990). Epidemiology and pathogenesis of cytomegalovirus disease. Semin Hematol *27*, 5-10.

Zaiss, D.M.W., de Graaf, N., and Sijts, A.J.A.M. (2008). The proteasome immunosubunit multicatalytic endopeptidase complex-like 1 is a T-cell-intrinsic factor influencing homeostatic expansion. Infect Immun *76*, 1207-1213.

Zhang, M., Pickart, C.M., and Coffino, P. (2003). Determinants of proteasome recognition of ornithine decarboxylase, a ubiquitin-independent substrate. EMBO J *22*, 1488-1496.

Zhang, Z., Krutchinsky, A., Endicott, S., Realini, C., Rechsteiner, M., and Standing, K.G. (1999). Proteasome Activator 11S REG or PA28: Recombinant REG alpha/REG beta Hetero-oligomers Are Heptamers. Biochemistry *38*, 5651-5658.

Zheng, P.-Z., Wang, K.-K., Zhang, Q.-Y., Huang, Q.-H., Du, Y.-Z., Zhang, Q.-H., Xiao, D.-K., Shen, S.-H., Imbeaud, S., Eveno, E.*, et al.* (2005). Systems analysis of transcriptome and proteome in retinoic acid/arsenic trioxide-induced cell differentiation/apoptosis of promyelocytic leukemia. Proceedings of the National Academy of Sciences of the United States of America *102*, 7653-7658.

Zhu, H., Cong, J.-P., Mamtora, G., Gingeras, T., and Shenk, T. (1998). Cellular gene expression altered by human cytomegalovirus: Global monitoring with oligonucleotide arrays Proceedings of the National Academy of Sciences of the United States of America *95* 14470-14475

Zhu, H., Shen, Y., and Shenk, T. (1995). Human cytomegalovirus IE1 and IE2 proteins block apoptosis. J Virol *69*, 7960-7970.

Zimmermann, A., Trilling, M., Wagner, M., Wilborn, M., Bubic, I., Jonjic, S., Koszinowski, U., and Hengel, H. (2005). A cytomegaloviral protein reveals a dual role for STAT2 in IFN-γ signaling and antiviral responses. The Journal of Experimental Medicine *201*, 1543-1553.

Abbreviations

(v/v)	ratio volume to volume
(w/v)	ratio weight to volumne
26S	26 Svedberg
ag	antigen
ALIS	aggresome-like induced structures
AMC	7-amino-4-methylcoumarin
α1-7	proteasomal α subunit 1 to 7
APC	antigen presenting cell
APS	ammonium peroxodisulfat
ATP	adenosine triphosphate
BCA	bicinchoninic acid protein assay
BCR	B cell receptor
βi-subunit	immunosubunit
Bp	base pairs
cDNA	complementary DNA
CMV	cytomegalovirus
CNS	central nervous system
CTL	cytotoxic T lymphocyte
Da	Dalton, unit equal to g/mol
DALIS	dendritic cell aggresome-like induced structures
DC	dendritic cell
DCFH-DA	2'-7'-dichlorofluorescin diacetate
DMF	dimethylformamide
DMSO	dimethylsulfoxide
DNA	desoxyribo nucleic acid
DRiP	defective ribosomal product
DTT	dithiothreitol
DUB	deubiquitinating enzyme
E1	ubiquitin activating enzyme
E2	ubiquitin conjugating enzyme
E3	ubiquitin ligating enzyme/ ligase
EAE	experimental autoimmune encephalomyelitis
EDTA	ethylene diamine tetraacetic acid
ELISA	enzyme-linked immunosorbent assay
ER	endoplasmatic reticulum
ERAD	endoplasmatic reticulum associated degradation
FACS	fluorescence associated cell sorting
FCS	fetal calf serum
FITC	fluorescein isothiocyanate

gpUS2	HCMV glycoprotein unique short 2
GSH	glutathione
GST	glutathione S-transferase, enzyme family
h	hour
HBSS	Hank's buffered salt solution
HCMV	human cytomegalovirus
HECT domain	homologous to E6-AP carboxy terminus domain
HeLa	cervical cancer cell line derived from patient Henrietta Lacks
hpi	hours post infection
HPRT1	hypoxanthine phosphoribosyltransferase 1
HRP	horse radish peroxidase
IAV	influenza A virus
IFN	interferon
IgG	immunoglobulin G
IKKε	IκB kinase ε
IL	interleukin
IP	immunoprecipitation
IPTG	isopropyl-β-D-thiogalactopyranoside
IRF3	interferon regulatory factor 3
ISG15	interferon stimulated gene 15
Jak	Janus kinase
K48	lysine at amino acid position 48
kbp	kilo base pairs
Lmp2	low molecular mass protein 2, i-subunit β1i
Lmp7	low molecular mass protein 7, i-subunit β5i
M1	matrix protein 1
MCMV	murine cytomegalovirus
MDA5	melanoma differentiation-associated protein 5
Mecl-1	multicatalytic endopeptidase complex subunit 1, i-subunit β2i
MEF	mouse embryonic fibroblast
MHC	major histocompatibility complex
min	minute
MOI	multiplicity of infection
MRC5	human lung fibroblast
MTT	3-(4,5-Dimethylthiazol-2-yl)-2,5-diphenyltetrazoliumbromid (Thiazolyl blue)
NADPH	nicotinamide adenine dinucleotide phosphate
NEM	N-ethylmaleimide
Nox	NADPH Oxidase, enzyme family
NS1	nonstructural protein 1
NTP	nucleotide triphosphate
o/n	over night

OD600	optical density at wave langeth of 600nm
ORF	open reading frame
PA28	proteasome activator 28
PAGE	polyacrylamide gel electrophoresis
PAMP	Pathogen-associated molecular pattern
PBS/PBST	phosphate buffered saline (with tween-20)
PCR	polymerase chain reaction
PE	phycoerythrin
PEST sequence	proline (P), glutamine (E), serine (S) and threonine (T) rich sequence
polyA-end	poly adenosine end
pp65	phosphoprotein of 65kDa
PRR	pattern recognition receptor
PSMB8	proteasome subunit beta type 8 (coding for β1i)
PSMB9	proteasome subunit beta type 9 (coding for β5i)
PSMB10	proteasome subunit beta type 10 (coding for β2i)
PSMD4	proteasome 26S non-ATPase subunit (coding for Rpn10)
PSME1	proteasome activator subunit 1 (coding for PA28α)
PSME2	proteasome activator subunit 2 (coding for PA28β)
PTM	posttranslational modification
PVDF	polyvinylidene fluoride
RIG-1	retinoic acid inducible gene 1
RING domain	really interesting new gene domain
ROS	reactive oxygen species
Rpn10	19S proteasome regulatory non-ATPase subunit
RT-PCR	reverse transcriptase polymerase chain reaction
SD	standard deviation
SDS	sodiumdodecylsulfoxide
sec	second
SMC	smooth muscle cell
Stat	signal transducer and activator of transcription
SUMO	small ubiquitin-like modifier
TAP	transporter associated with antigen processing
TBK1	TANK-binding kinase 1
TBS/TBST	tris buffered saline (with tween-20)
TCR	T cell receptor
TEMED	Tetramethylethylenediamine
TLR	Toll like receptor
TMB	tetramethylbenzidine
Tris	tris(hydroxymethyl)-aminomethan
U	unit
Ub	ubiquitin

Ubl domain	ubiquitin-like domain
UIM domain	ubiquitin interacting motif domain
UL83	HCMV unique long 83 (coding for pp65)
UPS	ubiquitin proteasome system
UV	ultraviolet
V	Volt
X-Gal	5-brom-4-chlor-3-indoxyl-β-D-galactopyranosid
ZBP1	Z-DNA-binding protein 1

List of figures

List of tables

Attachments

	fold increase transcription	
gene name	**4h HCMV infection**	**4h IAV infection**
E1		
UBA1	1,3	1,3
Selected E2		
UBE2L6	1,1	1
UBE2B	1,2	2,3
UBE2D1	1,1	1,9
UBE2D2	1,3	0,4
UBE2D3	1,5	3,6
UBE2DNL	9,7	1,2
UBE2CBP	23	1,5
ubiquitin		
UBC	1,01	1,08
i-subunits		
PSMB8	1,3	1,4
PSMB9	1,3	1,1
PSMB10	0,9	0,8
Nox enzymes		
Nox1	2,9	4,4
Nox4	1,7	2,1
Selected antiviral genes		
ZBP1	1,4	6,8
OAS1	1,8	58
OAS2	2	24
OAS3	6,4	2,7
IL6	1,2	17,3
IL11	1,1	2,3
NFKB1	1	1,6
NFKB2	4,2	5,7

Table 1 Effect of HCMV and IAV infection on the expression of selected genes. MRC5 fibroblasts were infected with HCMV Ad169 and HeLa cells with IAV at moi 3. After 4 hours of infection cells were harvested and RNA prepared as described for microarray analysis (Human U133 2.0 Plus; Affimetrix).

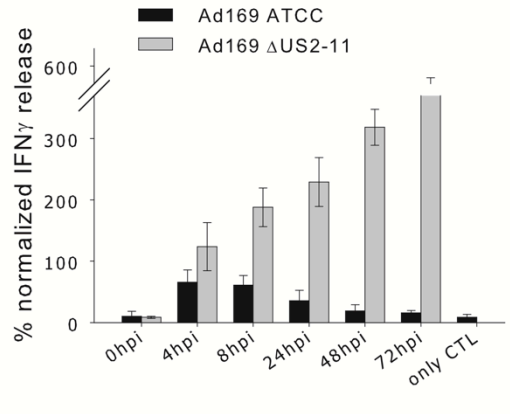

Figure 1 Presentation of the pp65$_{495-503}$ epitope is downregulated by the HCMV gene products of US2, US3, US6 and US11. MRC5 were infected either with HCMV Ad169 ATCC or the deletion mutant ΔUS2-11 at moi 5 for the indicated time points. IFNγ release by pp65$_{495-503}$ specific CTL was measured by ELISA and displayed as percentage of the response received by loading MRC5 with 1µg/ml pp65$_{495-503}$ peptide (n = 2, error bars represent ±SD).